UNIVERSITÀ
DEGLI STUDI
DI PADOVA

Head Office: Università degli Studi di Padova

Department of Land, Environment, Agriculture and Forestry

Ph.D. COURSE IN: LAND, ENVIRONMENT, RESOURCES AND HEALTH
SERIES XXXVI (36th)

EFFECTS OF DROUGHT/RECOVERY CYCLES ON TISSUE OSMOREGULATION, WATER RELATIONS AND ROOT EXUDATION IN PLANTS

Thesis written with the financial contribution of the Prima Programme, supported by the European Union's Framework Programme for Research and Innovation-Horizon 2020

Coordinator: Prof. Marco Borga
Supervisor: Prof. Giai Petit

Ph.D. student : dott.ssa Alessia Sartori

Index

Abstract

Not all organic compounds synthesized by plants undergo conversion into structural carbohydrates; conversely, a substantial portion of photosynthesized sugars is designated for the formation of non-structural carbohydrates (NSCs). Some of these NSCs become part of the root exudates. The root exudates include, besides a part of the non-structural carbohydrates, also amino acids, organic acids, and phenolic compounds.

The carbon emissions from roots are considerable, amounting to approximately 11% of the carbon fixed by leaves during photosynthesis and constituting 27% of the carbon allocated to the roots.

To elucidate the mechanisms triggering the release of root exudates in plants and their impact on the growth of soil microorganisms and other organisms (truffles, for example), two monitoring stations were established in different locations. These stations collected plant physiology data using sensors such as dendrometers, sap flow sensors, and environmental sensors. Analysis of environmental data revealed that truffle growth was not influenced by conventional parameters like humidity and temperature. Instead, it proved imperative to consider the physiology of the plant with which the fungus forms a symbiotic relationship and from which it derives nourishment.

Examination of dendrometer and sap flow data disclosed distinctions between truffle-producing and non-productive plants. Productive plants demonstrated superior dehydration control, attributed to osmoregulation mechanisms involving the accumulation of osmolites. The study also entailed experiments with maize and *Quercus ilex* L. plants to explore osmoregulation activities and the release of root exudates. Results suggested that osmolites, including sugars, could be released from roots after stress and recovery phases, as evidenced by changes in osmolality in leaf and root tissues during such cycles.

This research challenges prevailing beliefs regarding truffle growth conditions, presenting a fresh perspective that integrates the symbiotic nature of mycorrhizal fungi. The findings significantly contribute to a more comprehensive understanding of plant-water interactions and osmoregulation mechanisms, offering valuable insights into the release of root exudates and their potential effects on forest ecosystems.

1. Introduction

Climate change triggers changes in precipitation patterns and increases the frequency and intensity of extreme weather events, as evidenced by the Intergovernmental Panel on Climate Change. (IPCC, 2014). The ramifications of such extreme events, such as drought, reverberate through ecosystems, impacting the carbon equilibrium and inducing modifications in the productivity and stability of plants and their associated ecosystems (Zhao and Running, 2010).

Consequently, it is imperative to delve into a comprehensive understanding of the functions and mechanisms underlying organic compounds, which serve as invaluable resources within ecosystems. Notably, not all organic compounds synthesized by plants assume the form of structural carbohydrates; conversely, a substantial proportion of photosynthetically derived sugars is allocated to non-structural carbohydrates (NSCs). Maintaining a minimum threshold of non-structural carbohydrates (NSCs) is crucial for plants in order to osmoregulate, as highlighted by Martínez-Vilalta et al. (2016). Individuals with higher NSCs, such as starch, sucrose, and monosaccharides, exhibit prolonged survival during extreme drought conditions (Garcia-Forner et al., 2016). Some of these NSCs form, together with other compounds, the root exudates.

1.1 Root exudates

Root exudates constitute organic compounds predominantly composed of polysaccharides, amino acids, organic acids, and phenolic compounds (Bertin et al., 2003). Nevertheless, it is established that the composition of root exudates exhibits considerable variability. For instance, in an experiment involving *Quercus ilex* L., the composition of exudates demonstrated sensitivity to environmental conditions. In periods of drought, the exudates released by plants were primarily constituted of secondary metabolites. Conversely, during the recovery phase, marked by increased water availability, there was a surge in primary metabolites. This shift is attributed to the plant's necessity to utilize essential primary metabolites during drought, leaving predominantly secondary metabolites available for exudation (Gargallo-Garriga et al., 2018).

Divergent perspectives persist regarding the quantity of organic carbon released, ranging from 1% to 34%, with a prevailing consensus around 11% (Meharg and Killham, 1995;

Nguyen, 2003; Jones et al., 2009). Accurately determining the proportion of carbon in exudates remains challenging due to sampling issues, with no standardized methodology currently in place. While hydroponics is a widely adopted technique for growing plants and collecting their exudates, its limitations include influencing root morphology and physiology, and significant deviations from natural growth conditions (Dilkes et al., 2004; Oburger and Jones, 2018; Sasse et al., 2018; Canellas et al., 2019).

Experiments utilizing tracers like ^{13}C are fundamental for studying ground rhizodeposition, enabling the differentiation between deposited carbon and that pre-existing in the rhizosphere. This facilitates field studies under more realistic conditions compared to laboratory settings (Nguyen, 2003). However, these studies tend to be more expensive. Transferring plants from soil to hydroponics for exudate measurement could offer insights close to natural conditions but risks root damage during the transfer (Canarini et al., 2016; Oburger and Jones, 2018).

To address these challenges, a "microcosm" method has been developed, wherein plants grow in an agar substrate with microorganisms akin to those in the soil. This approach allows for the collection of approximately 90% of root exudates. However, it falls short in considering vital aspects of natural growth, such as nutrient competition and physical soil structure (Meharg and Killham, 1991).

1.2 Root exudates roles

The multifaceted roles of root exudates are underscored by various studies. Song et al. (2012) propose that the heightened release of root exudates observed in drought-resistant maize varieties, following a stress-and-recovery cycle, strategically enhances nutrient availability for the plant, potentially contributing to their increased drought resistance. Under water stress conditions, the proteases released by roots aid in nitrogen intake (Kohli et al., 2012).

Exudates released during stress and recovery cycles can elevate soil respiration rates, particularly when compared to exudates from non-stressed plants. This stimulation of microbial activity is postulated to be a consequence of the altered exudate composition (de Vries et al., 2019).

Root exudates play a protective role for root apices, crucial for soil exploration and interaction. Some exudates attract pathogens, while others inhibit or even eliminate them (Baetz and Martinoia, 2014).

A specific subset of root exudates, mucilages, acts as a physical barrier against harmful microorganisms, facilitates root growth, and increases the surface area for interactions with other organisms (Bertin et al., 2003; Baetz and Martinoia, 2014; Sasse et al., 2018). Mucilages contribute to nutrient accessibility and help maintain adequate rhizosphere humidity, as observed by Holz et al. (2018).

Exudates also play a pivotal role in promoting chemotaxis of beneficial soil microorganisms towards the plant. The organic acids in exudates solubilize phosphates of calcium, iron, and aluminum in the soil, making them available for plant uptake (Dakora and Phillips, 2002).

Root exudates may influence soil respiration dynamics and production. The allocation of photosynthesized carbon to the subsoil could vary based on the degree of root exudation, as observed by Karlowsky et al. (2018), impacting the rate of decomposition and the Birch effect.

Preece and Peñuelas (2019) emphasize the undervalued role of exudates in agriculture, noting that ancient varieties possess genetic traits beneficial for resistance to parasites, reduced dependence on fertilization, increased phosphorus availability, and positive associations with fungi and bacteria, mediated by root exudates. Additionally, exudates may promote allelopathy, exemplified by ailantone released from *Ailanthus altissima* Mill., which inhibits seed germination in certain species and stimulates root nodule formation in nitrogen-fixing bacteria (Heisey, 1990; Heisey, 1997; Bostan et al., 2014; Greer et al., 2016).

Understanding the release of allelopathic substances from roots, such as ailantone, holds potential implications for the development of new herbicides (Fracchiolla and Montemurro, 2007).

1.3 Root exudation is affected by plant and environmental conditions

The plant employs active transport, passive transport, or a combination of both for the release of root exudates. Sugars and amino acids are predominantly emitted through passive transport, the most frequently utilized mechanism (Dilkes et al., 2004). It is crucial to recognize that the plant exercises control over transport through various means, including modifying the expression of carrier protein genes, recovering previously exuded compounds, and regulating the activity of the root meristem (Canarini et al., 2019).

Exudation appears to be more closely associated with the rate of compounds allocated to the roots rather than the total amount of photosynthesized compounds produced. Furthermore, the exudation process is remarkably rapid, with photosynthesized compounds transferred to the soil in less than an hour following fixation (Dilkes et al., 2004).

The release of root exudates is influenced by water availability. During drought, the amount of exudates released decreases, but the proportion of photosynthesized compounds allocated to exudates increases, while the carbon destined for biomass decreases (Preece et al., 2018). Calvo et al. (2017) corroborate this observation, noting that water availability levels influence root exudation patterns in barley (*Hordeum vulgare* L.), where drought led to a higher hypogeal-to-epigeal biomass ratio and increased accumulation of ABA, proline, and potassium.

Sunflowers (*Helianthus annuus* L.) release significantly more carbon and nitrogen during recovery after drought stress, indicating a dynamic response to water availability (Canarini et al., 2016). The study also highlights qualitative changes in soybeans (*Glycine max* (L.) Merr.), where there is no increase in exudates, but a shift in composition favoring osmolytes.

Water stress conditions stimulate the emission of secondary metabolites, particularly volatile organic compounds (VOCs). VOCs can contribute to aerosol formation, act as nucleating agents for steam, and possess medicinal properties, as observed in *Salvia dolomitica* Codd. under drought conditions (Caser et al., 2019). VOCs also play a crucial role in plant protection against pathogens.

Different stresses, such as low-temperature soil, drought, and shade, induce varied responses in the release of root exudates, as observed by Karst et al. (2017). Stress plants allocate relatively more carbon to exudates than stress-free plants, and as the amount of non-structural carbohydrates (NSCs) allocated to the roots increases, the amount of root exudates also increases.

Water stress not only affects the soil but also the above-ground part of the plant. During drought periods, the reduction in shoot biomass and the simultaneous increase of the fine root biomass indicates that the drought induces an allocation of resources from the aerial part of the plant to other organs (Karlowsky et al., 2018). Fast-growing plants utilize carbon release to facilitate growth after drought, attracting beneficial microbes that aid in recovery (Williams and de Vries, 2019).

The release of root exudates is also influenced by nutrient presence. In an experiment by Högberg et al. (2010), increased nitrogen reduced carbon release after a year. Nitrogen enrichment negatively affects mycorrhizal fungi, primarily due to reduced carbon allocation by the plant (Hasselquist et al., 2016). Special conditions, such as CO2 enrichment, affect carbon release and root storage, potentially leading to increased carbon release in the soil (Jiang et al., 2020).

Root exudates play a pivotal role in phosphorus acquisition. Clausing et al. (2020) demonstrated that reducing carbon allocation to roots resulted in a phosphorus deficiency. Prescott et al. (2020) observed that the release of root carbon is linked to deficiencies in nitrogen, phosphorus, or water. In nitrogen or phosphorus deficiency the rate of cell division is reduced, while photosynthesis continues. Plants experiencing these situations, transform photosynthates into sugars and secondary metabolites. Releasing these compounds in form of root exudates could be a way of disposing of the C surplus.

The studies reviewed underscore the significant impact of water stress on resource allocation to roots and exudate production across various plant species and ecosystems. However, the precise mechanisms through which plants activate rhizodeposition, and whether this is linked to soil microorganisms, remain to be clearly established.

1.4 Root exudates and soil microorganisms

The relationship between microorganisms and roots is complex, exhibiting an ambivalence wherein root exudates can nourish microorganisms, yet microorganisms influence the release rate by creating a gradient out of the root (Canarini et al., 2019). This relationship plays a fundamental role not only in natural ecosystems but also in agricultural ones, emphasizing the importance of understanding their functioning to manage them and enhance ecosystem functionality (Battie-Laclau et al., 2020; Alaux et al., 2021).

To establish successful symbiosis between roots and rhizosphere microorganisms, it is imperative that the symbionts are metabolically active, capable of recognizing the plant and its exudates, able to move towards the root, successfully compete for root colonization against other microbes, and possess the ability to bind to the root and penetrate tissues (Sasse et al., 2018). Reciprocal sensing is essential, with root exudates containing chemical molecules that regulate symbiotic development and signal the fungus of potential host presence. Interestingly, these signals appear to overlap with those regulating communication with nitrogen-fixing bacteria in legumes (Dakora and Phillips, 2002).

Mycorrhizae, among the most critical microorganisms capable of symbiosis with roots, play a vital role in providing plants with water and nutrients, particularly under water stress conditions. For instance, under water stress, mycorrhiza positively affects the biomass production of *Triticum aestivum* L., whereas well-watered wheat does not benefit as much from the symbiosis, despite higher productivity (Al-Karaki et al., 2004). Mycorrhization with

Tuber melanosporum Vitt. in *Quercus ilex* L. plants influences leaf mass, conductance, and net photosynthesis, impacting stomatal duration (Nardini et al., 2000).

The benefits of mycorrhization extend beyond plants; fungi developing mycorrhiza demonstrate increased drought resistance compared to non-symbiotic fungi. The plants, through their roots, may reach deeper soil layers, acquiring water utilized by fungi (Castaño et al., 2018).

Considering the widespread occurrence of mycorrhizal symbiosis, colonizing the roots of 90% of terrestrial species, it is crucial to integrate mycorrhization into studies on root exudates (Wang and Qiu, 2006; Canarini et al., 2019).

In arid environments susceptible to desertification, the symbiosis between fungi and bacteria contributes to maintaining vegetation. *Anthyllis cytisoides* L. plants, inoculated with spores of mycorrhizal fungi and Rhizobium bacteria, exhibit enhanced survival during drought, increased size, elevated nitrogen and organic matter content in arid soils, and improved soil structure (Requena et al., 2001).

Mycorrhizal fungi, with their hyphae, can form soil aggregates, enhancing soil structure and porosity. This becomes crucial in situations of reduced soil water content, preventing alterations in root adhesion due to soil volume reduction. Mycorrhiza ensures contact maintenance, guaranteeing the plant a minimum water supply and nutrient access even under stressful conditions (Davies et al., 1992).

Understanding the regulatory mechanisms of mycorrhization is essential, not only for forest plants that typically exhibit high mycorrhization rates but also for species that are not consistently mycorrhized (Lehto and Zwiazek, 2011). For these species, the ability to develop advantageous symbiosis may influence their stress resistance and, on a broader scale, determine stand stability.

Another intriguing symbiosis involves fungi and bacteria, specifically mycorrhizal helper bacteria (MHBs). MHBs interact with ectomycorrhizal fungi, such as basidiomycetes and *Tuber melanosporum* Vitt. There are two types of MHBs: those aiding in mycorrhiza formation and those positively interacting with symbiosis. The bacteria receive benefits from the fungus, even in the absence of roots, hypothesized to be due to attraction to metabolites emitted by the fungus, forming a biofilm and creating a niche. These bacteria could be considered species-specific, influencing the growth of one fungus while inhibiting another. They hold potential applications in agriculture for promoting mycorrhization and reducing the presence of harmful fungi. Bacteria stimulate spore germination, mycelium growth, alleviate soil stress effects (e.g., restoring soil conductivity in drought conditions or removing toxic molecules),

enhance root system branching, and promote colonization by inducing substance release. Bacteria may have applications for nutrient mobilization, nitrogen fixation, and plant protection against root pathogens (Frey-Klett et al., 2007). This establishes a symbiotic relationship involving the plant, fungus, and bacterium.

1.5 Mycorrhizal fungi, ecosystem and drought

The establishment of symbiosis between plants and fungi has profound impacts on plant communities and ecosystem processes (Tedersoo et al., 2020; Alaux et al., 2021). Understanding the relationships between plants and fungi is crucial for several reasons. Firstly, mycorrhizal fungi associated with plant roots could serve as significant carbon storage (Treseder and Holden, 2013). Carbon compounds produced by microorganisms in the soil are known to be more resistant to decomposition (Allison, 2006; Prescott, 2010). The mycorrhizal mycelium, comprising 62% of the dominant pathway, facilitates the entry of carbon into the soil organic matter (SOM) pool, surpassing input via leaf litter and fine root turnover (Godbold et al., 2006). Moreover, certain mycorrhizal symbioses have economic significance, such as in truffle production (Samils et al., 2008; Reyna and Garcia-Barreda, 2014).

Numerous studies affirm the mutualistic benefits of mycorrhizal symbiosis for both plants and fungi. For example, plants gain resistance to stress (Al-Karaki et al., 2004), while fungi receive a portion of the photosynthetically fixed carbon for their development (Godbold et al., 2006). However, mycorrhizal associations are not universally mutualistic, with exceptions such as myco-heterotrophy, where the plant becomes a parasite of the fungus by not photosynthesizing (Leake and Cameron, 2010). Conversely, the fungus can turn parasitic, becoming a parasite of the plant and altering its lifestyle (Ballhorn et al., 2016).

The mycelium of mycorrhizal fungi appears crucial in controlling plant access to water, with about 20% of the total water uptake attributed to the mycorrhizal fungus (Ruth and Khalvati, 2011). Symbiotic organisms, like mycorrhizal fungi, significantly influence how tree roots respond to drought (Brunner et al., 2015). Despite the well-established substance exchange in symbiosis, where mycorrhizal fungi provide water and nutrients in exchange for sugars, the intricate links between root exudates and the rhizosphere remain less explored due to the challenges in quantifying root exudation in natural environments (Williams and de Vries, 2019).

As demonstrated by Sapes et al. (2020), if one plant linked to another via mycorrhiza undergoes a reduction in non-structural carbohydrates (NSCs), the other plant not subjected

to shading also experiences a decline in drought resistance. This happens because NSCs, initially allocated for osmoregulation, are redirected to mycorrhiza, creating a trade-off between resource allocation for osmoregulation and symbiont support. Thus, while fungi can enhance survival through hydraulic lift, they may concurrently diminish the plant's drought tolerance, contributing to the trade-off between sustaining symbionts and retaining water through NSCs.

Observations in the Northern Jarrah Forest of southwestern Australia indicate changes in the fungal community's specific composition due to decreased precipitation, resulting in water stress for plants. This shift involves an increase in certain species groups, like arbuscular mycorrhiza and saprophytic mycorrhiza, and a decrease in others, notably ectomycorrhizal fungi (Hopkins et al., 2018). This finding holds particular relevance, given that ectomycorrhizal fungi encompass economically valuable species such as Basidiomycetes (e.g., Boletales) and Ascomycetes, including truffles (genus Tuber).

1.6 Truffles: the most valuable mycorrhizal mushrooms

One of the most esteemed mycorrhizal fungi is the truffle, creating a multimillion-euro market in Italy, France, and Spain (Reyna and Garcia-Barreda 2014). However, the production of this sought-after wild food is steadily declining due to climate change and land abandonment. Truffle production fails to meet the internal demand in Italy, with 40-50% of the commercialized raw material currently being imported (MiPAAF 2018).

Conscious management of wild food products, such as truffles, is valuable not only for industrialized countries (Reyna and Garcia-Barreda 2014; Schulp et al. 2014) but also for developing nations (Negi et al. 2011; Stryamets et al. 2015). Fischer et al. (2017) recommend considering environmental characteristics when cultivating truffles, emphasizing the importance of pre-production and production operations, including irrigation, soil tillage, and pruning, as well as addressing potential predators.

The timing of pruning is crucial for plant growth. Winter pruning preserves carbohydrates stored in roots, while vegetative season pruning aids quicker healing (Fischer et al. 2017). Mycorrhizal fungi release allelopathic substances, forming areas devoid of herbaceous vegetation near truffle growth sites. A study on black truffle, *Tuber melanosporum* Vitt., revealed the inhibitory effect of its mycelium on other ectomycorrhizal fungi, influencing biodiversity (Napoli et al. 2010).

In Spain, the use of "truffle nests," peat containing spores inserted in orchard soil, results in rounder, less affected truffles with larvae positioned on the outside for better growth (Garcia-Barreda et al. 2020). The innovative "MRT" method, involving selective grass removal, deep operations, and intensive pruning, leads to accelerated production, deeper truffles, and reduced reliance on substances (Chevalier and Pargney 2014).

However, truffle cultivation faces challenges. Diverse mycorrhization methods yield varying results, affecting the number, diameter, and height of mycorrhized plants (Bruhn et al. 2013). Critical issues include unwanted species production and productivity decline after a few years, attributed to the difficulty of cultivating forest species (Bencivenga et al. 2009). Various methods to assess plant mycorrhization for truffle production underscore the importance of cultivation techniques (Fischer and Colinas 1996).

Cultivation times for truffles are prolonged, hindering timely assessment of mycorrhization results (Bruhn and Hall 2011). The truffle's slow growth is attributed to the small hyphal surface through which carbon is transferred from the plant (Deveau et al. 2019).

Truffles exhibit specific soil and environmental requirements. Soil analysis, considering texture and quality, is crucial for informed production management (Bragato et al. 2021). Optimal growth conditions involve a precise balance of exchangeable calcium in the soil (Raglione 2011). Mycorrhizal fungi production correlates with the basimetric area of the plant, emphasizing the importance of understanding species differences (Tahvanainen et al. 2016).

Precipitation significantly impacts truffle production, with summer months' rainfall being crucial (Garcia-Barreda and Camarero 2020). Drought periods may benefit truffles, prompting a reevaluation of irrigation systems to conserve water (Garcia-Barreda et al. 2019). Moderate irrigation between May and July proves effective in increasing mycorrhized apices (Olivera et al. 2014).

Different truffle species present varying challenges. *Tuber aestivum* Vitt. is adaptable to diverse soil conditions, pH levels, and temperatures, making it the most straightforward to cultivate (Bruhn and Hall 2011; Chevalier 2012; Robin et al. 2016). *Tuber magnatum* Pico, the most prized but challenging to cultivate, relies on nitrogen-fixing bacteria during ripening, resembling legume root nodules' nitrogen fixation (Barbieri et al. 2010).

Understanding the needs of truffles is essential for adapting cultivation methods to climate change. Predictions indicate potential expansion with slight emissions increase but reduced production with excessive emissions (Čejka et al. 2020). Spain, a southern European country,

anticipates a 29% reduction in truffle production by 2040 due to climate change (Fischer et al. 2017). Historic symbiotic relationships between truffles and their host plants during the post-glacial era, influencing their current distribution, highlight the importance of understanding these symbiotic organisms (Mello et al. 2006).

1.7 Understanding the trigger of root exudation: a new hypothesis

The elucidation of why plants release a substantial amount of fixed carbon remains elusive (Jones et al. 2004). Consequently, it is imperative to unravel the mechanisms governing the initiation of root exudation. A novel hypothesis associates stress-recovery cycles with the liberation of root exudates. Notably, moderate stress levels have been observed to enhance the accumulation of essential oils in the aerial parts of *Mentha x piperita* L., elevating medicinal qualities (Búfalo et al. 2016). Similarly, *Helianthus annuus* L., recovering from water stress, exhibited a remarkable 330% increase in root-released carbon compared to pre-stress conditions (Canarini et al. 2016).

Water stress induces a myriad of effects on plants, ranging from morphological alterations (reduced height, changes in leaf and root morphology, alterations in root/shoot and root/stem ratios, and stomatal development) to physiological and biochemical adaptations (photosynthetic capacity, osmotic regulation metabolism, drought-induced proteins, and biochemical and molecular adjustments) (Fang and Xiong 2015; R. Gobu et al. 2017; Ilyas et al. 2021; Yang et al. 2021).

Plants absorb water from the soil when the leaf water potential (Ψ) is lower than that of the soil (Taiz and Zeiger 2003). Consequently, during water stress, plants must reduce their leaf water potential to maintain the hydration of all living tissues and to sustain water flow to the leaves. Osmoregulation becomes pivotal in plants subjected to drought (Mehmood et al. 2020) or excessive salinity (Perri et al. 2018).

Crucial osmolites, including soluble carbohydrates, sugar alcohols, proteins, amino acids, and proline (Kavi Kishor et al. 2005; Ozturk et al. 2021), accumulate in cytoplasmic compartments, maintaining cell turgor (Rontein et al. 2002). This accumulation correlates with the severity of stress (Chakhchar et al. 2015).

Research by Yang et al. (2015) demonstrated that a drought-hardening treatment, involving the transfer of *Jatropha curcas* L. plants into a Hoagland's solution supplemented with PEG

6000, enhances drought tolerance, with osmoregulation identified as a key factor in increased tolerance.

Stomatal opening is regulated by the solute content in guard cells, with various metabolic pathways supplying osmotically active solutes. Talbott and Zeiger (1998) identify two osmoregulatory phases in guard cells, involving initial K+ accumulation and subsequent sugar accumulation.

Although osmolites accumulated in leaves may have detrimental effects, such as inhibiting cellular enzymes in the presence of ions (Waseem et al. 2011), the fate of these compounds after fulfilling their osmotic adjustment function remains unexplored.

The release of carbon from roots during stress, a seemingly inefficient choice for the plant, lacks a clear trigger. A plausible explanation based on plant physiology posits that, during a drought phase, osmoregulation prompts the accumulation of organic compounds in leaves, leading to a reduction in leaf water potential. Subsequently, as water availability resumes, the plant gains better control over water flow, obviating the need for sustained low leaf water potential. Consequently, excess osmolites accumulated in leaves are released as root exudates.

Preliminary analysis of literature reported minimum leaf water potential values reveals that many truffle-producing plants tend to reach low leaf water potentials, accumulating osmotic compounds to sustain water flow to leaves (Table 1). This observation provides a compelling avenue for comprehending why certain plants may not be conducive to mycorrhizal fungi production.

Truffle producing plants	**Minimum leaf water potential (Ψ)**	**Non truffle producing plants**	**Minimum leaf water potential (Ψ)**
***Ostrya carpinifolia* Scop.**	**-3** (Nardini et al. 2000)	***Acer pseudoplatanus* L.**	**-1.72** (Li, Feifel, et al. 2015)
***Quercus pubescens* Willd.**	**-4.5** (Tognetti et al. 1998)	***Fraxinus excelsior* L.**	**-2.1** (Li, Feifel, et al. 2015)
***Corylus avellana* L.**	**-1.8** (Li, Feifel, et al. 2015)	***Sorbus torminalis* L.**	**-1.53** (Paganová et al. 2020)
***Quercus robur* L.**	**-2.85** (Glatzel 1983)	***Prunus avium* L.**	**-2.5** (Centritto et al. 1999)
***Quercus ilex* L.**	**-6.5** (Tognetti et al. 1998)	***Crataegus laevigata* Poir.**	**-1.7** (Thomas et al. 2021)

***Carpinus betulus* L.**	**-2.35** (Li, Feifel, et al. 2015)	***Betula pendula* Roth.**	**-1.7** (Aspelmeier and Leuschner 2004)
***Quercus cerris* L.**	**-3.9** (Vannini et al. 2009)	***Ulmus minor* Mill.**	**-2.25** (Li, López, et al. 2015)
***Populus nigra* L.**	**-3.5** (Callister et al. 2006)	***Alnus glutinosa* L.**	**-2.25** (Eschenbach and Kappen 1999)

Table 1: minimum leaf water potential (Ψ) described in literature for plants suitable for the production of truffles and plants that do not develop symbiosis with fungi of the genus *Tuber*

The leaf transpiration rate is influenced by the vapor pressure gradient between the leaf and the atmosphere (Daly et al., 2004). The activation of sapflow, and consequently transpiration, is closely linked to Vapor Pressure Deficit (VPD) (Badalotti et al., 2000), signifying that higher VPD values lead to increased plant dehydration. As the leaf-to-air VPD serves as the primary driving force for transpiration (Dichio et al., 2006), it has been selected as a parameter to measure the likelihood of plant dehydration. This measure is then compared with the quantity of truffles collected to establish a correlation between production and dehydration.

2. Material and methods

The study is composed by distinct experiments conducted both within controlled laboratory settings involving young plants of *Zea mays* L. and *Quercus ilex* L. and in open fields where target plants underwent observation within natural environmental conditions.

2.1 Field experiment

The field experiment aims to investigate physiological disparities and water stress management between productive truffle-producing plants and non-productive ones. This work unfolds across two distinct sites: Caltrano (VI) and Carlino (UD).

Caltrano boasts a meticulously cultivated truffle orchard, specifically a hop-hornbeam plantation realized in 2001, with trees strategically spaced at 2 x 2.5 meters. After a decade, the plantation started producing truffles. Spanning an area of 2428 m^2 with a perimeter of 227 m, the site exhibits a slope ranging from 12° to 19°, a south/south-west aspect, and an altitude varying between 480 and 500 m a.s.l. It corresponds to cadastral parcel n. 123, situated in "Tezze" locality of the Municipality of Caltrano (VI) (figure 1).

Delving into geolithology, the area is characterized by limestone and dolomite, falling into the category of "Hills and pre-alpine mountains of medium and low altitudes." The substrate comprises limestone, dolomitic limestone, and flint limestone. Various soil types, including Eutric Cambisol, Leptic Luvisol, and Rendzic Leptosol, contribute to the composition. The Corine Land Cover classification designates the area as "Broad-leaved Forest". With a temperate macro-climate typical of the semi-continental-sub-continental temperate climate in the eastern part of northern Italy, the forest type is classified as the typical orno-ostryetum, with coverage ranging from 71% to 100%.

The plantation, predominantly composed of hop hornbeam (*Ostrya carpinifolia* Scop.) and supplemented by beech (*Fagus sylvatica* L.) specimens, features *Fraxinus ornus* L. as the most prevalent renewal (40% coverage). The herbaceous and shrubby layer includes ivy (*Hedera helix* L.), *Arrhenatherum elatius* L., *Hepatica nobilis* Schreb., *Allium* spp., *Taraxacum officinalis* Web., and *Viola odorata* L. Notably, the truffle orchard is diligently managed, with regular visits by the owner and manager, who employs a trained dog to discern mycorrhized plants that produce truffles from those that do not.

Measurements:

Eight target plants, all of the same species *Ostrya carpinifolia*, evenly distributed between productive and non-productive, underwent detailed analysis. Target plants have average dbh of 15 cm and average height of 15 meters. Each target plant was equipped with a dendrometer and a Granier-type sapflow sensor, providing accurate measurements of daily hydration cycles and sap flow rates.

The dendrometers, featuring potentiometers with a precision of one hundredth of a millimeter, were affixed to the plant trunks using screws (figure 2). These potentiometers, touching the bark, captured minute changes associated with daily hydration and dehydration cycles.

Sap flow sensors, utilizing two probes inserted into the trunk with a 10 cm separation, measured sap flow rates by detecting temperature differences between the probes (figure 3).

The upper probe is actively heated, and under conditions of high sapflow, it undergoes cooling as the sap carries heat away, resulting in a reduced temperature difference between the upper and lower probes. Conversely, during periods of low sapflow, such as at night, the temperature difference becomes more pronounced. This mechanism provides insights into the regulation of stomatal activity, allowing us to discern the phases of photosynthesis engaged by the plant (Lu et al. 2004).

This data, indicative of the opening and closing of stomata, offered insights into photosynthesis timings.

Additionally, two TDR soil sensors were strategically placed within the truffle orchard to measure soil water content (m^3/m^3), reflecting both its availability and continuous variation due to plant uptake and atmospheric evaporation.

A hygrometer, providing air temperature (°C) and relative humidity (%) measurements, was positioned installed. Utilizing temperature and relative humidity values, VPD (vapor pressure deficit) was calculated through the empirical Magnus formula (Formula n. 1)

$$\mathbf{VPD = (1\text{-}RH)\ a\ e(bT/T+c)} \qquad \textit{Formula n. 1}$$

The sensors, powered by a photovoltaic panel, transmitted data to a Campbell CR1000 datalogger, ensuring remote data download post-2022. Further, truffles were systematically collected, counted, and weighed every 2-3 days since 2021. The truffles collected under the area of the crown for each plant were attributed to that specific plant. In the case of *Tuber*

melanosporum it takes at least 6 months between the production of the primordia and the full development of ascocarps (Le Tacon et al. 2013). However, it should be noted that during the harvest, which took place with the help of a trained dog, the ripening level of truffles varied considerably after a few days or hours. In fact, it was not uncommon for the dog to find new ripened ascocarps for several consecutive days (and this suggests that in the previous days they were not yet ripened).

In 2022, detailed plant characteristics were recorded, including precise location (using submetric GPS, figure 4), status (productive or not productive), diameter at breast height (dbh) measured with a tree caliper, total plant height, and crown insertion height measured with a Trupulse laser hypsometer. Additionally, the distance covered by the crown along the north-south and east-west axes was measured. The crown volume, approximated as a cylinder, was calculated based on these values (specifically, by calculating the volume of a cylinder with the average radius of the four measured radii and a height equal to the crown height). However, the crown shape coefficient was not considered in the comparative analysis between productive and non-productive plants. All data were organized into graphs using a logarithmic scale for clarity.

Despite meticulous data collection, external factors such as weather conditions and biotic elements led to incomplete data series. These challenges were particularly pronounced in Carlino, where anthropogenic and animal-caused damages interrupted battery power, and tree falls resulted in station destruction. In Caltrano, ant activity led to the oxidation of datalogger structure.

Pre-dawn leaf water potential (Ψ) measurements were taken in September 2022 using a Scholander pressure chamber (PMS Model 600D) in Caltrano. Leaves were collected at the same height on the 8 target plants before sunrise, and their leaf water potential was immediately measured (taking 3 leaves from 6 of the 8 target plants). Other leaves were collected and immediately placed in ziplock bags with a damp piece of paper to prevent rapid dehydration, then stored in a thermal container in the dark. Their leaf water potential was measured at various water content levels, allowing gradual dehydration and providing valuable insights into plant water response and differences between productive and non-productive plants. The mapping of the area and data representation were achieved through QGIS software.

Statistical Analyses:

To extract meaningful insights from the extensive dataset, statistical analyses were conducted using the software R and Excel. The dataset comprised information on diameter fluctuations, sapflow, soil water content and temperature, air temperature, and relative humidity. Key analyses included determining the vapor pressure deficit (VPD), daily maximum and minimum differentials, calculating dehydration levels from dendrometer data, and deriving the percentage of flow during the day from sapflow sensor data.

Leaf water potential (Ψ) measurements collected in 2022 for each target plant were subjected to statistical analysis to discern plant water responses at various water content levels. Detrending of data obtained from dendrometers through Excel software highlighted daily swelling and shrinkage, excluding the effects of actual stem growth.

Graphical representations of the data were created using R, Excel, and QGIS, providing visual insights into trends and patterns. This comprehensive statistical approach allowed for a robust interpretation of the experiment's findings, enhancing the understanding of physiological differences and water stress management between productive and non-productive plants in the truffle orchard.

Figure 1: Aerial photo of the plantation of Caltrano (in red). The plantation is in the province of Vicenza in northeastern Italy. The truffle orchard lies in the hilly area of the Venetian Pre-Alps and borders the forest on one side and meadows on the other sides.

Figure 2: dendrometer installed on a tree. The potentiometer is fixed with two screws that sink into the deepest part of the trunk (not subject to movements), while the tip grazes the bark, and is pushed back and forth by the growth of the plant's radius, as well as from swelling and shrinkage due to daily cycles of hydration and dehydration

Figure 3: Sapflow sensors installed on white hornbeam (Carlino) and hop hornbeam (Caltrano). The sensors consist of 2 probes that are inserted into the trunk at a distance of about 10 cm from each other. The upper probe is heated and when the upward flow is consistent, it is cooled. In this way the temperature difference provides information on the intensity of the flow.

Figure 4: Representation of the distribution of productive plants (in red) and non-productive plants (in black) inside the truffle orchard of Caltrano.

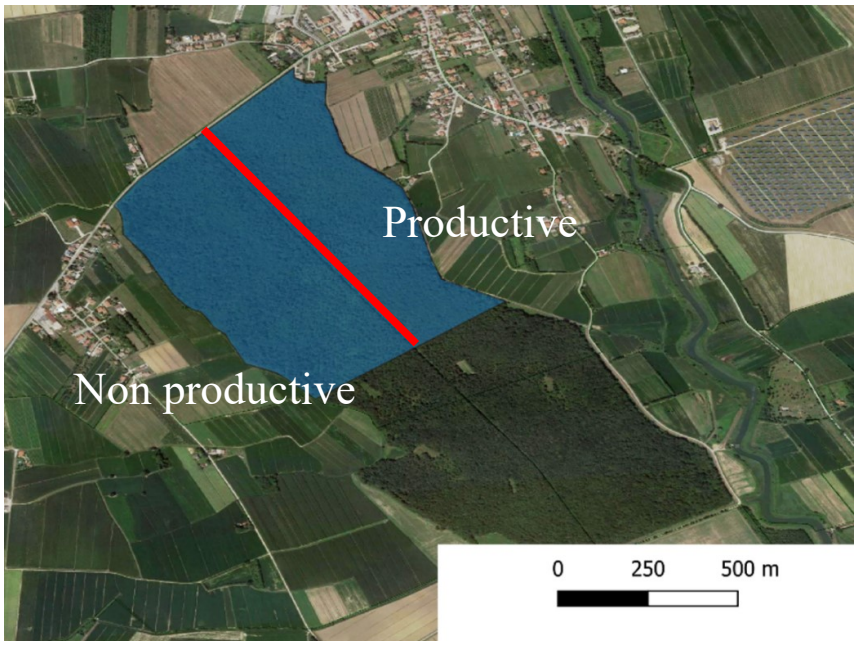

Figure 5: aerial image of the forest Sacile (Carlino site). The forest is located in the plain of Friuli, near the lagoon of Marano. It is divided into a part where in the past the white truffle was harvested (*Tuber magnatum* Pico, "Productive") and a part that instead has never been productive ("Non productive").

In Carlino, the forest predominantly comprises white hornbeam (*Carpinus betulus* L.), English oak (*Quercus robur* L.), and narrow-leafed ash (*Fraxinus angustifolia* Vahl). *Tuber magnatum* Pico, the prized white truffle, grows in this lowland forest. The site, historically divided into a productive and non-productive part (figure 5), now stands as a wholly non-productive forest.

Situated in the lower Friulan plain, the area corresponds to querco-carpinetum and carpinetum woods on silty-clayey sediments, occasionally mixed with sands and subordinate gravel. According to the Corine Land Cover classification, it falls under code 3.1.1, denoting "Broad-leaved woods."

In 2021, two sample areas were identified—one in the former production zone and another in the non-productive zone. Within each area, four target white hornbeam plants were selected for the installation of dendrometers and sapflow sensors. Additionally, a hygrometer and two TDR sensors were placed at different depths (0-20 cm and 20-40 cm) in each sample area. This configuration facilitates the detection of variations in aquifer movement between the two sites.

For each target plant in 2021, 5 leaves were collected, and their leaf water potential was measured at various water content levels using a Scholander pressure chamber (PMS Model 600D). This approach allows for the comparison of leaf water potential at different hydration percentages, offering insights into plant water response and discerning differences between the two forest areas.

Both sites are situated in northeastern Italy, specifically in the Veneto region. In this region, the average total annual precipitation for the reference period 1993-2020 was 1136 mm, while in 2021 was 971 mm and 774 mm in 2022. The summer precipitation in 2023 were 391 mm, a bit more than the reference period 1994 to 2022, corresponding to 323 mm.

During the reference period (summer from June to August) 1993-2020, the minimum average air temperature was 14.6°C, while the maximum average air temperature was 26.1°C. In 2021, the values aligned with the period's average, with an average minimum of 15°C and an average maximum of 26.6°C. However, in 2022 and 2023, the temperatures deviated, with values of minimum 16.1°C - maximum 28.3°C and minimum 15.7°C – maximum 26.8°C, respectively. (Summary of Weather and Agrometeorological Commentary for the Summer Period, Compiled by the Regional Department for Territorial Security of the Veneto Region-summer 2023).

2.2 Laboratory experiments

This section explains the materials used and the procedures applied for carrying out the experiments with *Zea mays* L. and *Quercus ilex* L.

2.2.1 Experiments with *Zea mays* L.

The laboratory experiment aimed to investigate the release mechanism of radical exudates in plants under water stress, particularly focusing on the osmoregulation process. The chosen plant for this hydroponic culture experiment was maize (*Zea mays* L.), specifically the P0423 hybrid obtained from the "Azienda Agricola Toniolo" in Legnaro.

The hydroponic culture setup involved the following phases:

Seed Cleaning (Day 1):

The initial step entailed cleaning maize seeds by removing their protective wax coating. Seeds were immersed in distilled water and gently stirred for an hour. Subsequently, they underwent a cleaning process with distilled water and 15% bleach for 5 minutes, followed by thorough rinsing. After cleaning, the seeds were left in distilled water overnight.

Germination (Day 2):

After absorbing water and swelling up, the maize seeds were placed on tissue paper in trays. Then, they were covered with additional tissue paper soaked in distilled water. Finally, the trays were sealed in plastic bags and kept in a dark, temperature-controlled environment.

Transplanting:

Upon the seeds' germination (4 days later), seedlings were transplanted into 500 ml pots for further growth. This process involved careful handling to avoid damage. Each pot featured an oxygenator to ensure a constant flow of air for optimal nutrient solution oxygenation.

The growth of plants occurred in a climatic cell, with controlled humidity, temperature and light conditions. The Hoagland solution (Table 2.1) was utilized, and its replacement occurred every 2-3 days.

Preliminary Test using *Zea mays* (2019):

A preliminary test was conducted in 2019 to assess biomass variation, exudate amount, and electrical conductivity in *Zea mays* L. during water stress induced by polyethylene glycol (PEG). During the four-day stress period, fresh weights, dry leaf weights, and carbon and nitrogen content were measured.

Tests using *Zea mays* (2021-22):

Test n. 1:

This test involved controlled stress conditions with variations in PEG concentrations. Measurements included monitoring solution conductivity changes, assessing relative water content (RWC) through turgid and dry weights, and determining sugar content in leaves and roots.

Test n. 2:

To refine the understanding, stress levels were increased, and measurements included growth parameters, osmolality of foliar and radical liquids, and gene expression related to stress.

Test n. 3:

This test aimed to evaluate the impact of nutrient solution concentration on growth. Electrical conductivity was monitored during growth, and observations were made on plant response to different nutrient solution concentrations.

Test n. 4:

Controlled stress conditions with PEG application were employed, measuring leaf water potential (Ψ) using a pressure chamber, calculating RWC, determining sugar content in leaves and roots, and analyzing gene expression related to stress.

Test using *Quercus ilex* (2023):

In 2023, an experiment with *Quercus ilex* L. was conducted, involving different stress scenarios with varied PEG concentrations. Measurements included fresh weight, turgid weight, dry weight, leaf water potential (Ψ) using a Scholander pressure chamber, osmolality of leaf and root using a dewpoint potentiometer, and sugar content in leaves and roots.

Statistical Analyses:

Data obtained from all experiments underwent rigorous statistical analysis, including techniques such as ANOVA and the Kruskal-Wallis test, supported by the Dunn post-hoc test. The statistical software R was employed for comprehensive analyses and graphical representation of the results. The emphasis on statistical rigor ensured the validity and reliability of the findings, contributing to the broader understanding of plant responses to water stress in hydroponic cultures.

The Hoagland solution used during the hydroponic cultures is described in Table 2.1:

MACROELEMENTS	**Name**	**mg/L**
KNO3	Potassium nitrate	1900
MgSO4-7H2O	Magnesium sulphate heptahydrate	370
KH2PO4	Potassium dihydrogen sulphate	170
Ca(NO3)2	Calcium nitrate	

MICROELEMENTS	**Name**	**mg/L**
MnSO4	Manganese sulphate	16.9
ZnSO4-7H2O	Zinc Sulphate Heptahydrate	8.6
H3BO3	Boric Acid	6.2
KI	Potassium Iodide	0.83
NaMoO4 – 2H2O	Sodium molybdate dihydrate	0.25
CuSO4 – 5H2O	Sulphate of copper pentahydrate	0.025
CoCl4 – 6H2O	Cobalt chloride hexahydrate	0.025

CHELATORS	**Name**	**g/L**
FeNaEDTA	Ferric Sodium EDTA	3.62 g

Table 2.1: list of macronutrients, micronutrients and chelators that compose the Hoagland solution used in this experiment.

For plant growth, a climatic cell was utilized, replicating variations in light between day and night.

Once the first leaf developed, the seedlings were transferred to groups of three in 500 ml pots. To achieve this, the plant stems were inserted into foam cylinders, threaded, and secured in holes in the pot lids. This arrangement ensured that the plants maintained an upright position, and their roots were well immersed in water.

Each pot included a small tube connected to an oxygenator, facilitating a constant flow of air to oxygenate the solution. The Hoagland solution was replaced every 2-3 days.

These initial steps are crucial, as any damage to the seedlings at this stage significantly affects the overall health of the mature plant. It has been observed that even a small portion of the root not in close contact with water can impede proper leaf development. Additional damage, visible during leaf development, may result from excessive agitation, a high bleach content during the cleaning step, and submersion of the seed in the solution during the initial growth phases (Figure 6).

Figure 6: Example of damage caused by criticality during growth. Plants that, for various reasons, did not have their roots fully immersed in water exhibit an inability to fully extend their initial leaves. Over time, the tips of these leaves have dried up and turned black.

Preliminary test using Zea mays

A preliminary test in 2019 was realized in order to test the hypothesis.

In the initial phase of the experiment, the impact of water stress on biomass variation (root and leaf) and the release of exudates in corn seedlings (*Zea mays* L.) was investigated. Polyethylene glycol (PEG, Polyethylene glycol 6000, HO(C2H4O)nh, Scharlau) was employed to induce stress. When dissolved in water, PEG takes on a dense, viscous consistency, forming a barrier on the root surface that restricts water absorption.

The plants were divided into three groups: a control group receiving nutrient solution (28 plants, SN), a group exposed to mild stress (8 plants immersed in a Hoagland solution with PEG at a concentration of 200g per liter), and a group subjected to intense stress (17 plants immersed in a Hoagland solution with PEG at a concentration of 400g per liter). The stress treatment spanned 4 days, following which the plants were returned to a nutrient solution. The contents of the bekers were collected during both the stress and recovery periods, transferred to falcon tubes, and subsequently lyophilized for the measurement of carbon and nitrogen content. Fresh weights and dry leaf weights were measured for each group.

In the second phase of the experiment, the variations in electrical conductivity (indicative of osmolite release from the roots) of the solutions were examined. Additionally, the osmolality of leaves and roots fluids was measured. The maize plants were divided into three groups (15 plants for each group): one group remained in PEG 200 for 19 hours, another group remained in distilled water for 19 hours, and a third group remained in PEG 200 for 14 hours and was then transferred to distilled water for 5 hours. The electrical conductivity of the solutions at different phases was measured using a conductivity meter, and the osmolality of leaves and roots fluids was determined.

In the 2021-22 period, a subsequent experiment involving *Zea mays* L. was conducted. The primary objective was to elucidate the response mechanisms of plants by employing a larger sample size. The experiment aimed to generate more precise data on the osmoregulation mechanism, including parameters such as the quantity of sugars in tissues and solutions, gene expression during stress phases, leaf water potential (Ψ), relative water content (RWC), along with the previously mentioned data on solution conductivity and osmolality.

During the initial growth phase of the experiment, several challenges were encountered, leading to the repetition of the experiment four times. Variations were introduced in stress intensity, the maize cultivation protocol, and concentrations of the hydroponic solution to ensure robust and reliable data collection.

Test n. 1 using Zea mays

In the initial trial conducted in January 2021, the experiment was originally planned for 90 seedlings. Unfortunately, during the growth phase, a significant number of plants exhibited drying and yellowing symptoms. Consequently, 51 robust individuals were selected to proceed with the experiment. Of these, 36 plants were placed in 500 ml pots in groups of 3, and 15 plants were placed in 250 ml bottles. The growth of plants occurred in a climatic cell with a temperature between 21°C (night) and 25°C (day), relative humidity of 55 %, a daytime of 14 hours and a nighttime of 10 hours. These settings were the same for next tests.

The selected plants, both in pots and bottles, were categorized into three groups: a control group (remaining in nutrient solution: 5 plants in bottles and 12 in pots), a group exposed to mild stress (5 plants in bottles and 12 in pots, subjected to 24 hours of immersion in a PEG solution with a concentration of 100 g/l, followed by 24 hours of recovery in nutrient solution, repeated for two cycles), and a group subjected to intense stress (5 plants in bottles and 12 in pots, exposed to 24 hours of immersion in a PEG solution with a concentration of 200 g/l, followed by 24 hours of recovery in nutrient solution, repeated for two cycles).

The rationale behind subjecting plants to a double cycle of stress-recovery was to investigate whether the release of root exudates resulted from osmoregulation cycles or if it was attributed to cell wall damage induced by severe stress. If the release of substances was due to damage, the effects would likely be visible only after the first stress cycle and not necessarily after the second.

To measure the release of osmolites from the roots, the conductivity of the solutions was measured using a conductivity meter, soaking it into the solutions.

To calculate the relative water content, the middle leaf and a small amount of root was taken from each plant.

The leaf was cut and weighed (fresh weight). Then it was immersed in distilled water for 3 hours, keeping it in the dark. After 3 hours, it could be obtained the turgid weight of the leaf. Finally, the leaf was placed in the oven for 24 hours at 70 °C, to obtain the dry weight. At this point, the RWC value was obtained applying the following formula (Formula 2):

$$RWC = \frac{Leaf\ fresh\ weight - Leaf\ dry\ weight}{Leaf\ turgid\ weight - Leaf\ dry\ weight} \times 100$$

The same procedure was applied to the roots.

Unfortunately, it was not possible to measure the osmolality of foliar and radical liquids due to an osmometer failure.

The plants at the beginning of the experiment were unfortunately already damaged, so that they all found themselves in a condition of stress. The plants of the treatment groups could not restore adequately during the recovery phases in nutritional solution.

Test n. 2 using Zea mays

During the second experiment conducted in May 2021, a total of 36 plants were distributed into 500 ml pots in groups of 3 (12 for each group), while 15 plants were placed in 250 ml bottles (5 for each group). Similar to the initial trial, both the potted plants and those in the bottles were categorized into three groups: a control group (remaining in nutritional solution), a mild stress group (subjected to 24 hours of immersion in a PEG solution with a concentration of 150 g/l, followed by 24 hours of recovery in nutrient solution, repeated for two cycles), and an intense stress group (exposed to 24 hours of immersion in a PEG solution with a concentration of 300 g/l, followed by 24 hours of recovery in nutrient solution, repeated for two cycles). In this case, the PEG levels were increased (mild stress 150 g/L, intense stress 300 g/L) with the aim of inducing a more pronounced response to stress.

Unfortunately, similar to the first trial, the plants did not exhibit vigorous and healthy growth, making it challenging for them to withstand the stress and recovery cycles.

Test n. 3 using Zea mays grown in nutrient solution at different concentrations

To evaluate the impact of nutrient solution concentration on plant growth, an experiment was conducted by cultivating maize seedlings in solutions with different concentrations, diluting the Hoagland solution with distilled water, in order to obtain different levels of conductivity.

The highest concentration had an initial conductivity of 540 μs, the intermediate solution had a conductivity of 300 μs, and the least concentrated solution had a conductivity of 100 μs. The 18 plants were grouped into three sets of six plants each and grown in nutrient solutions with different concentrations. Each of these three groups was further divided into two subgroups: a control group (4 plants), which remained in the solution at the same concentration for an additional 24 hours, and an experimental group (2 plants) transferred to nutrient solution with a concentration of 400 g of Polyethylene Glycol (PEG) per liter for 24 hours. After this period, all plants were transferred to distilled water. The electrical conductivity of the solutions was measured during each phase.

Throughout these initial experiments, challenges affecting the healthy growth of plants were identified, including issues such as parts of the root not being adequately wetted, excessive agitation, high bleach content during the cleaning step, and seed submersion in the solution during initial growth phases. These critical factors are detailed in the growth procedure outlined above.

Test n. 4 using Zea mays

In December 2021, the final maize experiment was conducted, commencing on the 21st day after seed sowing. The 17 pots were divided into 6 control pots and 11 treatment pots. The plants in the 6 control pots remained in the Hoagland solution, while the plants in the treatment pots were transferred to a solution containing 300 g of Polyethylene Glycol (PEG) per liter.

After 24 hours, on day 22, 2 control pots and 4 treatment pots were selected to collect plant material and solutions (both nutrient and nutrient + PEG). The plants (3 for each pot) were carefully removed from the solutions, and their roots were rinsed. For each plant, leaves and roots were separated by cutting the small stems, and the water potential was measured using a pressure chamber (PMS Instrument Company, Model 600D Pressure Chamber Instruments). Subsequently, a leaf, typically the middle one, was chosen from each plant for the calculation of Relative Water Content (RWC) using Formula n.2.

The leaves and roots of all plants in a single pot were then combined. Approximately 2/3 of the leaves and 2/3 of the roots from each pot were enclosed in aluminium foil and rapidly frozen in liquid nitrogen. These samples were stored in a freezer at -80°C and will be used for gene expression analysis.

About one-third of the leaves and one-third of the roots from each pot were placed in Falcon tubes, microwaved at 600 W for 3 minutes, and subsequently stored in a -20°C freezer. This portion of leaves and roots will be utilized to measure the sugar content. After 24 hours of recovery on day 23, biological material from the 4 control pots and the 4 stress pots is collected to calculate RWC, leaf water potential (Ψ), sugars, and gene expression, following the previously described method. Additionally, the growth solution is collected.

At the end of day 23, 3 treatment pots are subjected once again to PEG 300 solution. After 24 hours of water stress (second stress cycle), leaf and root material from the plants in the pots is collected to measure the sugar content. During each solution change over the 3 days, the solution is collected in Falcon tubes to measure the sugar content. Conductivity is measured multiple times during the experiment.

The sugar content measurements were conducted at the University of Udine by a research group from the Department of Agricultural, Environmental, and Animal Science, while gene expression and osmolality measurements were performed in Turin by a research group from the Department of Agricultural, Forest, and Food Sciences. Data were analyzed using ANOVA when applicable, or the non-parametric Kruskal-Wallis test and the Dunn post-hoc test. R software was employed for statistical analysis and graphical representation.

2.2.2 Experiment with *Quercus ilex* L.

In 2023, an experiment was conducted using 39 *Quercus ilex* L. plants grown in pots. These plants, 2-year-old holm oak specimens, were obtained from the Montecchio Precalcino (VI) nursery. After a meticulous cleaning of the roots from soil and a 2-day acclimatization period in a hydroponic solution (see table 1), the plants were divided into pots in subsets of four and placed in a hydroponic solution. Holm oak was chosen for this experiment conducted in October 2023 because it is an evergreen species, allowing the experiment to be carried out during this period.

The timing of stress and recovery cycles is crucial for triggering a response in the plant. Post-stress recovery during daytime hours, when the plant is photosynthesizing and the stomata are open, may hinder complete recovery. This is because the water transported from the roots to the leaves is used for transpiration rather than rehydration. On the other hand, if the recovery after the stress phase occurs during nighttime hours, the plant can rehydrate fully. During this phase, the stomata are closed, and the absorbed water can accumulate in the

tissues. This consideration likely contributed to the positive outcome of the preliminary test conducted in 2019. The measurements, regulated by the climate cell, were taken during the night rest, allowing the plants to recover completely.

For this reason, the experiment was structured in three phases: a first night phase, a diurnal phase, and a second night phase.

The pots containing four plants each were divided as follows:

- Three pots remained in nutrient solution throughout all three phases.
- One pot was in nutrient solution for the first two phases and in a solution with 280 g/L of PEG during the second night phase.
- Three pots were in PEG 280 g/L during the first two phases and in nutrient solution during the second night phase.
- One pot remained in PEG 280 g/L throughout all three phases.
- Two pots were in PEG 500 g/L for the first night and during the day, transitioning to nutrient solution during the second night phase.

Measurements included fresh weight, turgid weight, and dry weight, in order to determine RWC% (calculated using Formula 2). Leaf water potential (Ψ) was measured using a Scholander pressure chamber (PMS Model 600D). Hydroponic solution potentials (nutrient solution and solutions with varying PEG content) were measured with a dewpoint potentiometer WP4 (Decagon Devices, Inc., Pullman, WA, USA). The potentials were, approximatively: -0.05 for the nutrient solution, -1.7 for the PEG 280 g/L solution and -7 for the PEG 500 g/L solution.

Approximately 2 or 3 leaves and 1/3 of the roots of each plant were enclosed in foil and rapidly frozen in liquid nitrogen. These samples were stored in the freezer at -80°C and will be utilized for gene expression analysis.

Similarly, 2 or 3 leaves and 1/3 of the roots from each plant were placed in falcon tubes, microwaved at 600 W for 3 minutes, and then stored in the -20°C freezer. This portion of leaves and roots will be used to measure sugar content.

At each phase of the experiment, the solution was collected in falcon tubes for subsequent sugar content measurements. Conductivity was measured several times during the experiment. Osmolality of leaf and root samples, as well as sugar content in the hydroponic solution, will be analyzed by the laboratories of the Department of Biology and Plant Protection at the University of Udine. Simultaneously, samples for gene expression analysis

will be processed by the laboratories of the Department of Agricultural, Forestry, and Food Sciences in Turin (data not yet available).

3. Results

3.1 Field Experiment

In this section are presented the data related to the two field experiments, the one in Caltrano and the one in Carlino.

3.1.1 Type of data collected in field

Weather data

Figure 7 presents environmental data recorded at the Caltrano station in 2021. In Figure 7A, soil moisture is depicted as the mean value obtained from the two TDR probes installed at the station. This methodology is the same for the calculation of soil temperature showcased in Figure 7B. For air temperature (7C) and relative air humidity (7D), these fundamental values serve as the foundation for calculating Vapor Pressure Deficit (VPD) through the application of the Magnus formula (Formula 1).

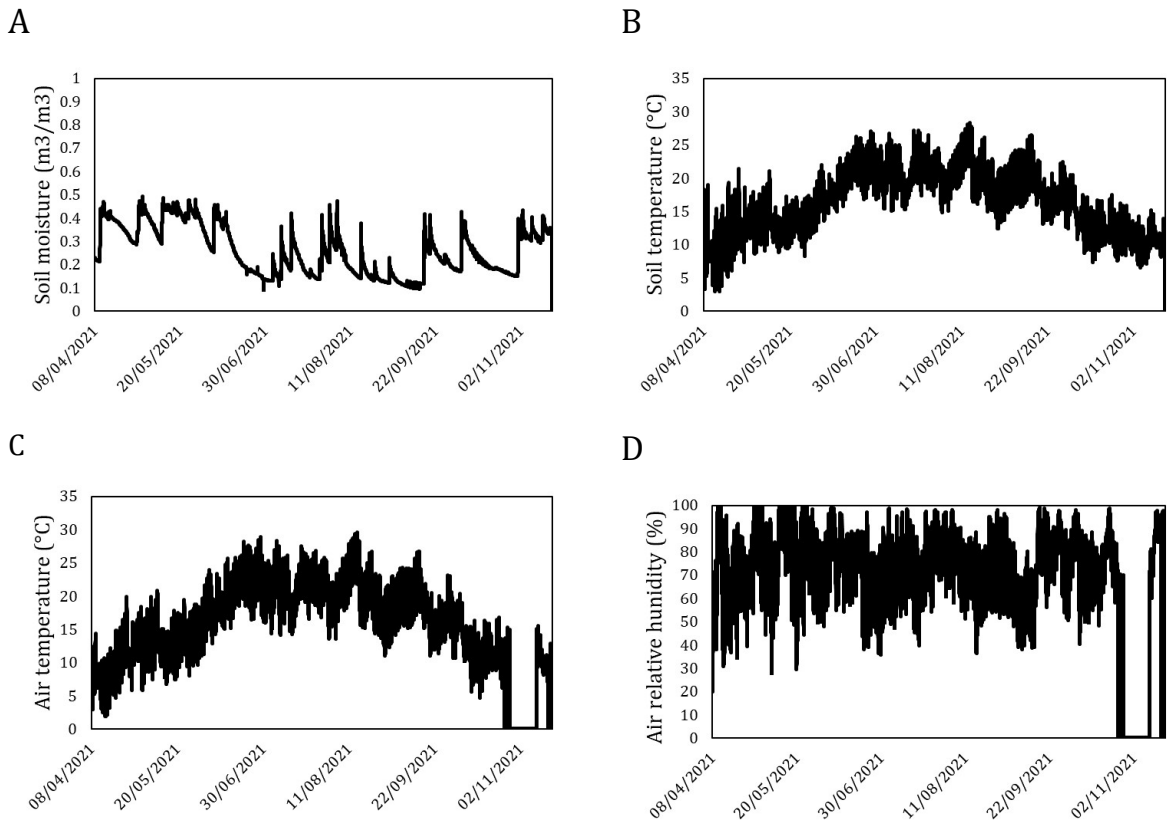

Figure 7: soil moisture (A), soil temperature (B), air temperature (C) and relative air humidity (D) data at Caltrano for 2021.

In Carlino, soil moisture data are determined as the average between the probe positioned closer to the surface and the deeper one. Figure 8A illustrates the soil moisture values recorded by the two TDR sensors in the former productive part of the forest. Figure 8B displays the values for the non-productive part of the forest. Notably, the difference in humidity between the two probes is more pronounced in this case, attributable to the shallower groundwater depth compared to scenario A.

A

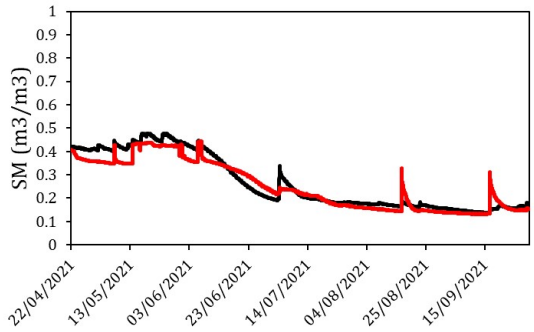

B

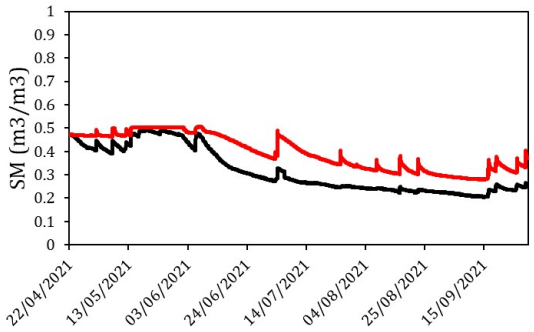

Figure 8: Soil moisture (SM) for the most superdicial TDR (black) and the deepest TDR (red) in Carlino in 2021. Graph A shows the data for the former production part and Graph B for the non-productive part.

Dendrometer data

The dendrometer data are derived from averaging between the readings of productive plants (in red) and non-productive plants (in black). Similar to Caltrano, in 2021 (Figure 9A), a noticeable difference in the amplitude of oscillations between productive and non-productive plants is evident. In 2022 (Figure 9B), both productive and non-productive plants exhibit a significant reduction in radius near the period of summer drought. In both cases, the diameter increase initiates in late April, reaches a peak in late June, and subsequently stabilizes. To emphasize the oscillations due to expansion and contraction (excluding diameter increase), the series are detrended.

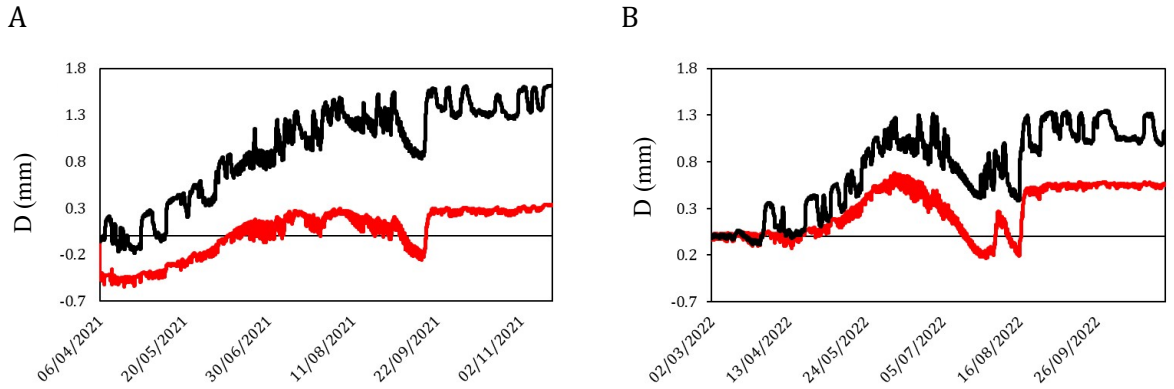

Figure 9: Increase in plant diameter (D) during the 2021 (A) and 2022 (B) seasons in Caltrano. The data are obtained by averaging the dendrometer values of productive plants (in red) and non-productive plants (in black). Diameter fluctuations in non-productive plants are much more pronounced than in productive plants

A comparable pattern is also noted at Carlino (Figure 10): a diameter increase that starts at the end of April and generally stabilizes by the end of June. Beyond that point, the plant stops the growth. Unlike Caltrano, there are no distinct differences in oscillation between the former productive plants and the non-productive plants.

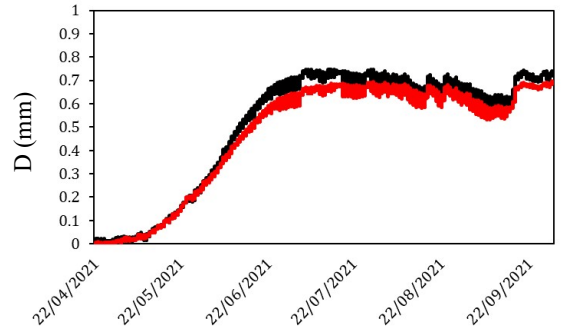

Figure 10: Increase in plant diameter (D) during the 2021 in Carlino. The data are obtained by averaging the dendrometry values of former productive plants (in red) and non-productive plants (in black).

Sapflow data

Sapflow data require significant processing, due to the presence of spikes and the fact that the series are not immediately comparable with each other (since they simply detect a change in temperature compared to an initial value). Figures 11 A and B shows raw data, which are difficult to interpretate. Initially, the data are cleaned to remove spikes, enabling a clearer identification of the daily oscillations (figure 12). The raw sapflow data primarily reflects the temperature difference between the two probes. During the day (higher sap flow), the peak is low because the difference between the probes decreases. Conversely, at night (no sap flow), the peak increases due to the rising temperature difference (Figure 12). However, this

presentation may not effectively highlight differences between the two groups, as, for example, the initial temperature between the probes could be slightly different. For this reason, the data are subsequently normalized to represent a percentage difference between day and night, as illustrated in the following pages.

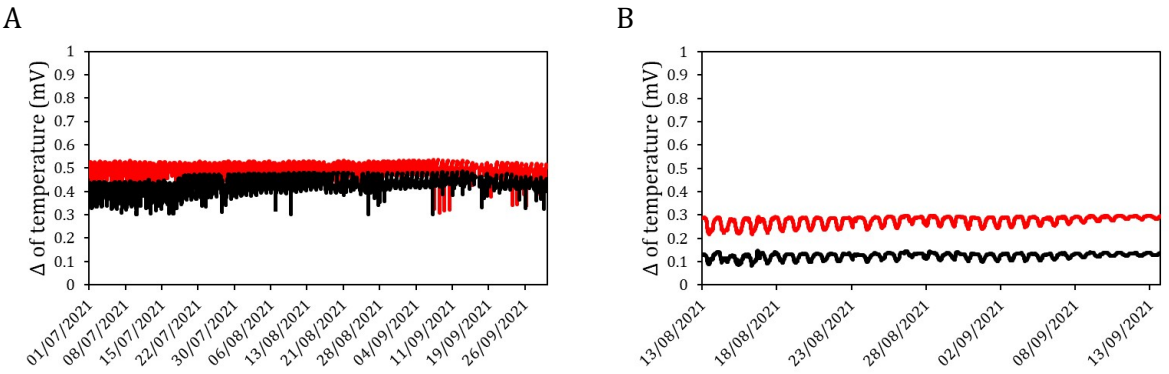

Figure 11: Raw data obtained in July-September 2021 from sapflow sensor in Carlino (A) and in August-September 2021 in Caltrano (B). In Carlino in red are data mediated between the former productive plants and in black among the non-productive ones, in Caltrano, in red the data mediated between productive plants and in black among non-productive ones. In graph A the interpretation of the data is rather complex, and even increasing the resolution (graph B) is not easy to obtain useful information. In both cases, the data is not immediately comprehensible and need to be elaborate.

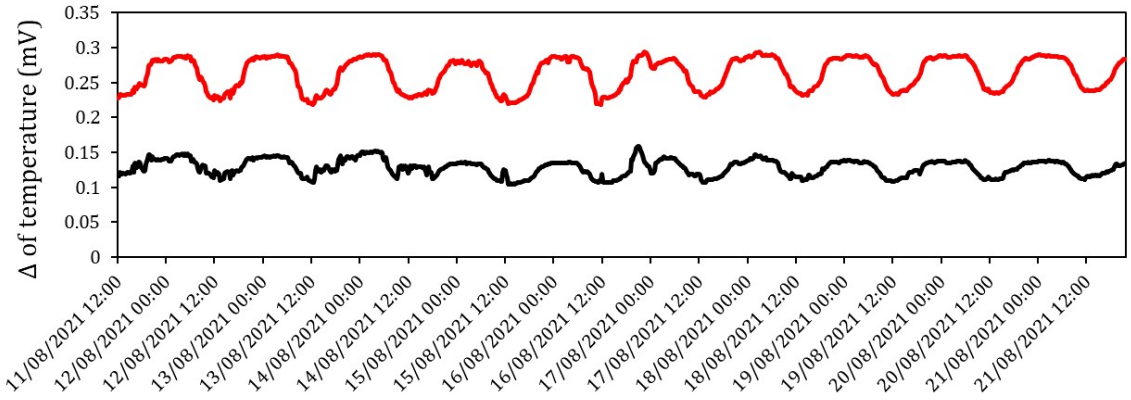

Figure 12 illustrates the raw data trend of sapflow sensors. The figure displays average values obtained from productive plants (in red) and non-productive plants (in black). During the night, when there is no flow, the difference increases, while during the day, the difference decreases.

3.1.2 Production and environmental parameters in Caltrano

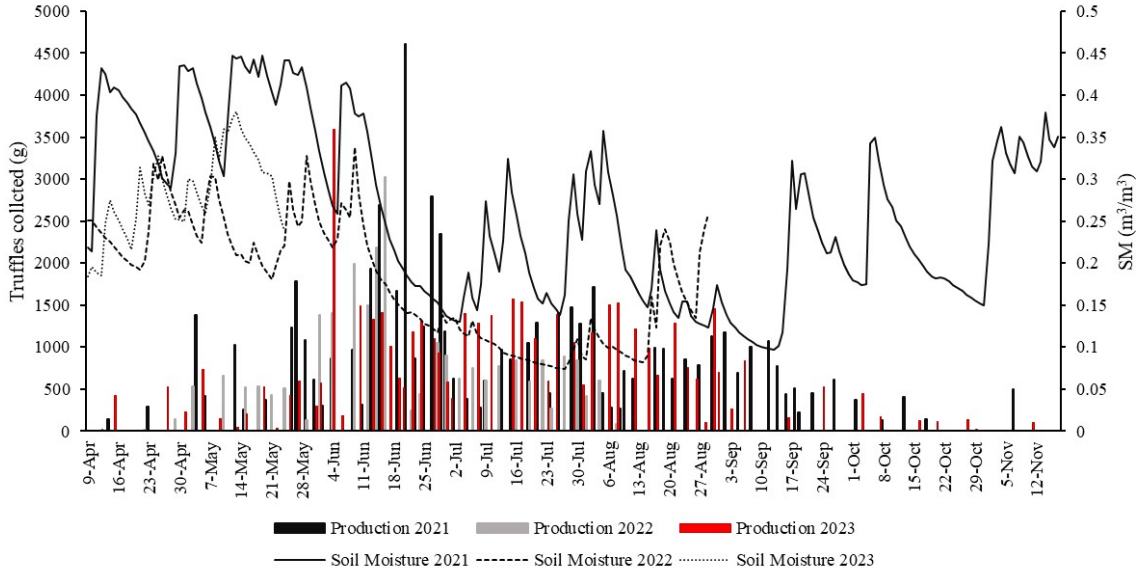

Figure 13: Truffles collected during the 2021 season (black columns), 2022 (grey columns), and 2023 (red columns). The harvest values pertain to the entire truffle farm. Regarding soil moisture (SM), the solid line represents the values of 2021, the dashed line represents 2022 values, and the dotted line represents 2023 values. The moisture values are obtained by averaging the readings from the two TDR probes.

The biomass of the truffle *Tuber aestivum* was meticulously measured on each harvesting day over three consecutive seasons: 2021, 2022, and 2023. Truffle production exhibited a concentration during the summer months, with a pronounced peak in June across all years, particularly in 2021 (Figure 13).

Traditionally, soil moisture and other environmental parameters are regarded as the primary predictors of truffle production. However, field-monitored environmental factors such as soil and air temperature and humidity did not exhibit robust correlations with truffle production.

In the subsequent analysis, production was compared with the following parameters:

Avg T_{air} (°C): average air temperature of the harvest day

Max T_{air} (°C): maximum air temperature of the harvest day

Avg T_{air} (°C) - 7 days: average air temperature of the 7 days before the harvest day

Max ΔT_{air} (°C) - 7 days: maximum difference of air temperature during the 7 days before the harvest day

Avg M_{air} (%): average air moisture of the harvest day

Δ M_{air} (%): maximum difference of air moisture during the harvest day

Avg M_{air} (%) - 7 days: average air moisture of the 7 days before the harvest day

Max ΔM_{air} (%) - 7 days: maximum difference of air moisture during the 7 days before the harvest day

Avg T_{soil} (°C): average soil temperature of the harvest day

Max T_{soil} (°C): maximum soil temperature of the harvest day

Avg T_{soil} (°C) - 7 days: average soil temperature of the 7 days before the harvest day

Max ΔT_{soil} (°C) - 7 days: maximum difference of soil temperature during the 7 days before the harvest day

Avg M_{soil} (m^3/m^3): average soil moisture of the harvest day

Δ M_{soil} (m^3/m^3): difference of soil moisture of the harvest day

Avg M_{soil} (m^3/m^3) - 7 days: average soil moisture during the 7 days before the harvest day

Max ΔM_{soil} (m^3/m^3) - 7 days: maximum difference of soil moisture during the 7 days before harvest day

Avg VPD (KPa): average vapor pressure deficit of the harvest day

Max VPD (KPa): maximum vapor pressure deficit of the harvest day

Δ VPD (KPa): difference of vapor pressure deficit of the harvest day

Max Δ VPD (KPa) - 7 days: maximum difference of vapor pressure deficit of the considered week

I examined the correlation between the daily truffle harvest biomass and the maximum and average air temperatures on each harvesting day to investigate whether higher temperatures influenced production and whether there was a short-term impact. Additionally, I explored the effects of the average air temperatures during the seven days preceding each truffle harvest, aiming to understand whether a prolonged period of warm temperatures could influence truffle production. Furthermore, I assessed the impact of the maximum temperature difference (Tmax-Tmin) in the seven days leading up to the truffle harvesting day. This exploration considers the plant's potential adaptive strategies, such as osmoregulation. The accumulation of osmotically active compounds during a "dehydration control" phase may lead to their release as root exudates during a rehydration phase, potentially influencing production.

Upon analyzing the impact of air temperature on truffle production (Figure 14), a slightly positive correlation is evident. A bettere correlation is observed with the maximum air temperature on the day of collection (Figure 14 - B), although the effect is comparable to the average temperature on the harvest day (A). The correlation with the average temperature of the 7 days before harvest is slightly lower, while the weakest correlation is found between production and the maximum temperature difference (T °C max - T °C min daily) in the 7 days prior. It's important to note that *Tuber aestivum* is a summer-ripening truffle species, and the data may reflect the impact of the maturation period (higher temperatures in summer) rather than the direct effect of temperature. However, truffle production seems constrained to temperature differences (Tmax-Tmin) in the seven days before harvest within the 9-11 °C range, with negligible production for lower and higher values (Figure 14 - D).

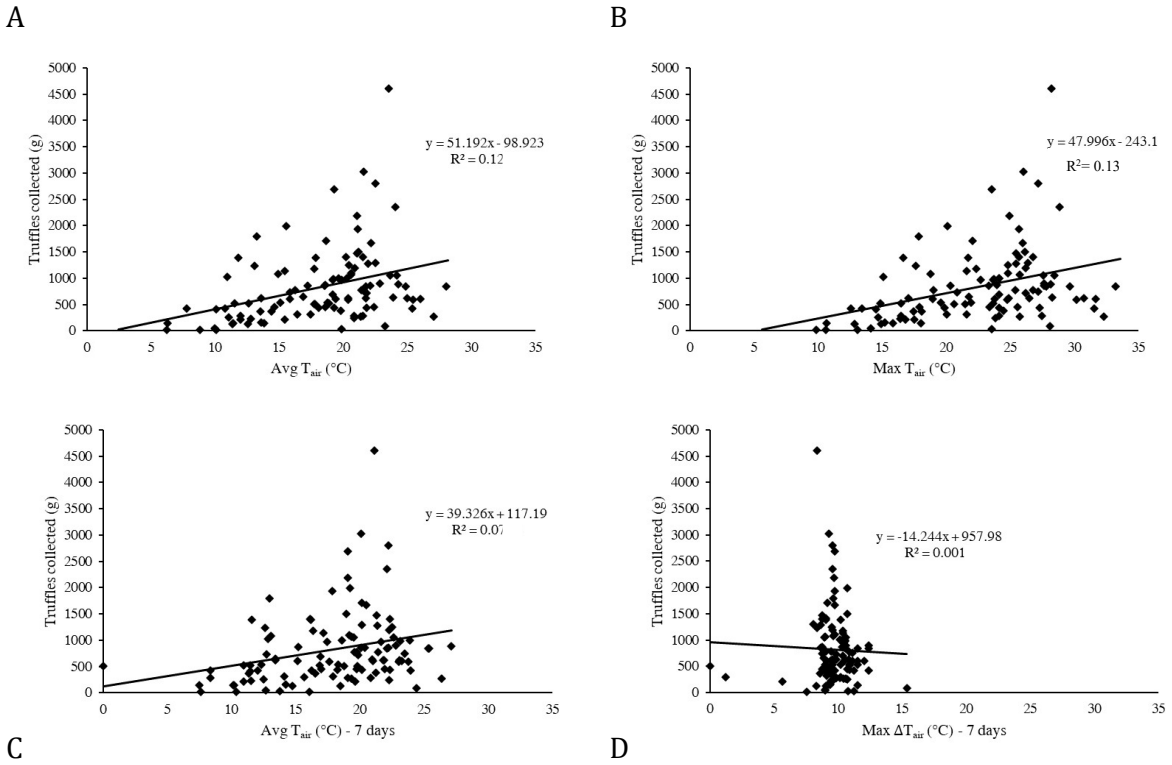

Figure 14: Relationship between truffle production and air temperatures. A) Average air temperature on the day of truffle harvest; B) Maximum air temperature on the day of truffle harvest; C) Average air temperature in the 7 days before harvest; D) Maximum daily temperature difference (difference) in the 7 days prior to collection. A slightly positive correlation is observed in graphs A, B, and C, while it is absent in graph D. The production values pertain to the entire truffle orchard.

Figure 15 illustrates the results of the correlation analysis between truffle production and air humidity. The average air moisture on the day of collection (A) does not exhibit a significant relationship with production. Similarly, the average humidity over the preceding 7 days (C) shows no notable correlation (in contrast to the observed temperature patterns in Figure 15 A and C). However, there appears to be a slightly more positive effect of the daily humidity difference on the day of collection (B) and the maximum humidity difference in the previous 7 days (D). A high difference value in humidity indicates substantial daily variation, which might necessitate the plant's adaptation to fluctuating humidity conditions through osmoregulation. This suggests that while air humidity may not directly influence the development of the fungus's fruiting body, it could exert an indirect effect. The plant's osmoregulatory adaptations, triggered by changes in humidity, might induce the release of organic compounds useable by the fungus.

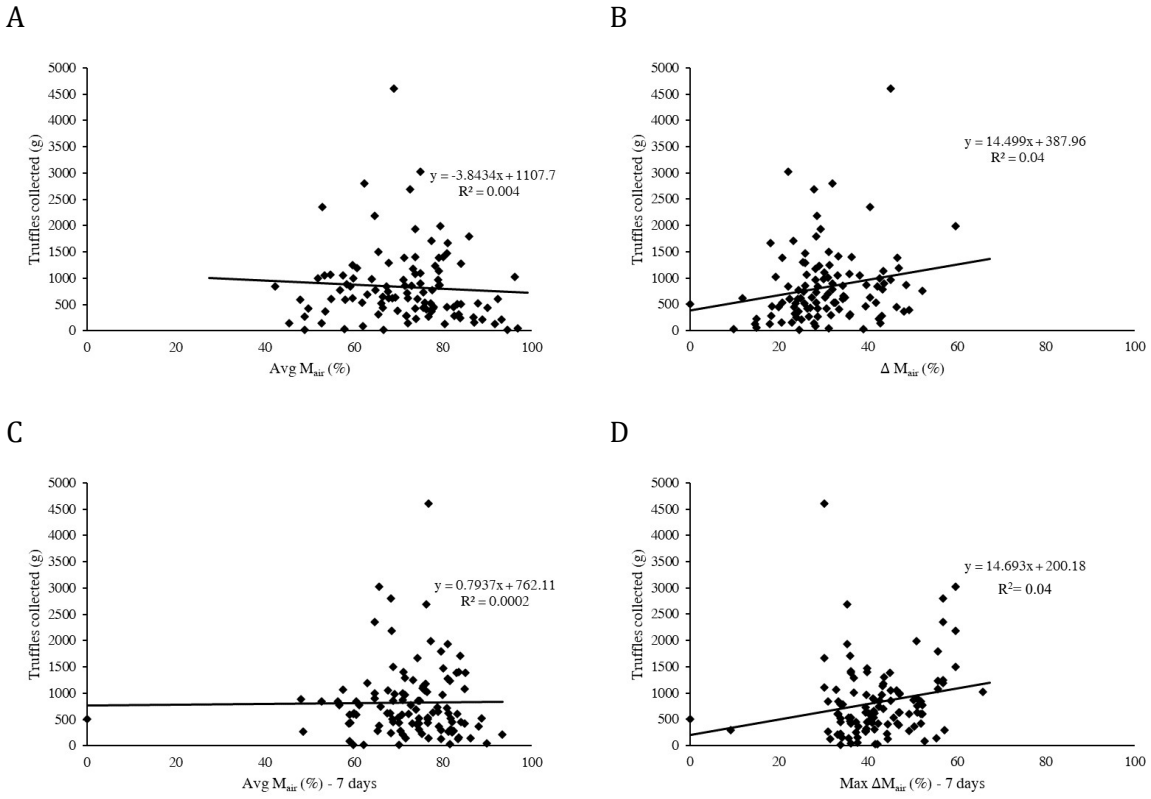

Figure 15: Correlation between truffle production and air moisture. Graph A depicts the correlation with the average humidity on the day of harvest, graph B illustrates the difference of air humidity on the day of harvest, graph C shows the average humidity of the air in the 7 days before the harvest, and graph D represents the maximum daily difference reached in the 7 days preceding the harvest. The correlation is more pronounced in cases where the humidity difference (B and D) is considered compared to the average humidity (A and C). The production values pertain to the entire truffle orchard.

As with the previous parameters, it is important to check whether the effect of soil temperature on production is immediate or not. Moreover, as for air temperature, the effect of the maximum temperature of the day of collection and the maximum temperature difference of the previous 7 days is compared with the production.

The average soil temperature seems to be positively correlated with production, and this is mainly true for the average temperature of the harvest day (fig. 16-A). A similar correlation is also observed with the maximum temperature reached during the day of collection (fig. 16-B) and with the average temperature of the 7 days preceding the harvest (fig. 16-C). On the other hand, the correlation between production and the maximum temperature difference seems to be negative in the 7 days before the harvest (fig. 16-D).

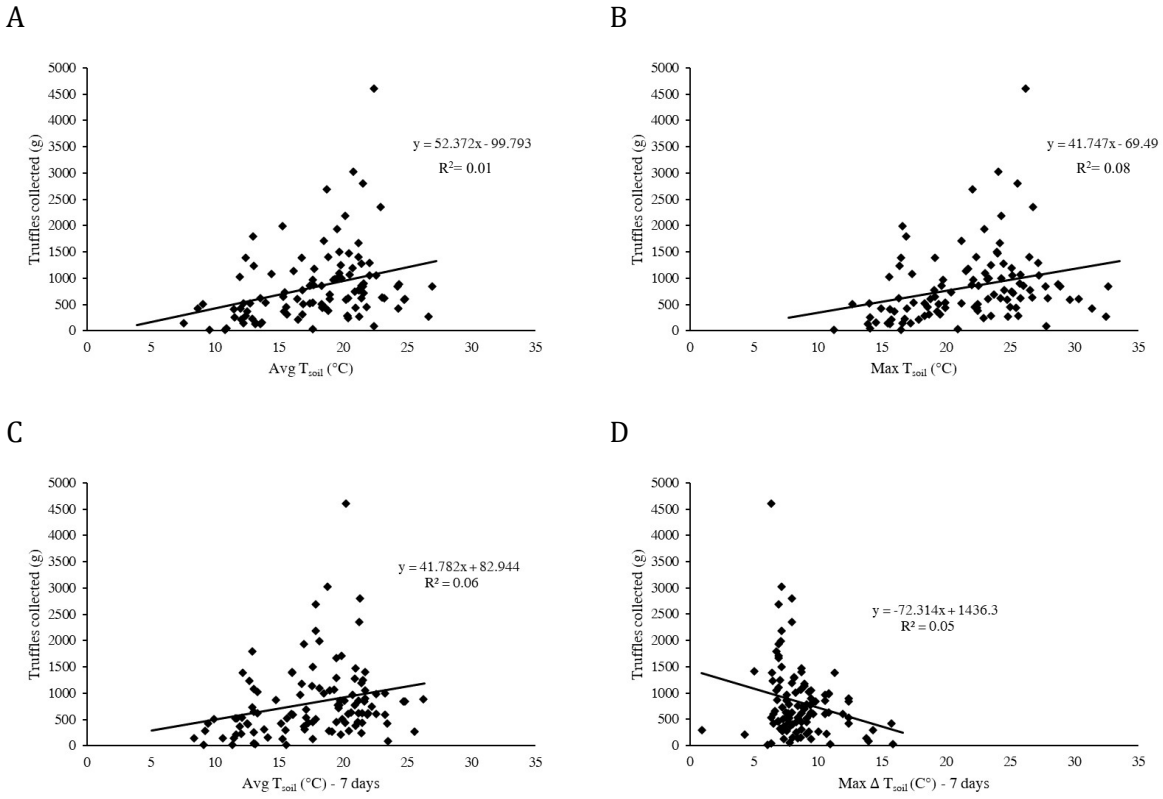

Figure 16: Correlation between production and soil temperatures. Graph A shows the correlation with the average soil temperature on the day of harvest, graph B the maximum soil temperature on the day of harvest, graph C the average soil temperature on the 7 days before harvest, graph D the maximum daily difference reached during the 7 days before the harvest. The correlation is positive with the mean and maximum temperature (A, B, C), but negative in the case of the maximum difference. In particular, production is concentrated within a narrow range of maximum difference, between 5 and 10 °C. The production values refer to the whole truffle orchard.

These observations may be correlated with the maturation period of *Tuber aestivum*. As depicted in Figure 17, the average soil temperature increases during the summer months (A), while, conversely, the temperature difference decreases (B). This dynamic could influence the correlation between truffle production and soil temperature.

A

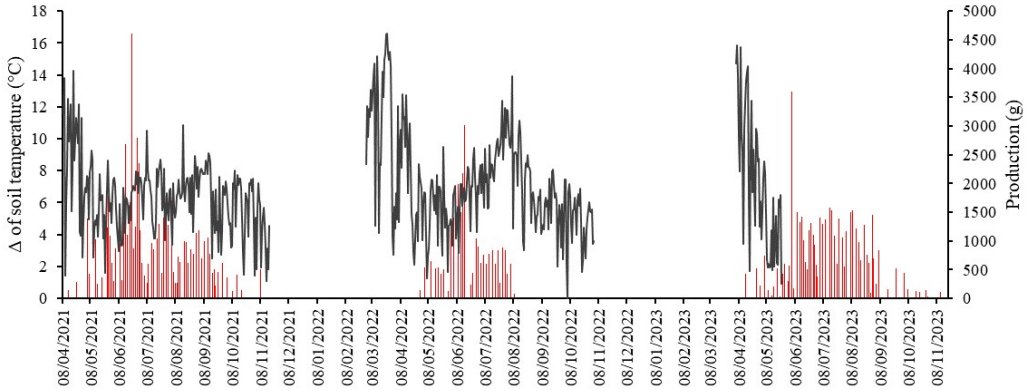

B

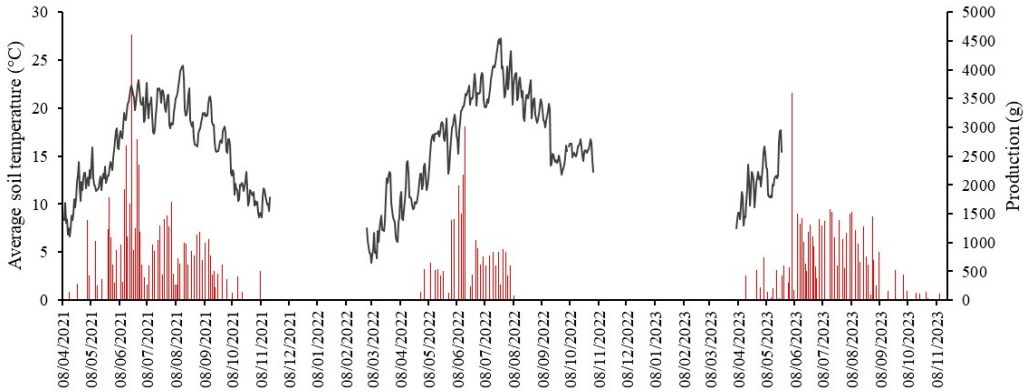

Figure 17: production trend compared to the soil temperature difference (A) and average temperature (B). The columns in red represent the production of the whole truffle orchard, while the lines in black respectively the difference of soil temperature and the average temperature of the soil. The temperature difference decreases during the summer season, while the average temperature increases.

Soil moisture is expected to significantly influence mushroom and truffle production, as suggested by literature and traditional truffle cultivation techniques. However, the graphs in Figure 18 reveal that, among all the parameters considered so far, soil moisture has the least impact on production. There is no observable correlation between the two variables, whether it is the average soil humidity on the day of harvest (A), the temperature difference on the day of harvest (B), the average humidity in the 7 days before harvest (C), or the maximum difference of humidity in the 7 days before the harvest (D).

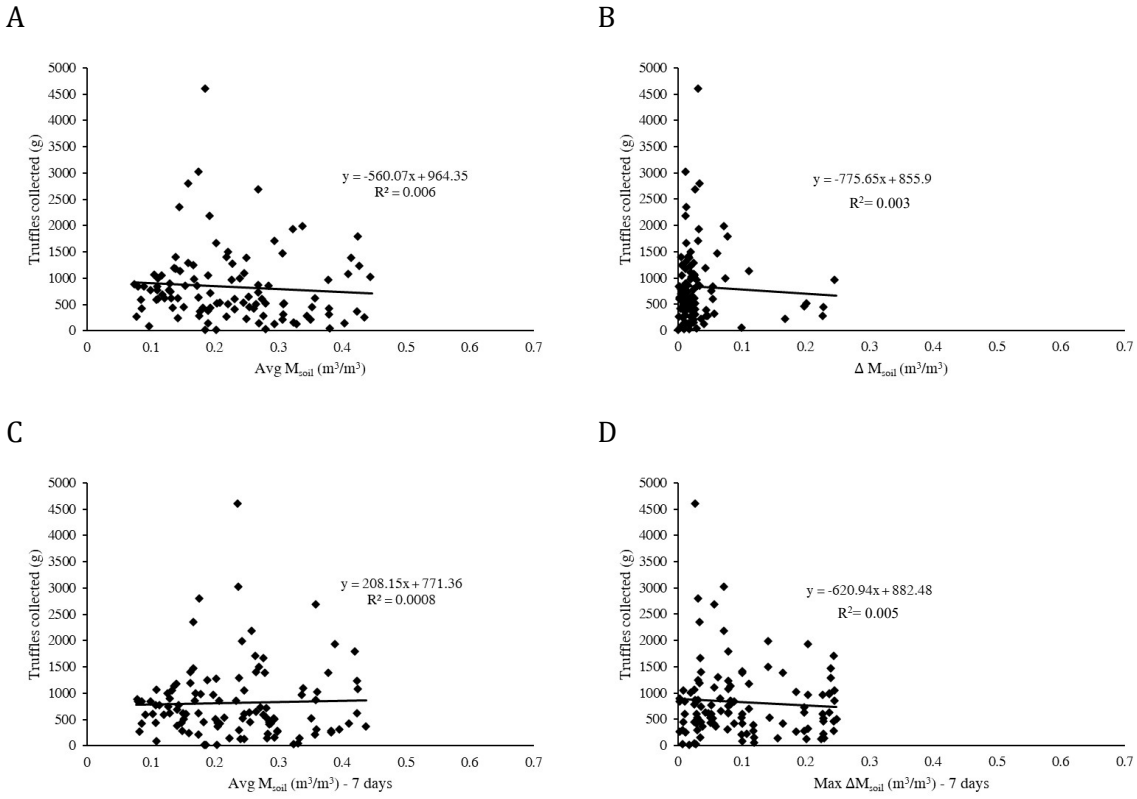

Figure 18: correlation between production and soil moisture. In graph A correlation between production and average soil moisture on the day of harvest, in graph B with the soil moisture difference on the day of harvest, in graph C the average humidity of the 7 days before the harvest and in graph D the maximum daily difference of humidity reached during the 7 days before the harvest. Humidity data were obtained by averaging the data of the 2 TDR installed. The production values refer to the whole truffle orchard.

For VPD (vapor pressure deficit) as well, I considered the average value on the day of collection, the maximum value on the day of collection, and the difference of VPD on the day of collection. In all these cases, the correlation seems to be slightly positive (Fig. 19).

The best result, however, was obtained by considering the weekly production in relation to the maximum difference of VPD reached during the week. A high difference of VPD indicates that the plant must adapt to a change in air humidity, which could lead to more or less transpiration. To adapt to these changes, also in this case, the plant must osmoregulate. It needs to accumulate osmotically active compounds to maintain a constant flow of water or reduce them to rebalance the difference in water potential between leaves and roots. This may suggest that production is influenced in some way by the plant's reaction to changes in environmental parameters, rather than by a direct response of the fungal organism.

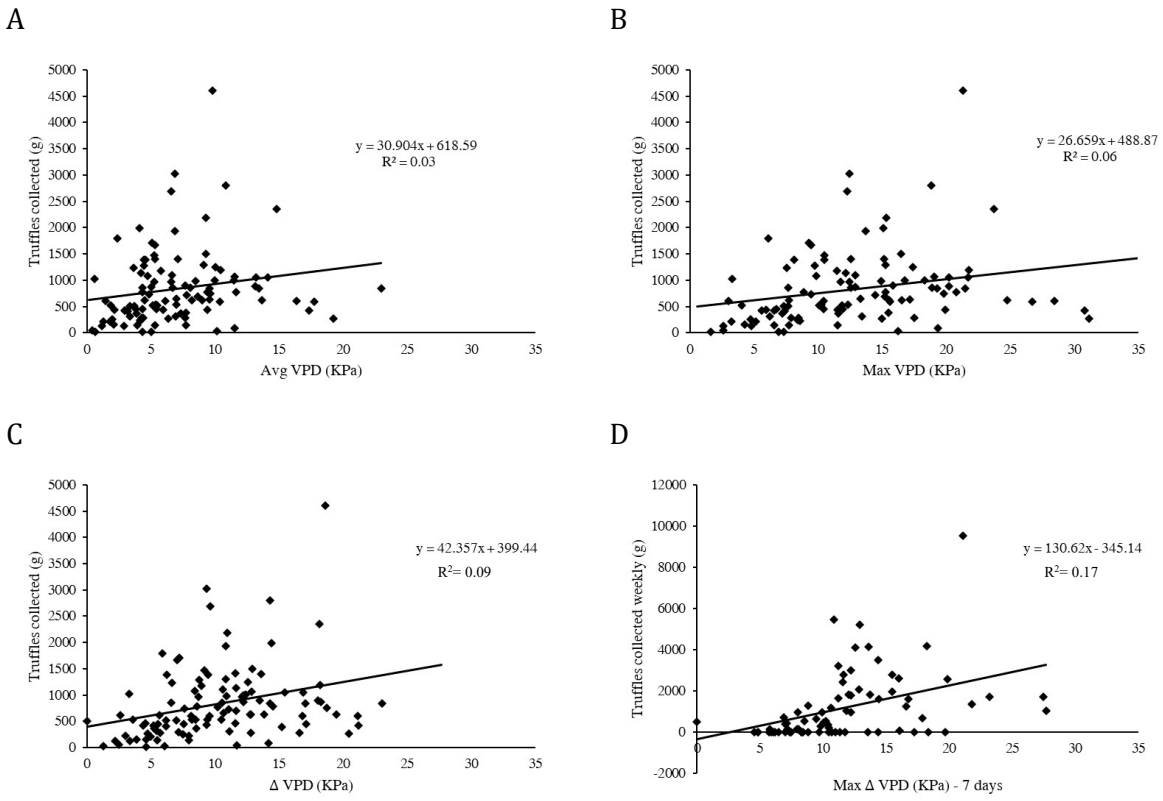

Figure 19: correlation between production and VPD. In graph A is the correlation between production and average VPD of the day of collection, in graph B the maximum VPD on the day of collection, in graph C the difference of VPD on the day of collection and in graph D the weekly production with the maximum weekly difference reached. Graph D reaches a value of R^2 higher than the others.

3.1.3 Productive and non productive plants' status and physiological parameters in Caltrano

At the truffle orchard in Caltrano, with the expertise of the truffle farmer, productive plants (producing truffles and thus mycorrhized) and non-productive plants (under which no truffles are harvested and, therefore, are not mycorrhized) have been distinguished.

Detrending the series become even clearer that non-productive plants have wider fluctuations: this means that they experience greater dehydration peaks than productive ones, and that the latter can better control water loss (fig. 20).
In 2021 (Figure 20A), oscillations are relatively limited throughout the initial part of the season, significantly increasing in September when soil moisture levels experience a sharp decline (Figure 13). Following this drought phase, productive plants return to low dehydration levels, while non-productive plants consistently maintain elevated peaks.
In 2022 (Figure 20B), dehydration levels increase in the middle of the season, with productive plants reaching peaks comparable to non-productive plants. This occurs as soil moisture values reach their absolute minimum (Figure 13). While plants recover in September, the productive ones do not return to zero, in contrast to non-productive plants that maintain wide oscillations. In 2023 (Figure 20C), with a shorter timeframe, a similar trend is observed, wherein non-productive plants exhibit significant fluctuations, while productive plants appear to better regulate dehydration levels.

A

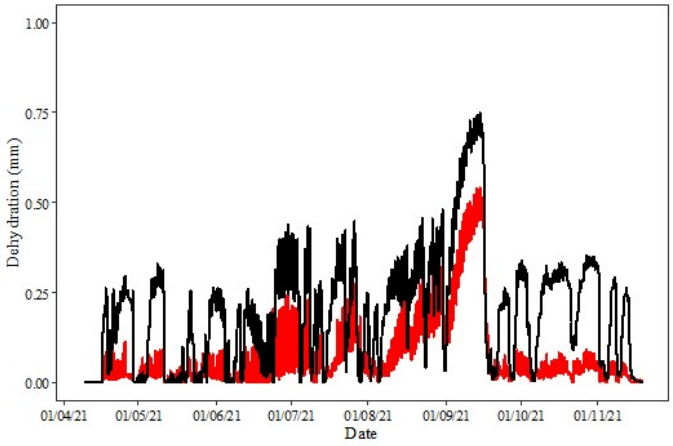

B

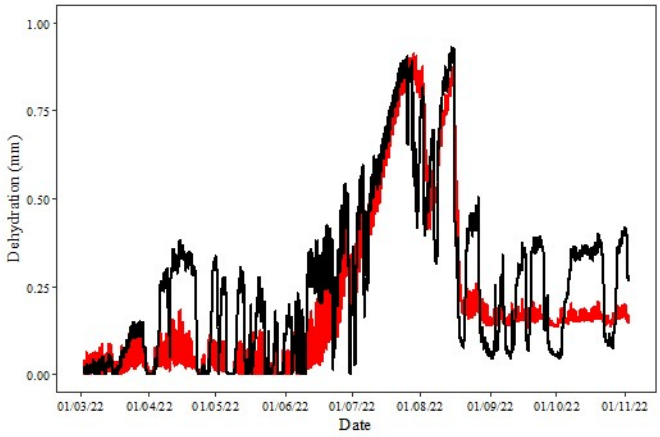

C

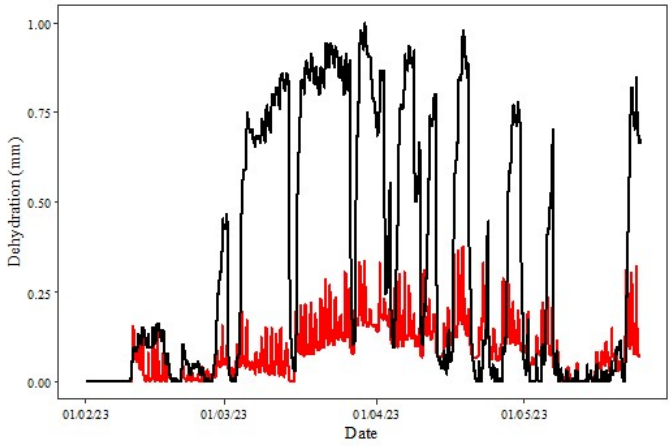

Figure 20: The graphs show the levels of dehydration of productive (red) and non-productive (black) plants expressed as reduction of stem radius in millimeters. The values were obtained by detrending the target plant data and averaging between 3 productive and 3 non-productive plants. In all years (2021-A, 2022-B and 2023-C) productive plants variations are much more limited than non-productive plants. In all 3 cases the Wilcoxon signed rank test for paired samples shows a p-value < 2.2e-16.

To conduct a more in-depth analysis of the dehydration data, it would be beneficial to present them alongside sapflow data.

In 2021, before the onset of production (Fig. 21 A), the variations in dehydration levels are more limited for productive plants compared to non-productive ones, which have already started to dehydrate more. Daily variations in sapflow levels are also limited. The situation changes when plants enter full production (Fig. 21 B). Specifically, June 21, 2021, coincides with the peak of production. During this period, the variations recorded by the dendrometers increase, and particularly between June 21 and 22, the levels of dehydration become higher. While non-productive plants dehydrate without recovering, productive plants recover completely (return to 0). Sapflow trends at this stage are also more regular. As production ends around September (Fig. 21 C), daily variations in dehydration levels become more limited, and the period of the day when sapflow is active is shorter than in previous months.

In 2022, a very dry year, the data in the first part of the season (Fig. 22 A) are very similar to those of 2021, with moderate fluctuations in dehydration values and limited variations in sapflow levels. During the peak of production (Fig. 22 B), the oscillations of the plant radius increase, but in this case, the productive plants are not able to fully recover, unlike what happened in 2021. In 2022, as mentioned earlier, production is slightly lower than in 2021.

Starting from 2022, there is a coupling between the sap flow data of productive and non-productive plants. This issue likely arose due to the system's difficulty in heating the probes, caused by shading from the photovoltaic panel due to the growth of branches and leaves. As a result, meaningful sapflow comparisons between productive and non-productive plants are not possible from June 2022 onwards.

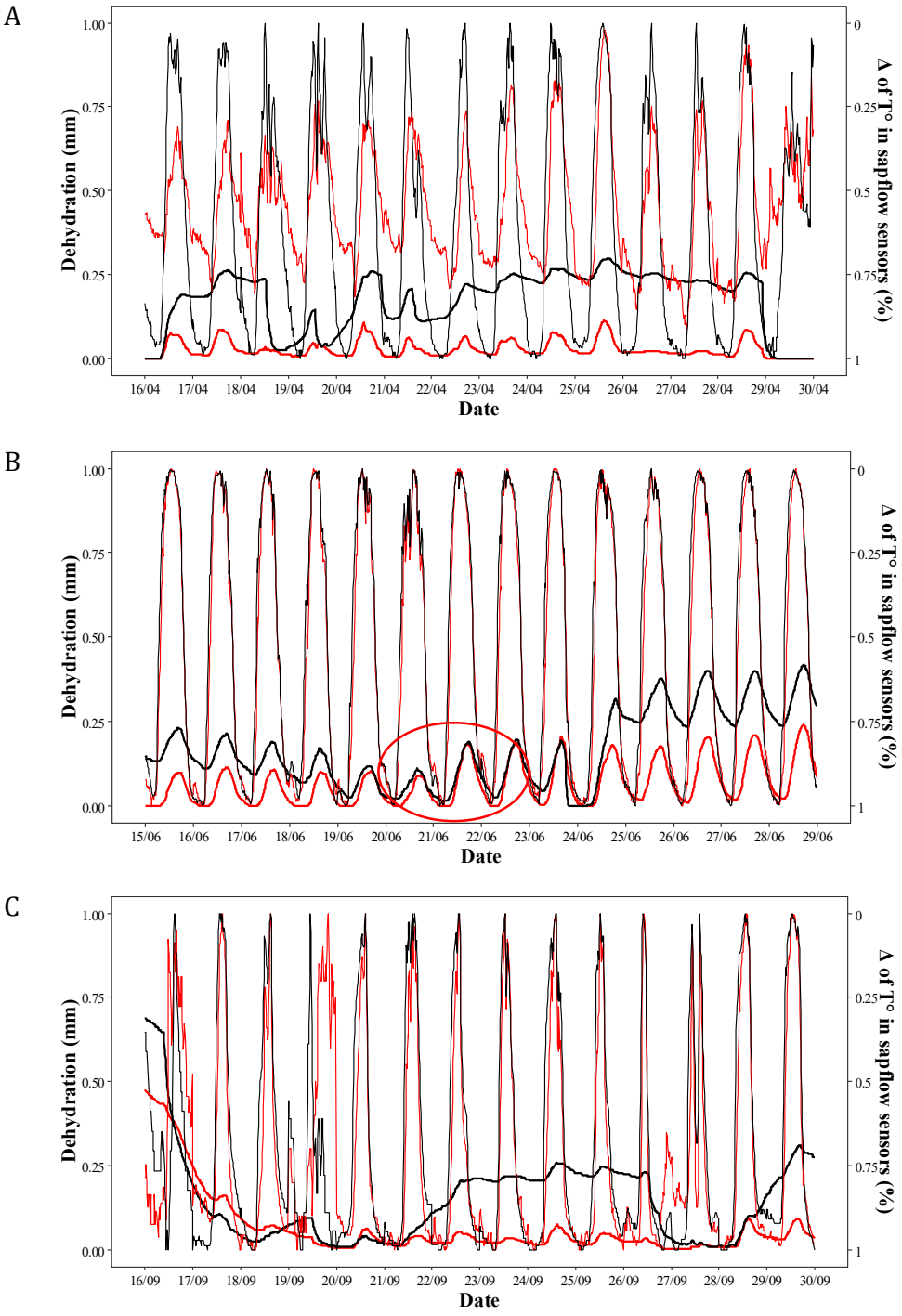

Figure 21: The bold red line represents the oscillation of the dendrometers for productive plants in 2021, while the bold black line represents non-productive plants. The red thin line shows the temperature difference of the Granier sensor probes, indicating the sapflow of productive plants, and the thin black line represents non-productive plants. In the first part of the season when production is not yet active (A), the fluctuations in the radius of productive plants are minimal, and sapflow levels are lower than those of non-productive plants. During the peak of production (B), the oscillations become wider, and the sapflow becomes more regular. At the end of the production season (C), the oscillations return to being limited for productive plants.

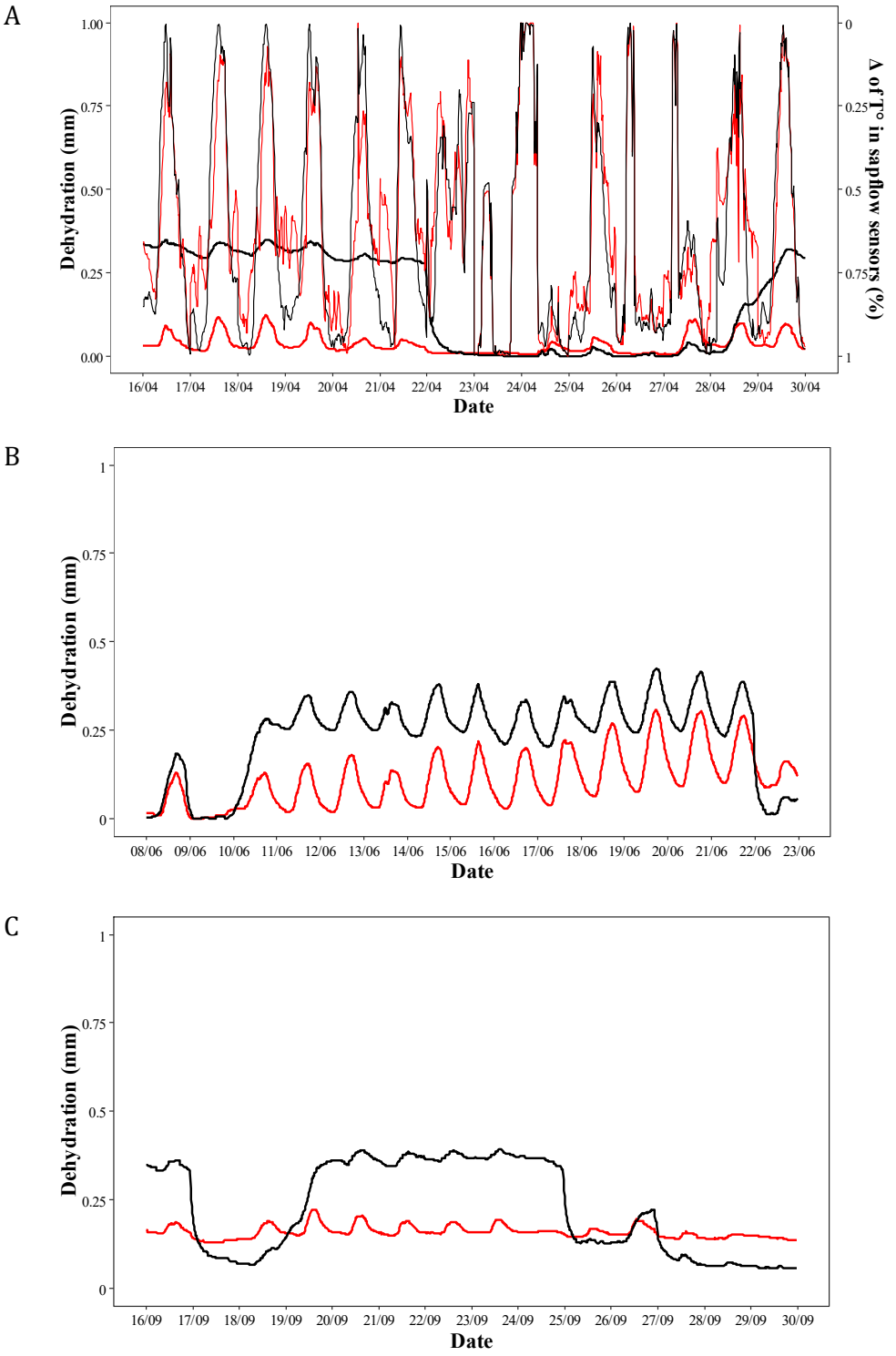

Figure 22: the bold red line represents the oscillation of the dendrometers for productive plants in 2022, while the bold black line represents non-productive plants. In panel A, the thin red line represents the temperature difference of the Granier sensor probes, indicating the sapflow of productive plants, and the thin black line represents non-productive plants. In this case, during the first part of the season (A), productive plants exhibit very limited daily variations, contrasting with non-productive plants. The sapflow is quite irregular. During the production peak (B), changes in hydration levels increase, and at the end of production (C), the productive plants can no longer recover the previous levels of hydration.

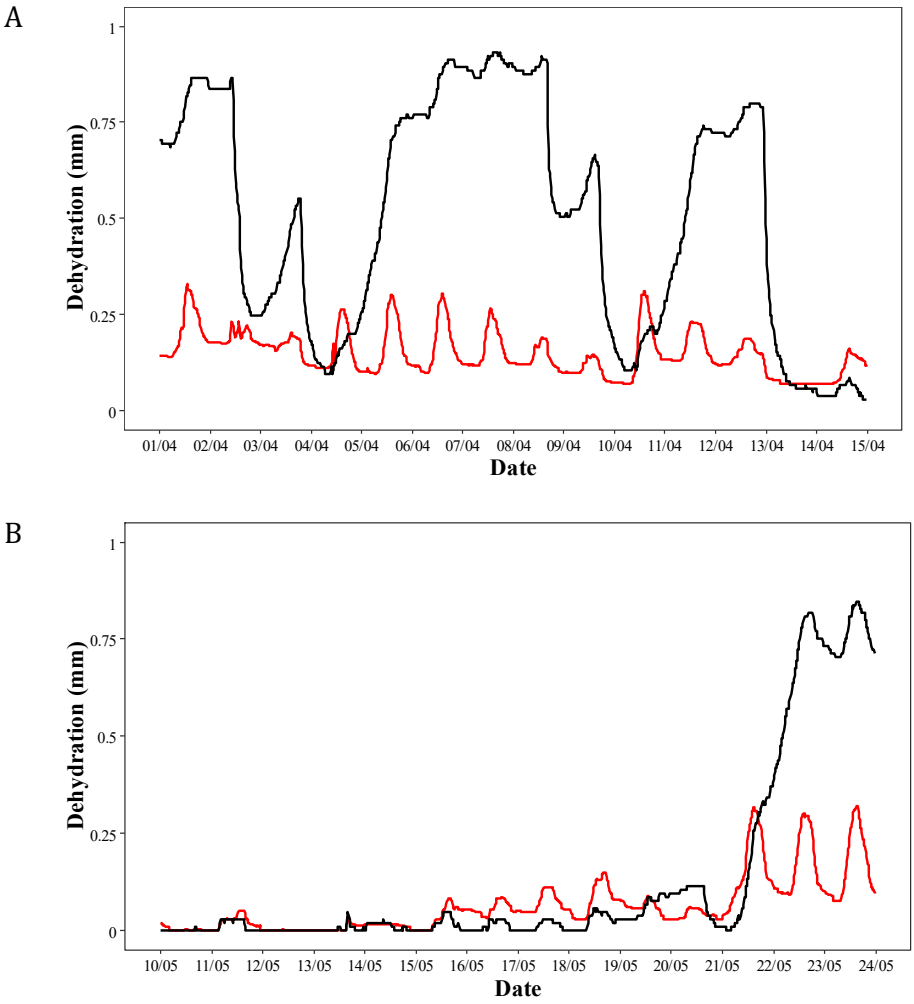

Figure 23: the bold red line represents the oscillation of the dendrometers for productive plants in 2023, while the bold black line represents non-productive plants. Both in graph A (pre-production period) and graph B (start of production period), dehydration levels remain limited in productive plants and wider in non-productive plants.

In 2023, changes in hydration levels remain higher in non-productive plants. However, unlike other years, productive plants also experience a certain degree of dehydration in April (Fig. 23 A), even though the soil moisture is comparable to that of the previous year (Fig. 13). In May (Fig. 23 B), between the 15th and 19th, the situation even reverses for a few days, showing higher levels of dehydration for productive plants. This change could potentially be an effect of the extreme stress experienced in the previous year.

For sapflow sensors, collected and processed data can initially suggest conflicting information. Specifically, in April 2021 (Figure 24, Graph A), it appears that the flow of productive plants remains constant during the night (when non-productive plants do not show flow signals), while during the day there is a small peak, which, however, is more contained than in non-productive plants. In June and September, it might seem that non-productive plants activate their flow earlier in the day compared to productive ones, suggesting greater efficiency (Figure 24, Graphs B and C). However, both groups reach the peak at the same time, and during the sapflow reduction, the curves of productive and non-productive plants overlap. It is essential to note that, as revealed by dendrometer data, productive plants exhibit higher osmoregulatory capacity.

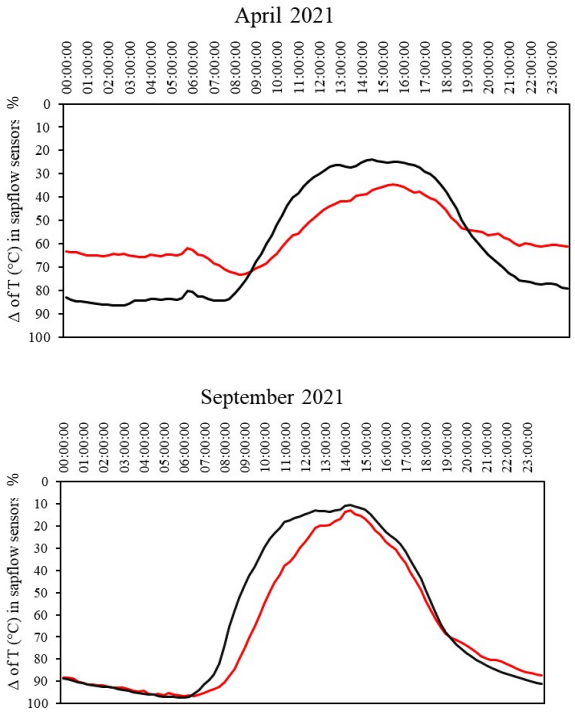

Figure 24: The graphs show the daily flow for productive plants (in red) and non-productive (in black), in the 3 moments of the production season: before its beginning (April), during the peak (June) and at the end (September). In April 2021 (Graph A) it appears that variations in the flow of productive plants (in red) are particularly small compared to non-productive plants (in black). Especially non-productive plants reach higher levels of flow. In June (Graph B) and September (Graph C) the flow peaks between the two groups are nearer, but always showing a later activation of the flow in the productive than non-productive. The flow levels of the productive ones are more limited regarding the not productive ones. The data presented were obtained by calculating the percentage of flow (given every 15 min) based on the daily minimum and maximum. Subsequently, the average was calculated between the values of 3 target productive plants and 3 target non-productive plants.

In April 2022 (Figure 25), a pattern similar to April 2021 is observed, with a small peak in the early hours of the day and then a subsequent peak in the afternoon. Activating the flow in the early hours could be a strategy to limit transpiration in the middle of the day. Moreover, the fact that the flow line of productive plants remains below that of non-productive plants during the central hours of the day suggests a less urgent need to activate the flow by productive plants, indicating greater efficiency in concentrating transpiration in the early morning hours.

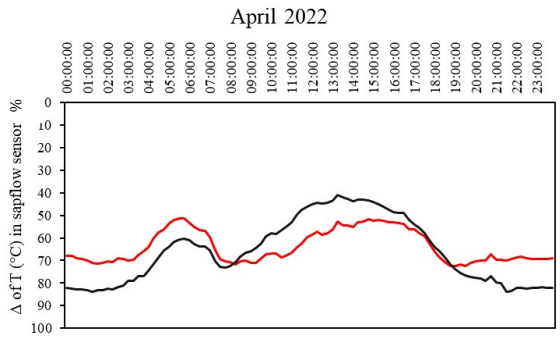

Figure 25: The graph depict the daily flow trend for productive plants (in red) and non-productive plants (in black) before the beginning of truffle production (April). The trend is similar to that observed in 2021, showing a small peak in the early morning when the stomata open, followed by a second peak in the afternoon. However, the flow levels of the productive plants remain lower compared to those of the non-productive ones.

A more detailed analysis of sapflow cycles during the peak production in 2021 (Figure 26) reveals a small nocturnal peak, more pronounced in productive plants than in non-productive ones. This is unusual, as plants typically transpire when the stomata are open during the day. Another notable feature is the shift in the activation of sapflow. It appears that non-productive plants initiate sapflow earlier compared to productive plants. They peak together in the middle of the day, and then the flow is reduced equally for both groups.

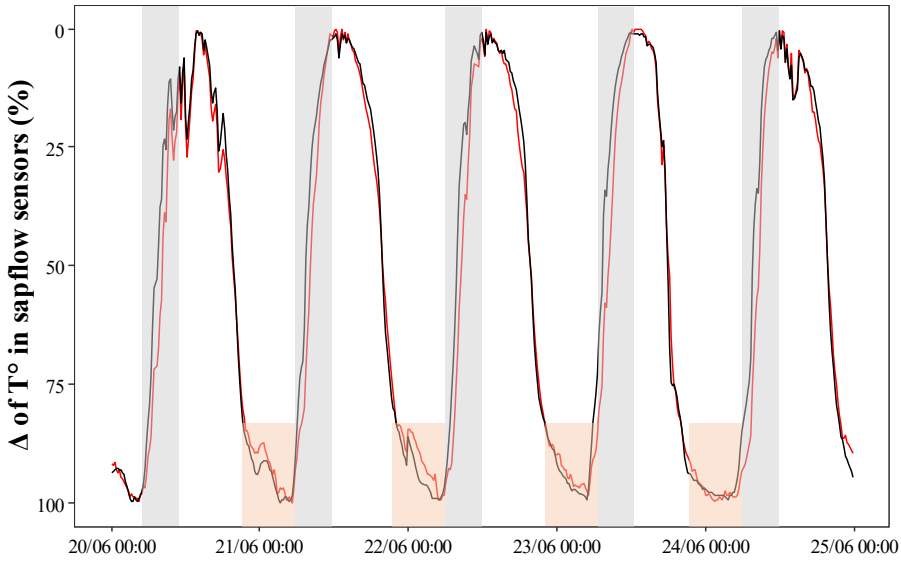

Figure 26: Analysis of sapflow performance for productive plants (red) and non-productive plants (black) during the peak production in June 2021. The values are derived from the average data of 3 productive plants and 3 non-productive plants. The grey shading represents the deviation between the two curves, while the pink shading indicates the night peak of sapflow. Initially, it appears that sapflow is activated later in productive plants.

It appears that non-productive plants have a greater capacity for transpiration. However, as shown earlier (fig. 20), productive plants are more hydrated. Given that the ability to cope with drought is closely related to the capacity for osmoregulation through the accumulation of sugars in tissues, it is crucial to investigate whether there are differences in the physiological structure of plants.

A B C

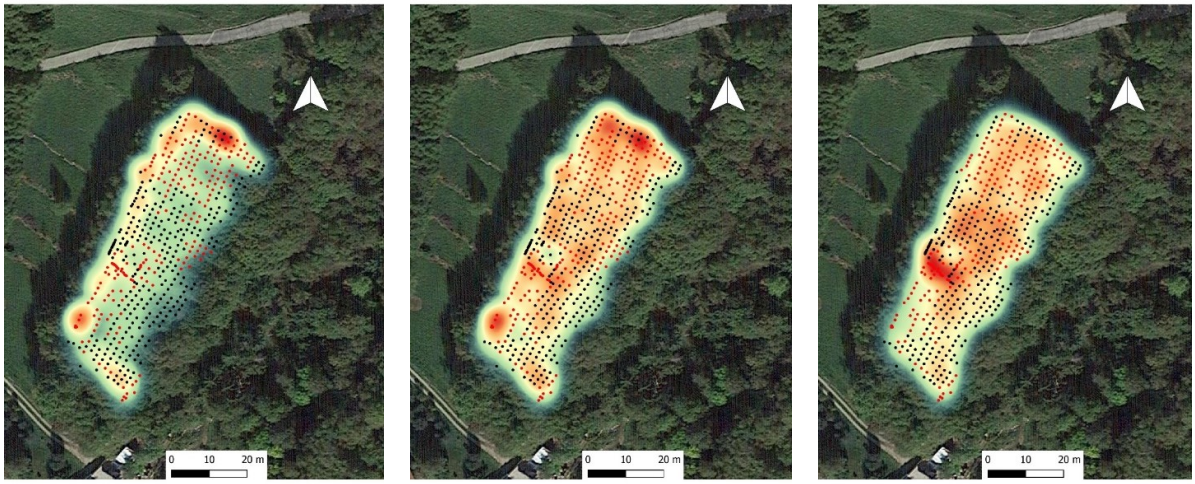

Figure 27: The red dots on the map represent the productive plants within the truffle orchard, while the black dots represent the non-productive plants. The map colors range from lower (colder) to higher (warmer) values. In Graph A, the crown volume is depicted, in Graph B, the trunk volume, and in Graph C, the height.

In the truffle orchard, plants with larger canopy volumes are situated along the north and west sides, corresponding to the areas where the truffle orchard borders the meadow (Figure 27A). It doesn't appear that the groups of productive plants are localized solely in areas with greater foliage growth; instead, they are dispersed across areas with smaller foliage as well. The distribution of trunk volumes seems more uniform in the truffle orchard, along with the distribution of heights (Figure 27B and C).

The biomass of woody plant species is predominantly composed of dead mass (Vanninen et al., 1996), which does not contribute to the metabolic functions of the organism. The greater the crown-to-stem volume ratio in favor of the part that photosynthesizes, the more it is reasonable to expect a surplus of sugar (and therefore carbon not stored in the form of wood). It raises the question of whether productive plants, with the same crown volume, could produce more sugar due to their greater height, potentially making them dominant over non-productive plants.

For the construction of the linear model, edge plants are excluded from consideration to obtain a more homogeneous sample in terms of crown distribution.

The results do not indicate differences in the ratio between crown volume and stem volume (Figure 28) and between canopy volume and height (Figure 29); the two groups are equivalent.

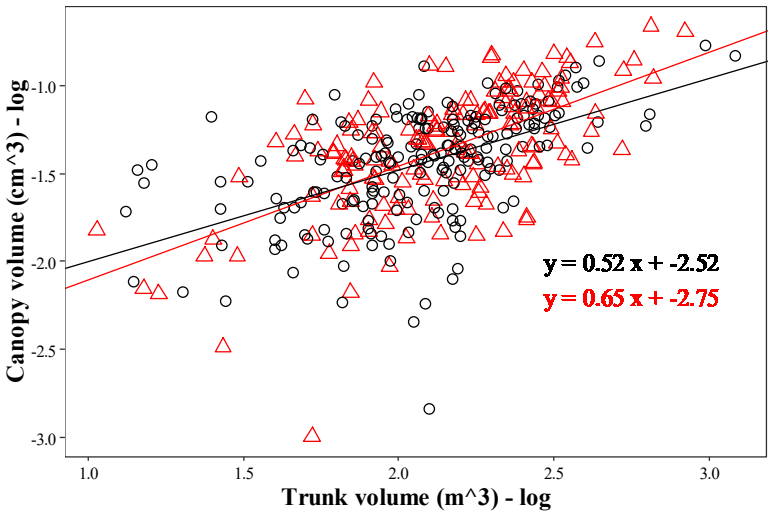

Figure 28: The ratio between crown volume and stem volume is displayed in log-log scale, with productive plants represented in red and non-productive plants in black. The differences between the groups are not statistically significant (p-value from linear model regression = 0.25).

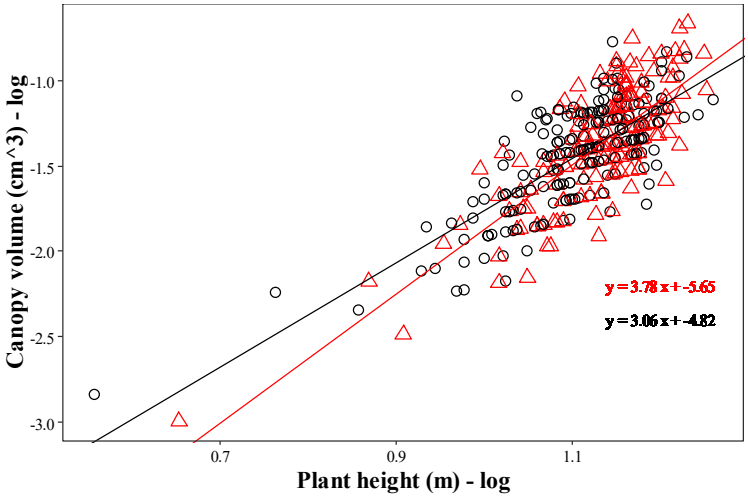

Figure 29: The relationship between the volume of foliage and height is depicted in log-log scale, with productive plants shown in red and non-productive plants in black. The differences between the two groups are not statistically significant (p-value from linear model regression = 0.33).

In September 2022, pre-dawn leaf water potentials were measured for both productive and non-productive plants to assess potential differences in nocturnal recovery.

The results indicate no statistically significant difference in pre-dawn leaf water potential between the two groups (fig. 30). Although the leaf water potentials are generally very low (<-1 MPa), there is increased variability in the potential of non-productive plants, although the groups cannot be considered distinctly different.

Additionally, leaves were collected and their weight, leaf water potential as they dehydrated in the air, and dry weight were measured. This was done to determine potential differences in the ratio of potential to water content during dehydration. The relationship between leaf water potential and water content appears to be consistent between productive and non-productive plants (fig. 31).

This reaffirms the earlier observation in figure 30 that there are no significant differences in leaf water potential between the two plant groups.

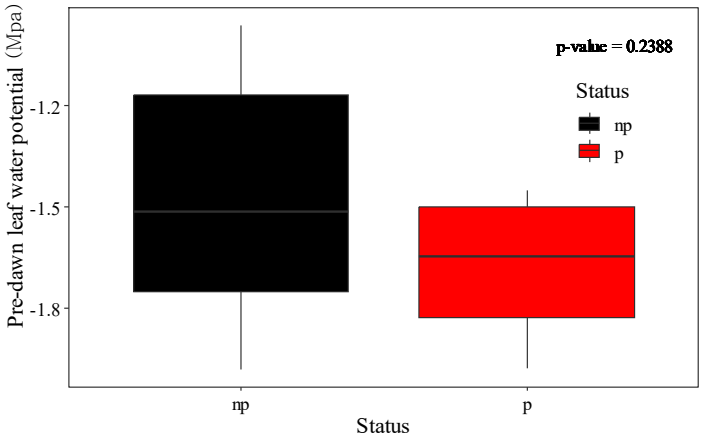

Figure 30: The figure displays pre-dawn leaf potential values, with non-productive plants represented by black and productive plants by red. Both groups exhibit low leaf water potential (Ψ) values, and the p-value of 0.24 confirms that there are no statistically significant differences between them.

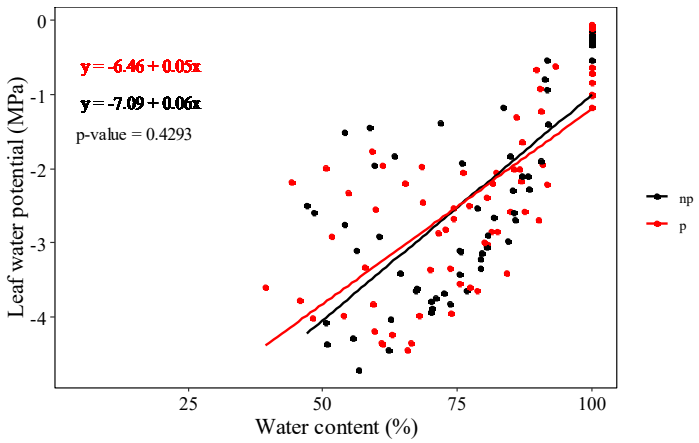

Figure 31: The graph illustrates the relationship between leaf water potential and water content, with productive plants depicted in red and non-productive plants in black. The analysis indicates no statistically significant difference between the two groups.

Certainly, the ability of productive plants to better control dehydration may be attributed to their efficient allocation of resources, potentially including the accumulation of sugars in various organs. This sophisticated resource management could contribute to their resilience in maintaining optimal hydration levels.

3.1.4 Differences in physiological response in two parts of forest in Carlino affected by different levels of aquifer

At the Carlino site, a discernible contrast exists in the soil water content. This is likely due to the different height of the soil profile between the erstwhile production segment and the non-productive sector (refer to Figure 32). Specifically, the aquifer height in the former production site is lower, whereas in the non-productive area, it registers as higher. This discrepancy implies that vegetation situated in the non-productive section may experience comparatively enhanced accessibility to water resources, particularly during periods of drought.

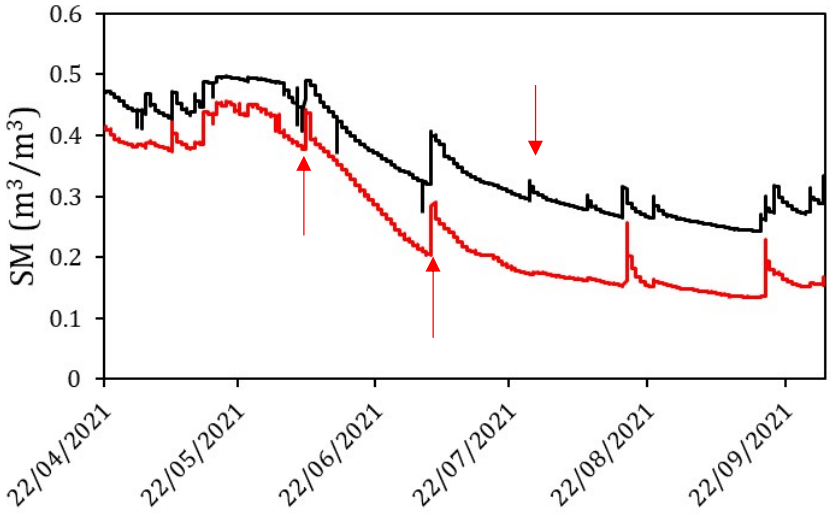

Figure 32: soil moisture trend throughout the summer season of 2021. Notably, the values for the former production sector (depicted in red) are lower compared to those for the non-productive area (depicted in black). These values are derived from the averaging of data collected by two Time Domain Reflectometry (TDR) sensors strategically positioned at distinct depths within the respective forest sections. Peaks observed in the graph align with precipitation events. The arrows indicate 5 June, 4 July and 8 August, focus dates in the description of site dynamics

Throughout the month of June, notable disparities in hydration and dehydration cycles of plants between the two areas are not prominent (see Figure 33 A). However, it is noteworthy that, despite the higher aquifer levels, plants in the non-productive area often exhibit elevated levels of dehydration during this month. This discrepancy becomes more pronounced in July (see Figure 33 B) and intensifies further in August (see Figure 33 C).

On specific dates, such as June 5th and July 4th, there were discernible peaks in soil moisture levels (refer to Figure 32), corresponding to a reduction in dehydration peaks as depicted in Figure 2. At June 5th (Figure 33A) and July 4th (Figure 33B), hydration increases, especially in the production area (in red) in June. Moreover, during the season the plants of the non-productive area dehydrated more than those of the former production area (Figure 33C).

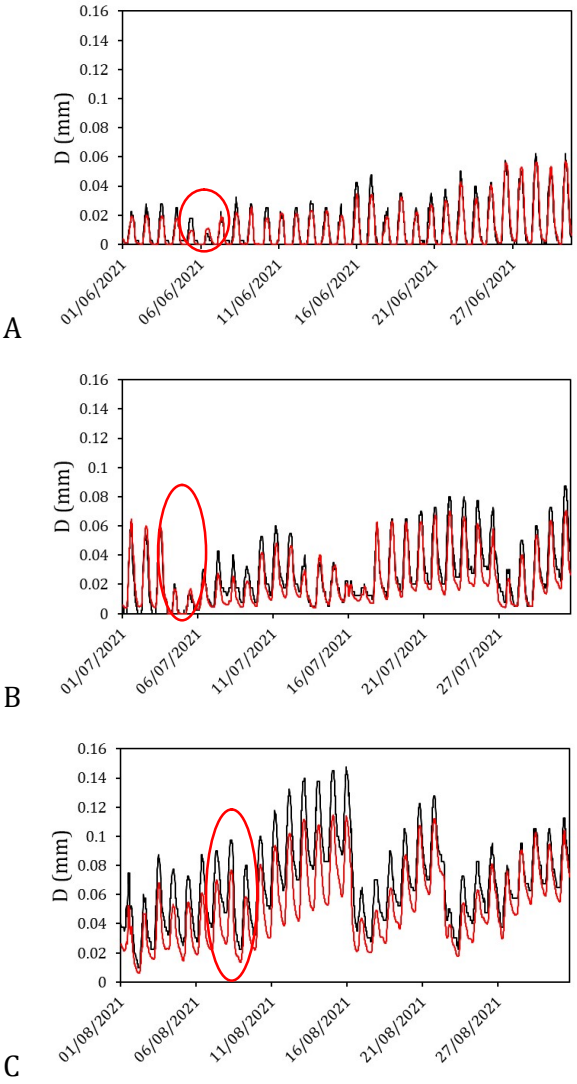

Figure 33: dendrometer trends observed throughout the 2021 season. In this representation, dehydration values for plants in the former production area are presented in red, while values for plants in the non-productive area are shown in black. These values were derived by detrending the series, accounting for the increase in diameter due to growth, and subsequently averaging the data from individual dendrometers. Graph A corresponds to the month of June, graph B illustrates trends in July, and graph C portrays the dynamics observed in August. The color-coded presentation facilitates a visual comparison of dehydration patterns between the two areas across these specific months. The circles indicate 5 June, 4 July and 8 August, focus dates in the description of the site dynamics

On August 8th, 2021, a notable peak in soil moisture was exclusively recorded on the non-productive side (Figure 32), resulting in a reduction of dehydration levels, as illustrated in Figure 33 C. Despite this isolated event, the disparities between the former production area and the non-productive area persist prominently throughout the month of August.

On July 4th, a day characterized by increased water availability, an alignment in the flow dynamics of plants from both parts of the forest is discernible. On other days, there appears to be a tendency for the "productive" plants to initiate sapflow later and close stomata at a delayed pace. This observation extends into the month of August, where, similar to the case in Caltrano, the former productive plants often exhibit a sustained minimum level of nocturnal flow (Figure 34).

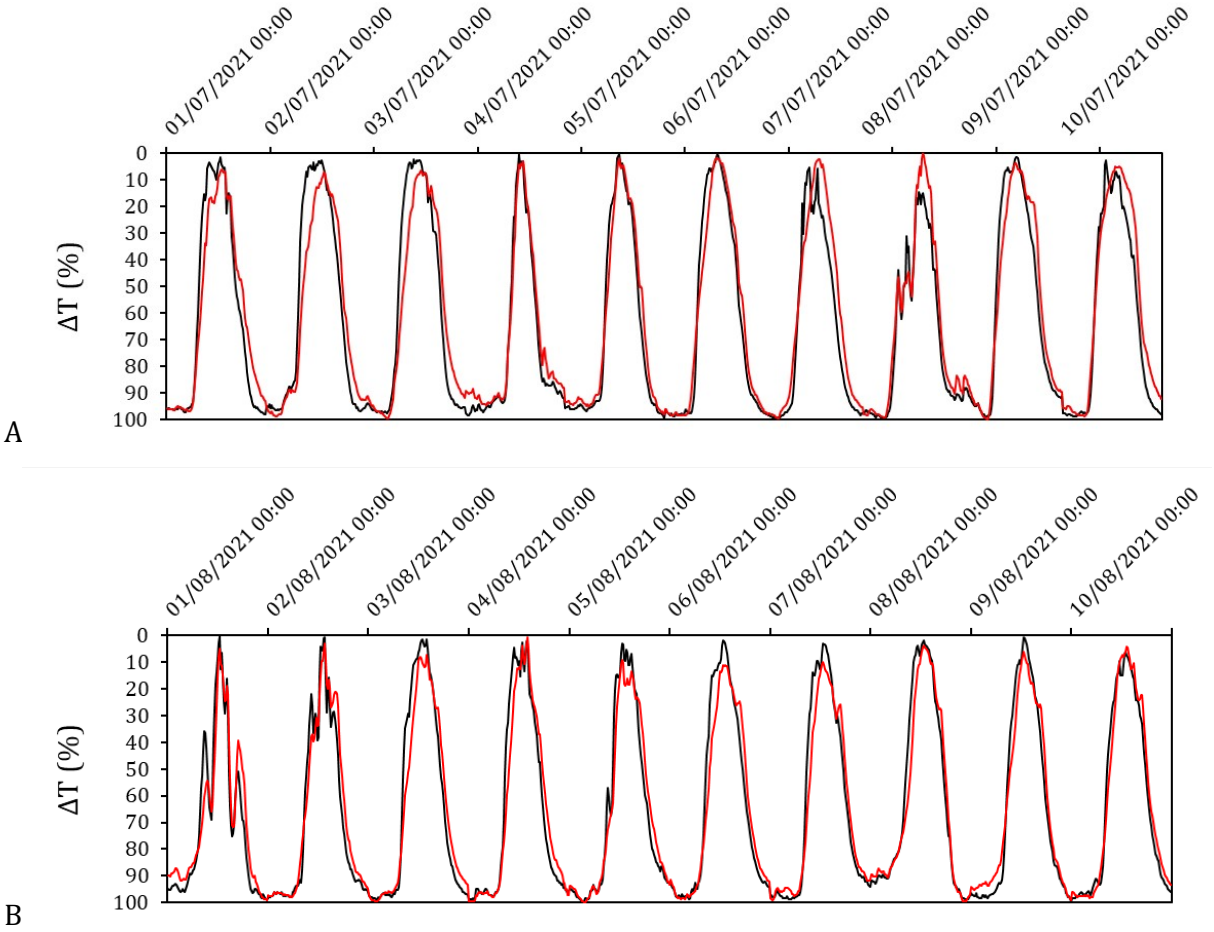

Figure 34: sapflow dynamics during the initial ten days of July (Graph A) and the first ten days of August (Graph B) for plants in both the former production area (depicted in red) and the non-productive area (depicted in black). A small delay merges between the two curves, suggesting that former productive plants tend to reach their sapflow peak at a slower rate and exhibit a delayed closure of stomata when compared to their non-productive counterparts.

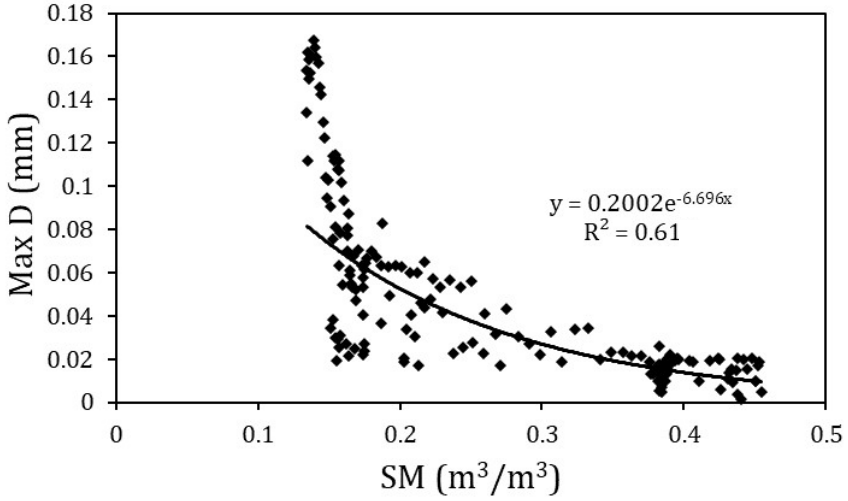

Figure 35: relationship between maximum daily dehydration (D) and soil moisture (SM). Notably, dehydration levels exhibit constancy up to a critical threshold of approximately 0.3 m^3/m^3. Beyond this threshold, there is an exponential increase in dehydration levels, highlighting a significant relationship between soil moisture content and the observed dehydration patterns.

The dehydration levels exhibit stability up to a critical threshold of approximately 0.3 m^3/m^3, beyond which there is an exponential escalation in dehydration: when the humidity drops below 0.2 the plant can no longer recover hydration and continues to have high levels of dehydration (Figure 35). Upon reaching the 0.3 threshold, plants encounter challenges in regulating dehydration. Notably, for the former production area, this threshold is surpassed towards the end of June, while for the non-productive segment, it occurs in August, as depicted in Figure 32. Despite the similarity in the amplitude of daily fluctuations in soil moisture levels during August, plants in the production area demonstrate a more effective control over dehydration throughout the season, as illustrated in Figure 33.

In the dataset for 2022, spanning from late July to late August, the disparity in soil moisture levels is sustained, attributable to variations in aquifer depth (Figure 36). Unfortunately, no other data are available due to damage to the technical equipment, caused by wildlife activity and some wind damage. Noteworthy hydration peaks in the soil are observed, such as on July 26th, where an increase in soil moisture is recorded in both forest sections. However, this increase does not manifest evident effects on hydration and dehydration cycles, except for a minor peak in dehydration, as indicated in Figure 37. The unique and highly restricted nature of the observed cycles during this period may be attributed to the extreme drought conditions, as daily cycles are markedly narrow compared to those observed in 2021. The

slight peak in dehydration might signify the plants' attempt to initiate transpiration in response to the modest increase in water availability. Analysis of the flow patterns during this period suggests that plants are still maintaining active sapflow (see Figure 38). However, examination of the daily oscillation ranges of dendrometers reveals a significantly constrained fluctuation, which means that the plant is experiencing a situation of severe water shortage (Figure 37).

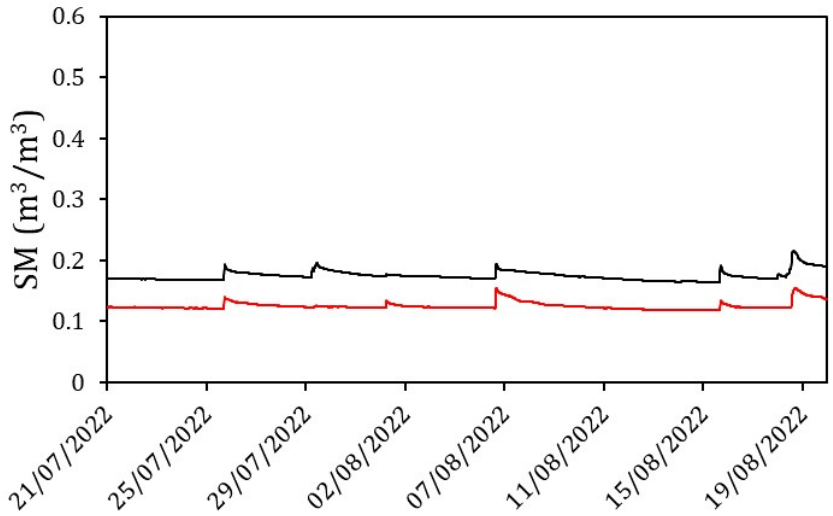

Figure 36: progression of soil moisture levels between July and August 2022. Notably, values for the former production area (depicted in red) are lower compared to those for the non-productive area (depicted in black). These values were computed by averaging data from two Time Domain Reflectometry (TDR) sensors strategically positioned at different depths in the respective forest sections. Peaks in the graph align with precipitation events.

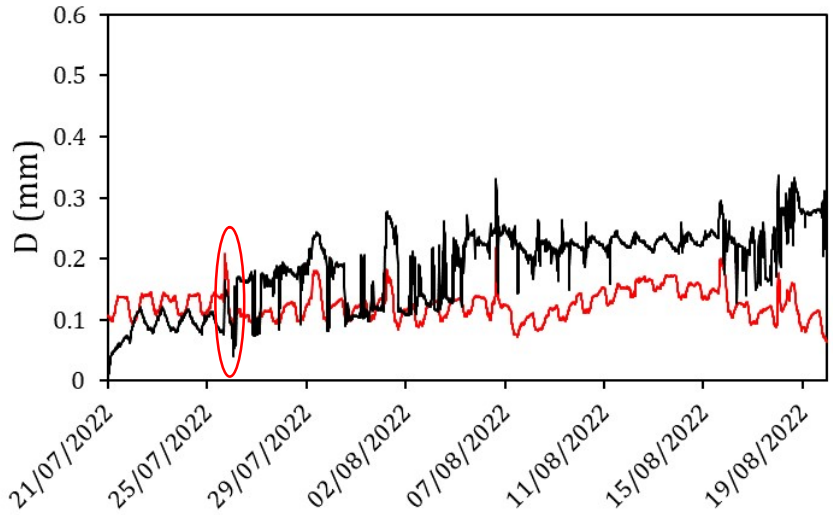

Figure 37: dendrometer trends observed between July and August 2022. Dehydration values for plants in the former production area are depicted in red, while those for plants in the non-productive area are represented in black. These values were derived by detrending the series, accounting for the increase in diameter due to growth, and subsequently averaging the data from individual dendrometers.

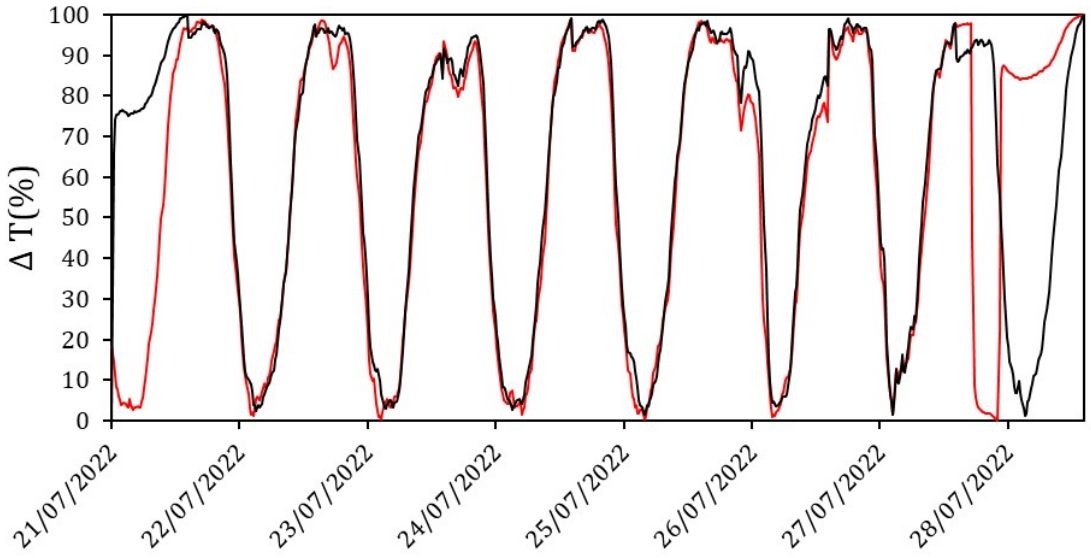

Figure 38: sapflow performance during the final week of July 2022. Notably, there are no discernible differences between the plants in the former productive zone (illustrated in red) and the non-productive zone (depicted in black). Despite extremely low soil moisture levels, plants in both areas exhibit an attempt to engage in photosynthesis. This observation raises the possibility that plants may be accessing deeper soil water through their root systems to sustain essential physiological processes.

By applying a linear regression model it was possible to compare the relationship between leaf water potential and water content in plants from the former production area and the non-productive area, revealing no statistically significant differences (figure 39). Nevertheless, it is noteworthy that, at equivalent water content levels, plants in the former productive area tend to exhibit less negative leaf water potential than their counterparts in the non-productive area, despite the lower aquifer level in the former. In addition, the relative water loss (compared to the full turgor) could be lower in non-productive.

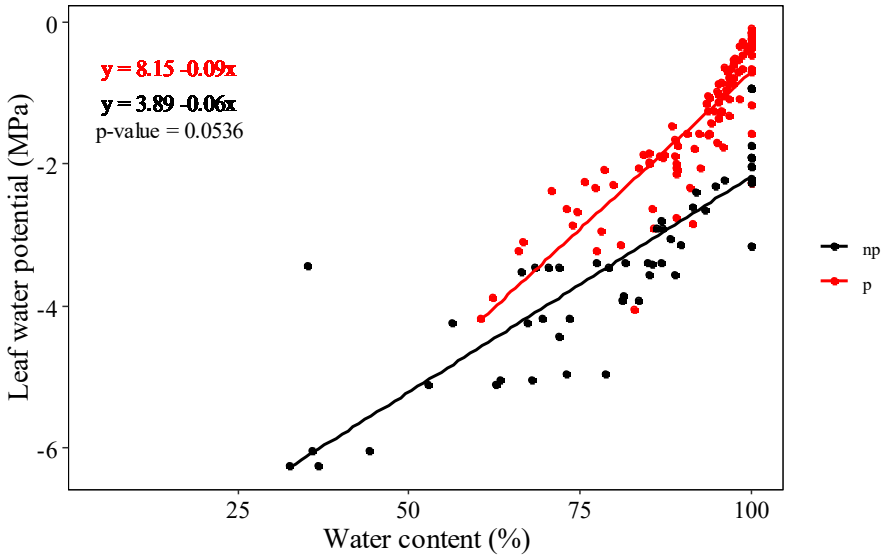

Figure 39: relationship between leaf water potential (Ψ) and relative water content for former productive plants (depicted in red) and non-productive plants (depicted in black). Despite the apparent difference in leaf water potential at the same hydration level, statistical analysis indicates no significant difference between productive and non-productive plants.

3.2 Laboratory experiment

This section presents the data related to the two laboratory experiments, the one using *Zea mays* L. and the one with *Quercus ilex* L.

3.2.1 Laboratory experiment using *Zea mays* L.

Preliminary experiment

Figure 40 presents the preliminary findings from the 2019 experiment. In this experiment, due to the programming of the climate cell, the plants were subjected to the recovery phase during the night hours, when the stomata were closed, and the cells could rehydrate. Sampling took place during the pre-dawn phase.

In graph 40-A, the carbon content of hydroponic solutions used for maize cultivation is illustrated. The red columns represent carbon content during the stress phase, while the black columns represent the recovery phase. Notably, the release of carbon in the recovery phase is significantly higher in stressed plants (exposed to peg 200 and peg 400) compared to plants in the control group, where such release is absent as these plants consistently remain in the nutritional solution.

Figure 40-B reveals the relationship between the electrical conductivity of solutions and carbon content, indicating that conductivity can serve as a reliable predictor of actual carbon content (R^2=0.85).

Figure 40-C displays the osmolality of both root and foliar liquids during the stress phase (depicted in red) and the subsequent recovery phase (depicted in grey). During the recovery phase, a reduction in osmolality is observed in both leaves and roots. This suggests the release of osmotic content, as the decrease is consistent across all tissues, indicating a uniform alteration rather than a differential allocation within the plant.

A

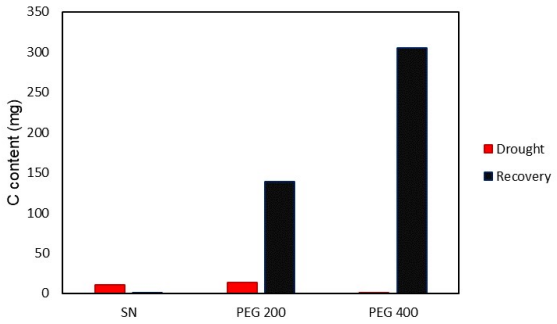

B

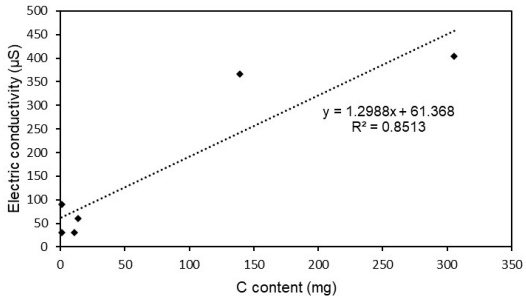

C

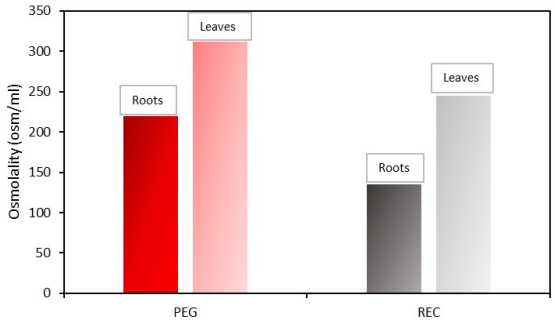

Figure 40: a comprehensive overview of the experiment conducted in 2019. In Graph A, the carbon content in plant growth solutions is presented. The red columns represent the carbon content during the stress phase for the control group (SN), the group with an intermediate peg level (peg200), and the group with a high peg level (peg400). The black columns denote the carbon content of the nutrient solutions to which the plants were transferred during the recovery phase. Graph B depicts the relationship between carbon content and the electrical conductivity of the solutions. Notably, the data suggests a correlation, demonstrating that electrical conductivity can serve as a predictor of carbon content, as indicated by the coefficient of determination (R^2). Graph C illustrates the osmolality levels of both radical and foliar fluids during the stress phase (peg) and the subsequent recovery phase (rec). The reduction in osmolality during the recovery phase in both leaves and roots implies the release of osmotic content, supporting the hypothesis that such content has been mobilized uniformly across various plant tissues.

Test n. 1

In 2021, a parallel experiment was conducted, encompassing a control group consistently exposed to nutrient solution (designated as "c" in the graph in Figure 41), a treatment group subjected to mild stress (marked as "m"), and another group experiencing intense stress (denoted as "i"). The experiment comprised four distinct phases: the initial stress phase (1, first day), the first recovery phase (2, second day), the second stress phase (3, third day), and the second recovery phase (4, fourth day). To mitigate potential cell damage in the root apexes due to dehydration, two stress cycles were implemented.

In this experiment, the treatments (stress and recovery) start in the morning, while the sampling was carried out during the day hours.

The graph in Figure 41 illustrates the Relative Water Content (RWC) of leaves (depicted in red) and roots (depicted in black) during the different phases of the experiment: 1-first stress

phase, 2-first recovery phase, 3-second stress phase, 4-second recovery phase. Notably, the levels of dehydration do not exhibit significant variations, a finding corroborated by statistical analyses (ANOVA and Tukey test). These analyses were conducted to ascertain potential differences in RWC between leaf and root tissues within the same group and among RWC values of different experimental groups.

Within the same experimental group, a statistically significant difference between root RWC and leaf RWC is evident for the "i1" and "m1" conditions (p-value < 0.05), specifically during the first stress phase. However, in all other instances, this difference is not statistically significant. Furthermore, when comparing root RWC among different experimental groups, no statistically significant difference is observed (p-value > 0.05).

Regarding leaf RWC, statistically significant differences (p-value < 0.05) are identified only in specific group-to-group comparisons, reported in table 3:

	C1	M1	I1	C2	M2	I2	C3	M3	I3	C4	M4	I4
C1												
M1												
I1	*			*			*					
C2												
M2			*									
I2			*									
C3												
M3									*			
I3						*	*			*		
C4												
M4			*						*			
I4												

Table 3: the matrix shows between which RWC leaf group there is a statistically significant difference.

There is a plant response to stress, confirmed by the diversity of leaf hydration levels in the various groups and the difference in leaf and root hydration levels during the first stress phase (m1 and i1). However, along the experiment, it seems that the reduction of hydration levels occurs only after intense stress. In addition, there are no clear differences between the control and treatment plants. This may be since the plants showed signs of stress (yellowing and withering) already at the beginning of the experiment.

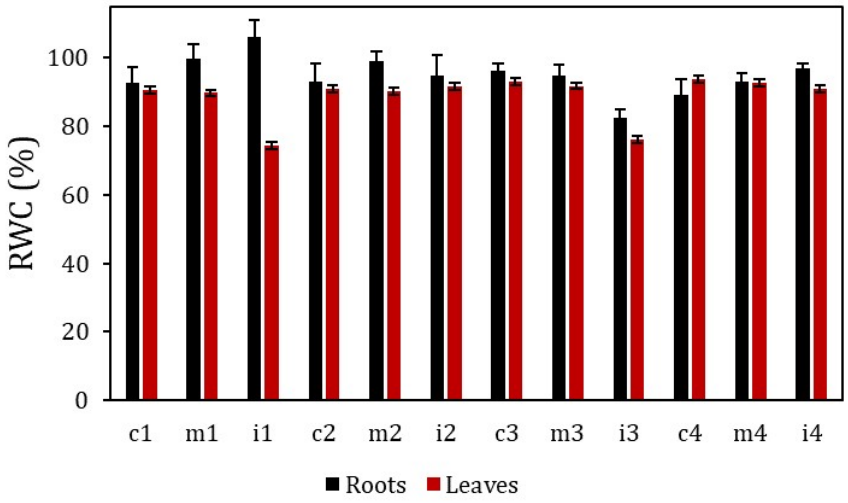

Figure 41: representation of root Relative Water Content (RWC) (depicted in black) and leaf RWC (depicted in red) across various phases of the experiment. The experiment included three groups: "C" (control group, consistently in nutrient solution), "M" (group subjected to two cycles of moderate stress with peg 100, followed by recovery in nutrient solution), and "I" (group subjected to two cycles of intense stress with peg 200, followed by recovery in nutrient solution). The numbers correspond to different phases of the experiment: 1 represents the first stress phase, 2 denotes the first recovery phase, 3 signifies the second stress phase, and 4 indicates the second recovery phase. The average values were calculated by averaging the RWC values for both leaves and roots within each group. This visualization offers insights into how root and leaf RWC fluctuate during distinct phases of the experiment across different stress conditions.

The graph in Figure 42 depicts the percentage variation in electrical conductivity of the solutions during various phases of the experiment. The data are expressed as a percentage in order to highlight the changes in conductivity, since the starting solutions do not all have the same conductivity. Notably, for plants subjected to intense stress (depicted in red), an increase in conductivity is observed during the stress phase, potentially attributed to substances released due to damage to the root tissues. However, this increase is not observed during the recovery phase. However, in this case the experiment was conducted by subjecting the plants to the recovery phase during the day. Sampling also took place during daylight hours, and this may have affected the results: the plants could not have fully recovered because they kept the stomata open for transpiration. Conversely, the reduction in conductivity, likely resulting from nutrient absorption, is less pronounced during the recovery phase for plants subjected to intense stress and more evident for those subjected to moderate stress.

The observed differences in the stress response between plants subjected to intense and moderate stress conditions suggest that the pre-existing stress condition experienced by plants prior to the experiment may have influenced their subsequent stress responses.

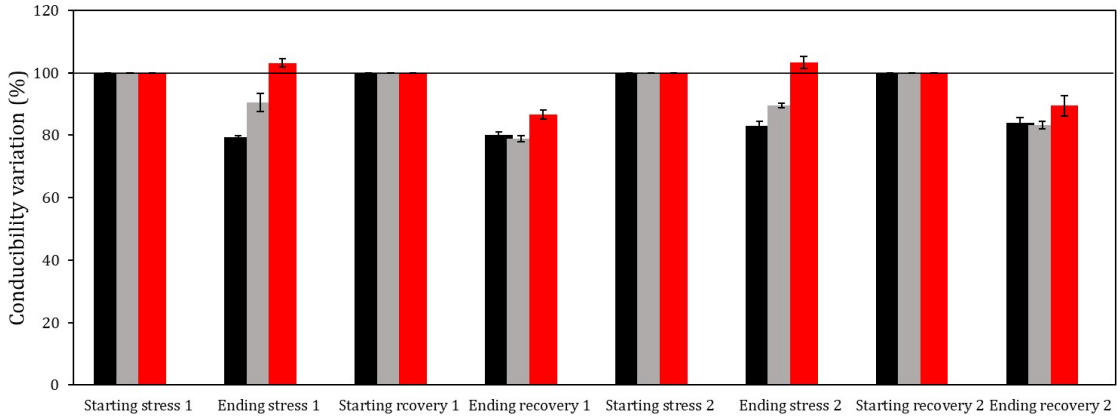

Figure 42: percentage change in the conductivity of the solutions throughout different phases of the experiment. In the graph, values corresponding to plants subjected to intense stress are depicted in red, those for plants subjected to intermediate stress are in grey, and values for the control group plants (consistently in nutritional solution) are represented in black. At the initiation of each phase, the value is set at 100. After the conclusion of the recovery or stress phase, values may exhibit positivity (>100, indicating potential substance release) or negativity (<100, suggesting likely absorption of osmotically active compounds).

During Test 2, the plants exhibited clear signs of severe stress during their growth phase, rendering it impractical to complete the experiment. The observed stress indicators (change of color of the leaves that become yellow or black, withering and desiccation) likely compromised the viability of the experimental conditions and the reliable collection of data. Understanding the causes and manifestations of stress in the plants was crucial for refining experimental protocols and obtaining meaningful results in subsequent attempts.

Test 3

During test 3, maize seedlings were divided into three groups. Each group was grown in a nutrient solution at different concentrations: 540 µs, 300 µs, and 100 µs. After growth, each group was in turn divided into two groups, one remaining in nutrient solution for other 24 hours (540 µs, 300 µs, and 100 µs) and the other transferred to PEG 400 for 24 hours, thus obtaining 6 groups. The 6 groups were then all transferred to distilled water. Figure 12 shows the conductivity of the distilled water into which the plants subjected to 6 different treatments were transferred. Notably, the conductivity is higher in plants that experienced

stress for 24 hours, especially in the case of the less concentrated solution. This difference diminishes as the concentration of the starting nutrient solution increases (figure 43).

An analysis of variance (ANOVA) reveals no statistically significant differences between the release of root exudates from plants stressed using PEG 400 solution and those grown in the most concentrated solution (p-value=0.53). So, this suggests that an excessively concentrated solution could induce plants to osmoregulate as much as a water stress. Consequently, the decision was made to continue using the original (or less concentrated) nutrient solution concentration in order to minimize potential osmotic stress effects on the plants.

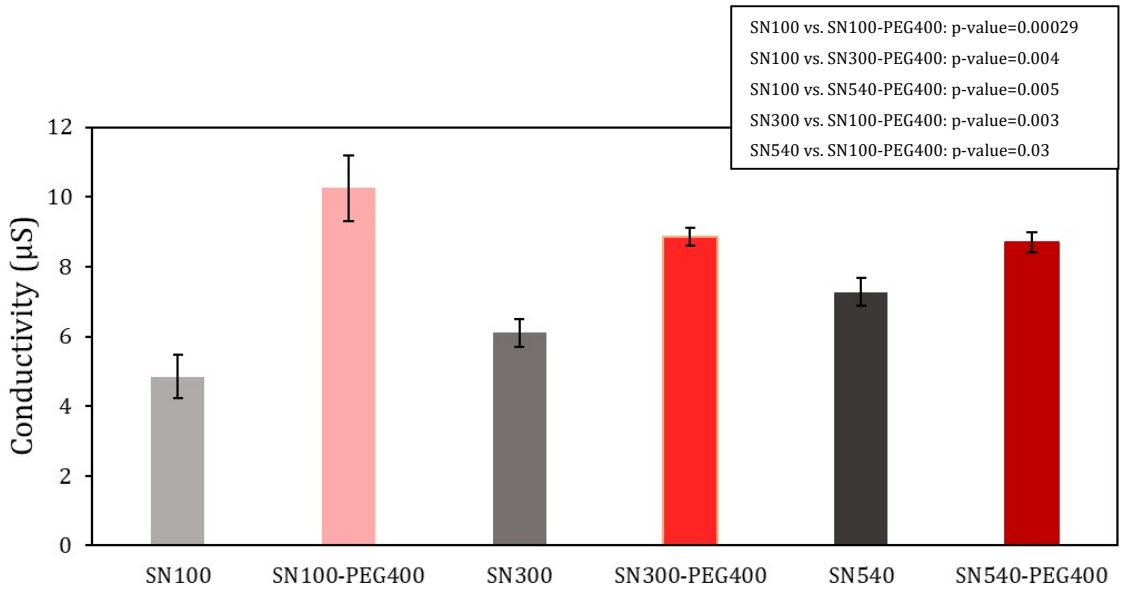

Figure 43: mean levels of electrical conductivity in distilled water, in which plants were placed for recovery after 24 hours of induced water stress using a solution containing 400g/L of polyethylene glycol (PEG). The graph illustrates the average conductivity values for two distinct conditions: plants that consistently remained in nutrient solution are represented in grey, while plants that underwent a 24-hour water stress event are indicated in red.

Test 4

Also in this test, the treatments (stress and recovery) start in the morning, while the sampling was carried out during the day hours.

Graph A in Figure 44 demonstrates the significant concentration of osmolites in leaf tissues following a water stress phase. However, during the subsequent recovery phase, osmolality returns to pre-stress levels, indicating the transfer of these substances out of the leaves. An intriguing confirmation of this hypothesis lies in the quantity of osmolites present in the roots, as illustrated in Figure 44, graph B.

During the stress phase, roots exhibit an increase in their osmolite content as a mechanism to withstand water stress. However, after the recovery period, the quantity of osmolites decreases, mirroring the trend observed in leaves and, notably, reaching levels even lower than in plants that remained in a control condition. Unfortunately in the analyzed solutions there are no traces of exudates, and this suggests that probably the stress to which the plants were subjected was too intense.

A

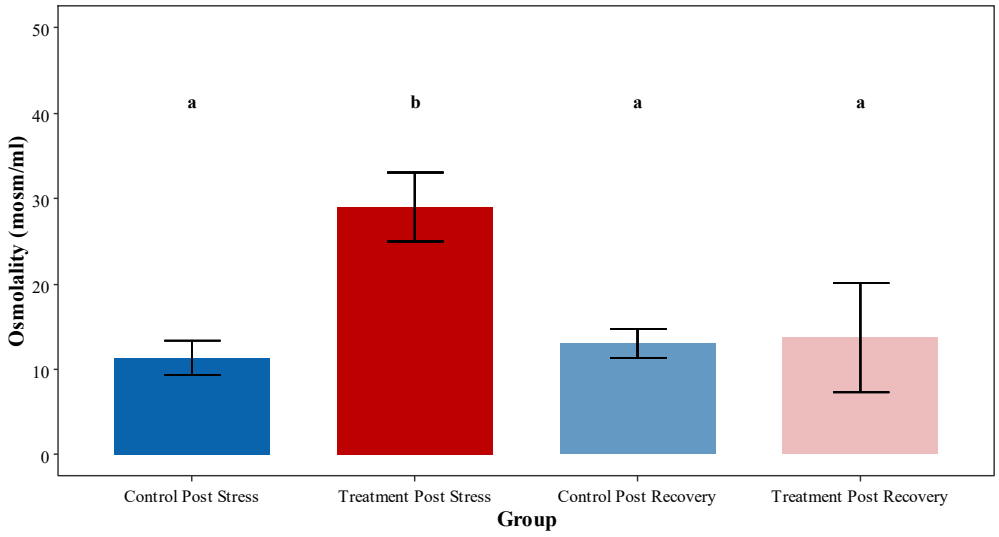

B

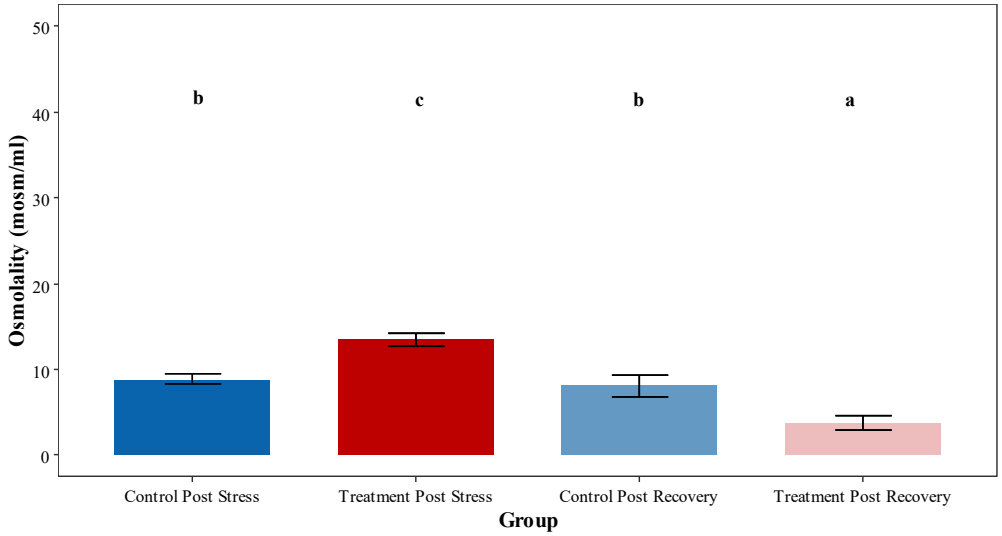

Figure 44: osmolality of leaf tissues (graph A) and root tissues (graph B) in maize, observed during a water stress phase and a subsequent recovery phase. Notably, there is an apparent increase in osmolality for both leaves and roots in the post-stress phase for the treated group. The letters above the columns in the graphs indicate the ANOVA results, confirming a statistically significant difference between the stress group and the control group.

Nevertheless, a critical consideration arises from the findings in Figure 45: the reduction in Relative Water Content (RWC) observed in stressed plants. This reduction might have led to an increase in osmolite concentrations not necessarily due to differential allocation but potentially as a consequence of reduced water content. Careful interpretation of these results is crucial for a comprehensive understanding of the dynamics involved.

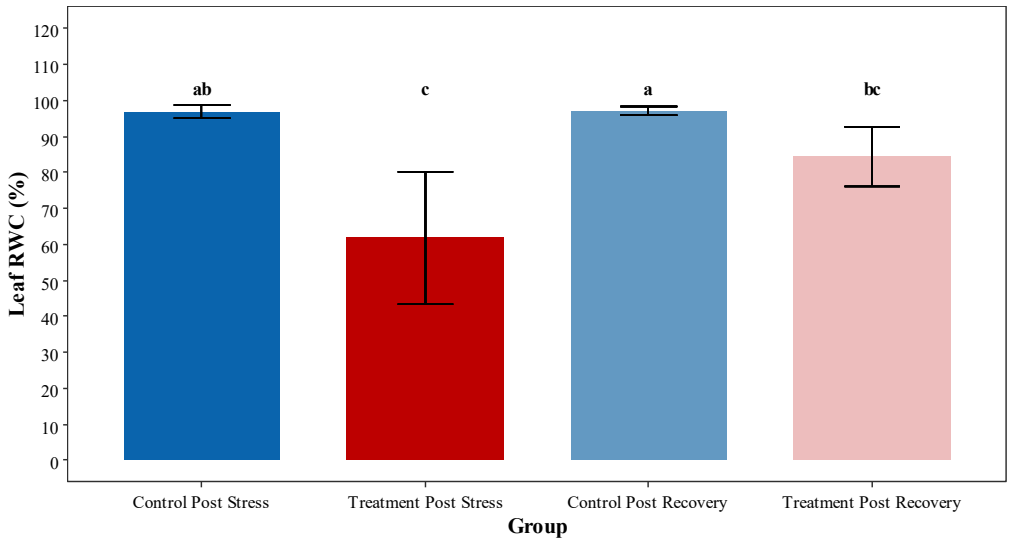

Figure 45: Relative Water Content (RWC) for leaf tissues in graph A. A significant difference in RWC is observed between the values of the Treatment Post Stress phase and those of the control group.

Regarding leaf water potential, there is a significant decrease following a period of stress (Figure 46), validating the plant's response to water stress and its strategy to sustain hydration by reducing the water potential. Upon reintroduction into the nutrient solution, the water potential resumes an upward trend. This observation indicates that the plant has not experienced stress to the extent that it cannot recover, affirming its resilience to the imposed stress conditions.

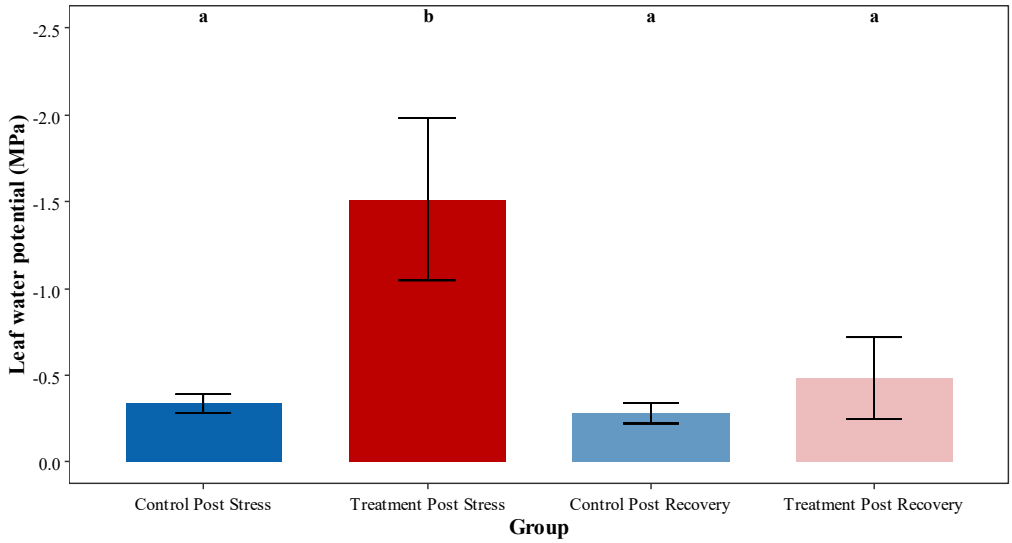

Figure 46: evolution of leaf water potential during the experiment. The leaf water potential undergoes a reduction in plants subjected to water stress, followed by a subsequent increase during the recovery phase, eventually returning to levels comparable to those of control plants (depicted in blue).

Graph 47 illustrates the conductivity of the distilled water used for leaf immersion. Notably, the highest conductivity is observed for leaves that underwent intense stress, indicating that these plants had accumulated osmotically active compounds as a response to drought. This observation suggests that osmoregulation (graph 44) may play a more substantial role in determining osmolality values than dehydration alone (graph 45).

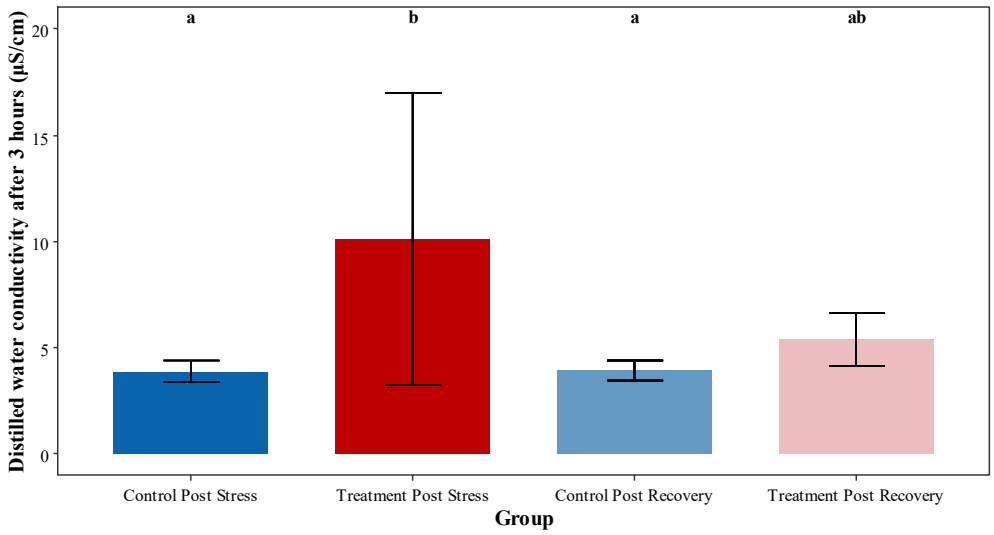

Figure 47: conductivity of the distilled water in which leaves were immersed for 3 hours to facilitate rehydration to full turgor and enable the calculation of Relative Water Content (RWC). The conductivity is notably higher for plants transferred to a PEG 300 solution (depicted in red). During the recovery phase (depicted in rose), the conductivity decreases, while it remains relatively constant for plants in the control group (depicted in blue).

3.2.2 Laboratory experiment using *Quercus ilex* L.

The experiment involving holm oak is detailed through the graphs in figures 48, 49, and 50. The labels correspond to the following conditions:

1_1: Control group, exposed to nutrient solution during the night (phase 1)

1_2: Control group, exposed to nutrient solution during the day (phase 2)

1_3: Control group, exposed to nutrient solution during the night (phase 3)

2_3: After the initial two phases (night and day) in nutrient solution, followed by phase 3 (second night) in PEG 280

3_1: Treatment group consistently exposed to PEG 280, during the night (phase 1)

3_2: Treatment group consistently exposed to PEG 280, during the day (phase 2)

3_3: Treatment group consistently exposed to PEG 280, during the night (phase 3)

4_3: After spending the first two phases (night and day) in PEG 280, followed by phase 3 (second night) in nutritive solution

5_1: Treatment with PEG 500 during the first two phases (night and day), with measurements taken after the night (phase 1)

5_3: Treatment with PEG 500 during the first two phases, followed by recovery in nutrient solution during the night (phase 3)

Graph 48 depicts changes in leaf water potential during the experiment. For plants consistently exposed to nutrient solution (1_1, 1_2, and 1_3), the leaf water potential is higher. Group 2_3 underwent two phases in nutrient solution (night and day), and the measurement displayed in the graph corresponds to the third stress phase (the night spent in PEG 280). The plants exhibit water stress control by lowering the leaf water potential, indicative of osmoregulation.

Plants 3_1, 3_2, and 3_3 remained in PEG 280 for the entire experiment. Notably, in 3_2 (and also in 1_2), the leaf water potential is lower. This is attributed to transpiration activity, as these measurements were taken during the day after stomatal opening.

In the case of group 5_3, no recovery is observed, possibly indicating that the stress was too intense, and the plants were unable to recover during the night. Generally, it is observed that the initial leaf water potential is already relatively low, placing the plants in a condition of slight stress from the beginning of the experiment. This could be attributed to the process of cleaning the roots from the soil where the plants initially grew, potentially causing slight damage to the root system.

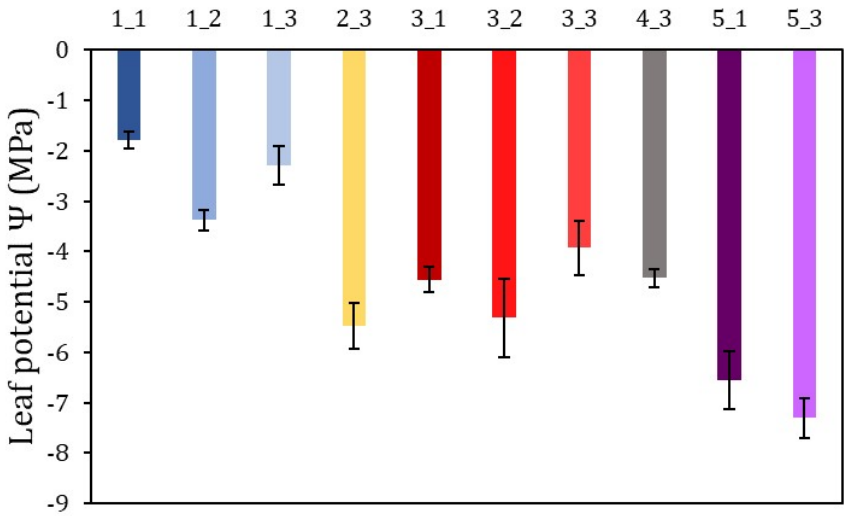

Figure 48: leaf water potential (Ψ) of holm oak plants throughout the experiment. The values represent the average of individual plant values for each group. Plants consistently exposed to nutrient solution (1_1, 1_2, and 1_3) exhibit lower leaf water potential compared to plants subjected to water stress. Groups 4_3 and 5_3 show leaf water potential after recovery from lighter and more intense stress, respectively. In the case of 4_3, the potential decreases relative to the situation in 3_2, suggesting a continued impact even after recovery from lighter stress. Conversely, in 5_3, the leaf water potential is higher than during stress (5_1), indicating that the plant has not fully recovered after more intense stress. These findings provide insights into the varying responses of holm oak plants to different stress conditions and recovery phases.

Figure 49 displays variations in root Relative Water Content (RWC) during different phases of the experiment. In groups 3_1, 3_2, and 5_1, under stress, the loss of RWC is noticeable but not substantial, indicating that the plant has accumulated sugars to mitigate drought effects. During the stress recovery phase (4_3), RWC experiences a further decline compared to the stress phase (3_2). Moreover, the leaf water potential (Ψ) at this stage remains constant (as observed in Figure 48). This suggests that the sugars accumulated by the plant must have been transferred elsewhere, as retaining them within its tissues would have led to an increase in RWC.

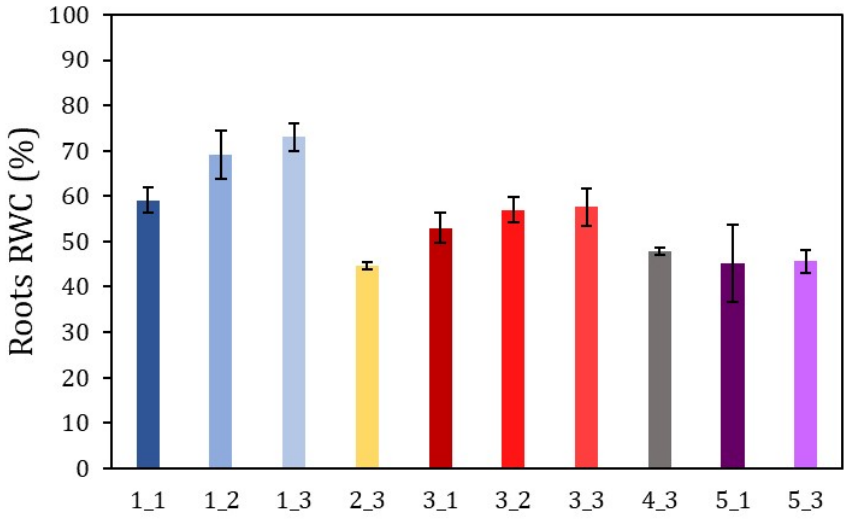

Figure 49: Root Relative Water Content (RWC) at different stages of the experiment. Notably, root RWC tends to be lower than foliar RWC as depicted in Figure 19. In the control group exposed to nutrient solution, root RWC is higher, whereas upon transfer to PEG 280 (2_3), it decreases. In plants placed in recovery after a night and a day of stress (4_3), RWC decreases. In plants subjected to intense stress, RWC remains consistently low both during stress and recovery phases.

Leaf Relative Water Content (RWC), as illustrated in Figure 50, is generally higher than root RWC (Figure 18). This observation indicates that to support leaf transpiration, the roots do not necessarily need to be turgid. An excess of sugar could potentially limit the root, as its cells might experience significant pressure due to water uptake following the osmotic gradient. It is important to note that RWC might also decrease due to the plant's challenge in acclimating to the new root submersion conditions.

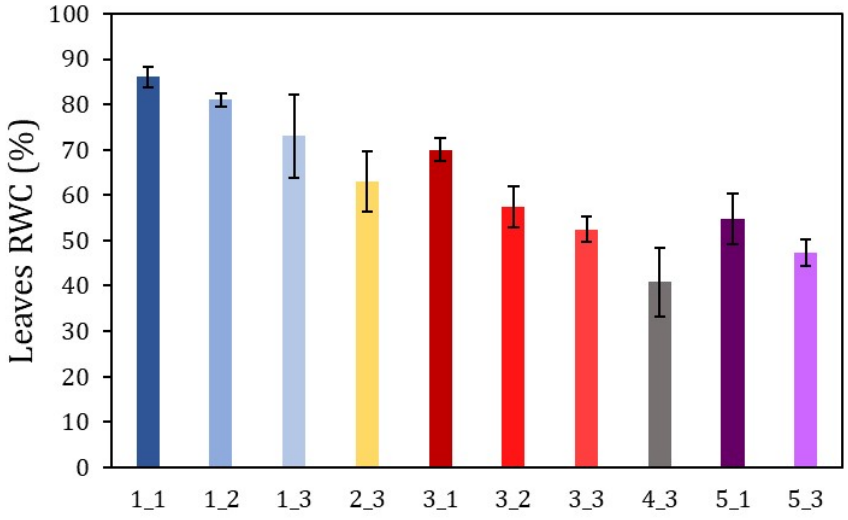

Figure 50: Relative Water Content (RWC) of the leaves at different stages of the experiment. Generally, foliar RWC is higher compared to root RWC as shown in Figure 18. In the nutrient solution (1_1, 1_2, and 1_3) groups, RWC is higher, even though it gradually decreases. A lower RWC is observed during the stress recovery phase (4_3), highlighting the impact of stress and recovery on foliar water content.

4. Discussion

The discussion of the results is structured for clarity according to the order of presentation of the results, discussing first the work done in the field and then the experiments conducted in the laboratory.

The investigation into the field experiment reveals noteworthy trends in *Tuber aestivum* production, particularly during the summer months (Figure 13). Across all observed years, a consistent pattern emerges, indicating the highest truffle yield during summer. Notably, in the drier years of 2022 and 2023, there is a discernible reduction in production. This observation suggests a plausible association between truffle harvest and environmental factors, emphasizing the potential impact of climate on truffle productivity, as suggested by Büntgen et al. (2019) and Le Tacon (2016).

Examining temperature dynamics (Figure 14), a slightly positive correlation is observed between truffle production and both maximum daily temperature and average temperature on the day of collection. The correlation with the average temperature of the 7 days preceding the harvest is marginally lower. Intriguingly, the weakest correlation is noted between production and the maximum temperature difference (T °C daily max - T °C daily min) in the 7 days before harvest. It remains unclear whether increased temperature directly corresponds to enhanced truffle production. The ripening period of *Tuber aestivum* occurring in summer (Büntgen et al. 2017) introduces complexities, as higher temperatures during this season may reflect the natural maturation process rather than a direct temperature effect.

An observation emerges regarding temperature differences in the seven days prior to harvest, indicating that truffle production is notably constrained within the range of 9-11 °C. Production appears to be negligible below or above this range. Soil temperature analysis also yields positive correlations, likely attributable to the maturation period. Notably, a negative correlation is apparent between harvested truffles and the maximum difference of soil temperature in the seven days before harvest. This observation may be influenced by seasonal variations, as temperature differentials between day and night are typically more pronounced in autumn and spring.

Turning attention to air humidity, a lack of correlation is observed when considering average air humidity levels. However, correlations become more pronounced when assessing the

difference of daily humidity on the day of collection and the difference of maximum humidity over the 7 days preceding harvest. This insight is pivotal, as a substantial difference in humidity signifies rapid adaptations by the plant to humidity fluctuations, potentially influencing transpiration (Niglas et al. 2014). In scenarios of reduced humidity, the plant engages in osmoregulation (Mehmood et al. 2020), while decreased osmolite content in foliar tissues may occur in response to humidity increase. This nuanced understanding underscores the complex interplay between truffle production and humidity, elucidating the need for a comprehensive examination of these environmental factors.

The observed positive correlation with the difference of air humidity suggests that the truffle may derive benefits from the plant's regulatory mechanisms against environmental changes. Traditionally, mushroom production has been linked to soil moisture; however, our study challenges this notion, revealing that soil moisture is the least influential parameter among those considered (Figure 18).

A noteworthy correlation is established with the vapor pressure deficit (VPD), especially when considering weekly production relative to the maximum difference of VPD reached during the week. A high VPD difference indicates the plant's necessity to adapt to fluctuations in both relative humidity and air temperature (Badalotti et al. 2000) This, akin to air humidity, implies that truffle production is influenced by the plant's response to environmental parameter changes rather than a direct response from the fungal organism to the environment.

In the Caltrano site, where all plants are of the same species, age, and planted in the same year, and the truffle grounds are uniformly treated (for example, with thinning on the *Fraxinus ornus* renewal), there is observed variability in truffle production. Some plants exhibit productive symbiosis, while others do not. The study identifies physiological distinctions between productive and non-productive plants. For instance, it is evident that productive plants exhibit superior control over dehydration levels compared to non-productive plants (as illustrated in figures with dendrometer oscillations in 2021, 2022, and 2023). In 2021, this difference persists throughout the season, up until September when the most severe drought is encountered. Productive plants utilize sugars produced through photosynthesis to activate osmoregulation (Kavi Kishor et al. 2005; Ozturk et al. 2021), effectively controlling dehydration, unlike non-productive plants.

In 2022, beyond a certain threshold of drought, productive plants begin to resemble non-productive ones. This might be attributed to the fact that, due to water scarcity, productive

plants can no longer photosynthesize at previous rates, resulting in insufficient sugars for osmoregulation. Furthermore, post-reaching the maximum drought level, productive plants do not fully recover from dehydration. This phenomenon suggests that complete rehydration would require plants to retain a substantial amount of fluid in their tissues, achievable only with an adequate supply of osmotically active compounds. It appears that towards the end of the season, when plants diminish vegetative activity, accumulating sugars becomes challenging and resource-intensive (Martel et al. 2005). Interestingly, during this period, in contrast to 2021, truffle production ceases. It can be hypothesized that insufficient sugars hinder both plant rehydration and transfer to the fungus for completing its life cycle. At this juncture, the correlation between production and physiological parameters of the plant becomes more apparent, suggesting a stronger link with the plant's vital status than with environmental parameters, which indirectly influence the plant's condition and, consequently, sugar transfer to the fungus.

A preliminary insight into the mechanism by which plants transfer sugars to fungi is obtained by focusing on the period of peak production in 2021 (figure 26). Notably, production experiences a significant surge on June 21, coinciding with productive plants initiating an increase in dehydration levels. The dehydration observed is moderate, suggesting that plants can potentially regulate it through the osmoregulation mechanism. This inference is supported by the fact that during nighttime hours, dehydration levels return to zero in productive plants, a phenomenon not observed in non-productive plants. This implies that productive plants accumulate sugars in their tissues during the day and, during the night when stomata are closed, successfully rehydrate. In contrast, non-productive plants experience daytime dehydration without the ability to recover hydration at night due to closed stomata. Similar patterns are evident in 2022.

Concerning the data from flow sensors, an initial observation may suggest conflicting information compared to dehydration data. It appears that sapflow is activated later in the day in productive plants (refer to the figure depicting hourly flow trends) compared to non-productive plants. At first glance, this might imply that productive plants transpire less than non-productive plants, thus potentially having fewer water resources available.

What emerges from most of the literature in many cases is that mycorrhizal plants (which in this case correspond to productive plants) have more available water (Ruth and Khalvati 2011), and therefore, they should exhibit a faster flow activation and a greater amount of

transported water. This leads to the question of whether productive plants need to rehydrate more. However, the answer to this question is negative because, as seen before, dehydration data indicate that productive plants experience less dehydration compared to non-productive plants.

Of equal importance is the small peak of sapflow observed at night. This is especially unusual, since during the night the plants close the stomata, as a result should be absent any type of flow.

A possible explanation may come from osmoregulation, the mechanism through which plants regulate their water response (Rontein et al. 2002). The osmotic potential of cells, from roots to leaves, must balance along a gradient from soil to the atmosphere, becoming progressively more negative to allow water passage (figure 51). This gradient fluctuates throughout the day. Cells in productive plants, as we have seen, have greater osmotic capacity, generating more turgor. If the cell is in a turgid state, water can be easily extracted. This suggests that, during full hydration, morning transpiration in productive plants with turgid cells may initially be sustained not by sapflow, but rather by fluids in leaf tissues. Only later the plant will need to activate root flow. Non-productive plants have lower turgor, so they activate root flow earlier.

After the transpiration phase follows stomatal closure. However, leaves of productive plants still contain many sugars at this point, and this could cause a continuous flow of water towards the canopy even if the stomata are already closed. Over time, this continuous flow might damage cells due to excessive water content. This could push sugars downward and toward the roots, allowing the plant to regulate the osmotic gradient. The increased sugar concentration in the lower parts of the plant could trigger a small nocturnal flow peak, rebalancing the osmotic gradient. Such flow would be greater with a higher sugar concentration, explaining the observed larger peak in productive plants. However, it's essential to consider the possibility of excessive sugar loading. In this case, the plant would be forced to expel them through the release, for example, of root exudates.

Contrary to a perceived delay in the activation of sapflow in productive plants, the situation is more nuanced: these plants are indeed transpiring, but they utilize water accumulated in their tissues during the night. This dynamic leads to a side effect crucial for soil microorganisms, namely the release of root exudates. Consequently, a subtle positive correlation between air moisture difference or VPD and the biomass of harvested truffles may be observed. This

underscores the intricate interplay between plant transpiration, water dynamics, and the consequential release of compounds that significantly impact the soil microbial environment.

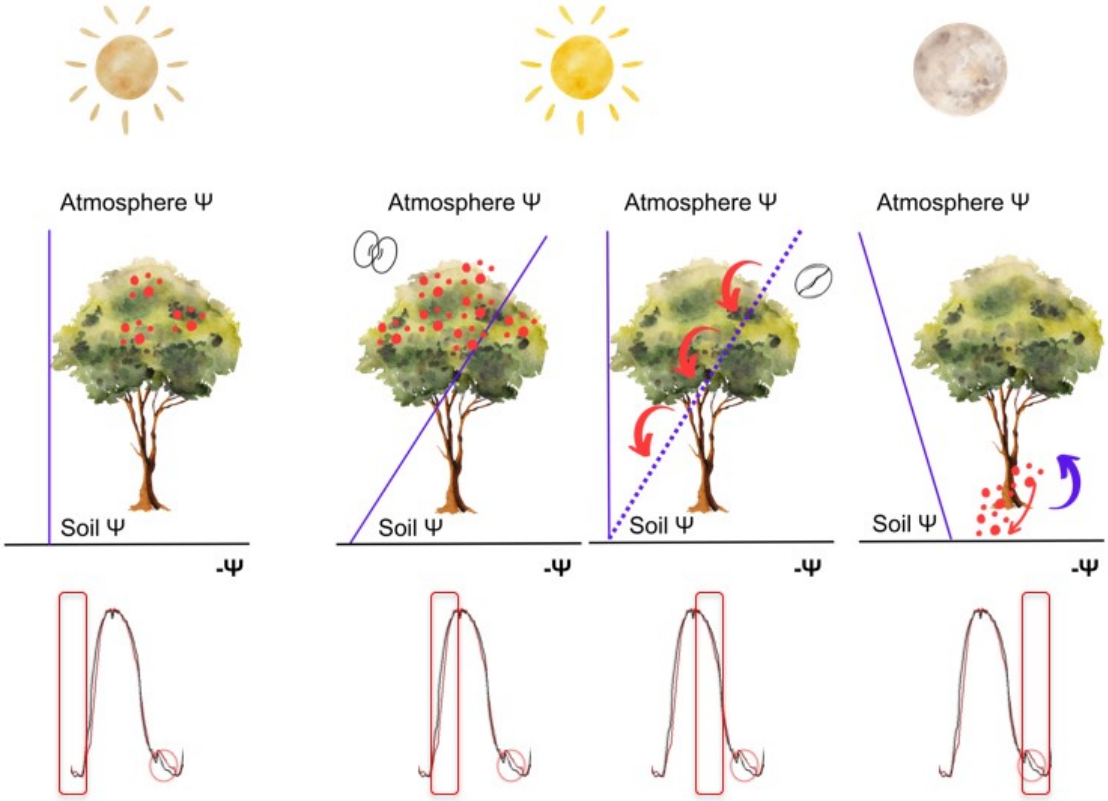

Figure 51: The representation illustrates the process of osmoregulation in plants throughout the day, with the blue line depicting the osmotic gradient. In the early morning, the osmotic gradient is minimal, indicating a lower potential for water movement. As the morning progresses, the gradient increases when the stomata open, initiating transpiration. To sustain adequate hydration levels, the plant engages in osmoregulation, adjusting its internal solute concentrations. After a certain period, typically in the afternoon, the plant undergoes stomatal closure. During this phase, the plant initiates rehydration, drawing up water resources and, notably, transferring sugars stored in the leaves. This transfer of sugars plays a crucial role in maintaining osmotic balance and facilitating the rehydration process. The osmotic gradient reflects these dynamic changes, showcasing the plant's adaptive response to varying environmental conditions throughout the day.

The factors contributing to the enhanced efficiency of productive plants in controlling dehydration and their superior osmoregulation abilities remain elusive (in fact, the adaptations that a plant can make to face the drought are several (Lo Gullo and Salleo 1988; Grzesiak et al. 1997).

The study aimed to investigate potential differences in the relationship between the photosynthetically active portion of the plants, known as the crown, and the segment comprising non-productive cells, namely the stem. If the ratio favours the crown in productive plants, it could imply that they possess an advantage over non-productive plants by producing

more sugar. Alternatively, non-productive plants may adopt a strategy centred on the production of structural carbohydrates to promote growth and optimize light absorption. This investigation seeks to shed light on these intricate dynamics within the plant physiology that may contribute to the observed variations in dehydration control and osmoregulation efficiency.

However, there are no discernible differences in either the ratio between the volume of the crown and the volume of the stem or the ratio between the volume of the crown and the height of the plant between the two groups. Therefore, it can be asserted that productive plants do not derive an advantage from a broader photosynthetically active portion.

Moreover, there are no distinctions between productive and non-productive plants concerning leaf water potential at pre-dawn (as otherwise reported by Yuste et al. 1999). This indicates that productive plants, having been rehydrated during the night, attain the same leaf water potential levels as non-productive plants, despite demonstrating superior control over dehydration during the day compared to their non-productive counterparts.

Similarly, in the relationship between leaf water potential and leaf water content, no distinctions are evident among productive plants. This implies that, with an equivalent osmotic content, the water content remains consistent across plants. Therefore, the observed difference does not lie in the dehydration process itself, such as the ability to sustain greater hydration at similar leaf water potential levels. Instead, the variation is attributed to the plant's capacity to accumulate varying quantities of osmotic compounds within foliar tissues.

At the Carlino site, the data indicates a lower groundwater level in the formerly productive region compared to the non-productive section. However, an interesting observation emerges as plants in the former production area exhibit lower levels of dehydration than those in the non-productive area. This distinctive trait is shared by the productive plants in Caltrano. One plausible hypothesis is that previously productive plants, potentially in conditions of greater water availability, demonstrated enhanced resilience against dehydration. This ability allowed them to effectively osmoregulate and produce sufficient quantities of sugar, thereby initiating the development of truffle fruit bodies of the *Tuber magnatum* Pico species.

In the context of sapflow data, subtle differences are noted between the two areas of the forest. Specifically, it appears that sapflow is activated later in the former productive part compared to the non-productive part. Notably, a small nocturnal flow peak is often present,

similar to the observations in Caltrano, although not consistently (the work of Deng et al (2021) suggests that groundwater depth can cause difference sap flow velocity).

This observation could serve as a confirming clue to the predisposition of this plant population to engage in symbiosis conducive to the development of fruiting bodies belonging to the Tuber genus. However, the cessation of production remains unclear, making it challenging to envision treatments that could reactivate this process. It is plausible that by regulating the aquifer's height through the existing channeling on the site, it might be feasible to augment water availability in the former productive area, aligning it with the levels observed in the non-productive area. This approach aims to ensure equal access to resources. Consequently, leveraging the advantage demonstrated by plants in the "productive" area in terms of dehydration control could potentially result in increased sugar production and subsequently greater release into the soil.

An analysis of the correlation between soil moisture and dehydration levels reveals that, beyond a certain threshold, plants lose their ability to control dehydration. By employing water channeling systems to regulate groundwater and thereby delaying the approach to this critical threshold, it may be feasible to sustain plants above the point at which they can no longer manage dehydration effectively.

While there are no statistically significant differences observed when comparing the relationship between leaf water potential and water content in plants from the former production area to those in the non-productive area, there is a noticeable trend. Despite equal water content, the former productive plants appear to exhibit less negative water potential than their non-productive counterparts. This suggests the possibility that productive plants may require less negative leaf water potential to maintain hydration, even in conditions of lower groundwater. To establish definitive differences in the physiology of the two groups, further comprehensive analyses are imperative.

In the case of 2022, soil moisture levels are further diminished, and hydration and dehydration cycles exhibit an exceptionally narrow range. This narrow range is likely a consequence of the intense water stress experienced by the stand plants. Sapflow persists, yet the distinct delay observed between the two areas in 2021 is no longer evident. It seems as though, following the severe drought, trends have become more uniform.

Laboratory experiments are designed to substantiate the hypothesis that the release of radical exudates is instigated by the osmoregulative processes activated by the plant during stress

and recovery cycles. These experiments aim to provide empirical evidence supporting the connection between plant osmoregulation and the subsequent release of root exudates in response to varying environmental conditions (Canarini et al. 2016, Preece et al. 2018).

Regarding the initial pilot test, the initial hypothesis finds confirmation. Specifically, the carbon content in the recovery solution is found to be directly proportional to the stress levels experienced by the plants. The activation of the osmoregulation process, facilitated by the transfer in polyethylene glycol (PEG), is further substantiated by the higher osmolality observed in foliar and radical liquids during the stress phase.

Regrettably, in the subsequent three experiments, the hypothesis has not consistently held true, primarily due to challenges encountered in the growth of maize. These challenges are particularly evident in the Relative Water Content (RWC) values, which remain unchanged across the control group, mild stress group and intense stress group. Additionally, there is no discernible increase in electrical conductivity in the solutions following the recovery phase.

However, in the test with plants grown at different concentrations of nutrient solution, the plants performed the recovery phase in distilled water. In this case the increase in electrical conductivity of the solutions was evident, confirming a release of probably radical exudates and showing an effect of mild stress caused by the concentration of solutes in the most concentrated nutritional solutions.

Upon repeating the experiment with healthy maize plants, the initial hypothesis was partially validated: during the stress phase, roots augmented their osmolite content as a response to water stress. However, following the recovery period, their quantity decreased, mirroring the trend observed in leaves and reaching levels even lower than those in plants that remained in a control condition. This preliminary evidence supports the hypothesis that excess osmolites, including sugars, can potentially be released in the form of root exudates by the roots following a stress and recovery phase. Further investigations are necessary for a comprehensive understanding of this phenomenon.

The reduction in Leaf Relative Water Content (RWC) during the stress phase might initially suggest that the increase in osmolality is a straightforward consequence of dehydration. However, the conductivity measurements of the distilled water in which the leaves were immersed for 3 hours (aimed at restoring turgor for RWC calculation) reveal a higher conductivity in the case of stressed plants. This indicates that the elevated osmolality is, in

fact, attributable to a higher concentration of osmotically active compounds, emphasizing the active role of such compounds in response to stress conditions.

The experiment conducted on holm oak plants shows how plants control water stress by lowering the leaf water potential, and thus osmoregulating. Typically, measurements taken during the day yield lower leaf water potential values, reflecting diurnal transpiration. Notably, plants subjected to intermediate stress were capable of returning to the same leaf water potential levels as control plants. In contrast, plants exposed to high stress levels maintained or even reduced their leaf water potential, signalling an inability to recover from the imposed stress conditions. This observation suggests a limitation in their capacity for physiological rebound under severe stress.

During the stress phase, plants initially reduced their root Relative Water Content (RWC), and in the subsequent recovery phase, the RWC continued to decrease. Despite the reduction in RWC during recovery, the leaf water potential (Ψ) remained constant. This implies that the sugars accumulated by the plant must have been transferred elsewhere. If retained in the tissues, the RWC during the recovery phase would have increased.

Notably, the foliar RWC is consistently higher than the root RWC. This suggests that, to support leaf transpiration, roots do not necessarily need to be turgid. An excess of sugar could even be limiting for the roots, as their cells might experience heightened pressure due to water influx following the osmotic gradient. However, it is important to consider that RWC could also decrease due to the plant's challenge in acclimatizing to the new condition of root submersion.

5. Conclusions

This study has elucidated a mechanism that regulates the release of radical exudates based on cycles of osmoregulation (stress phase) and recovery (return to water availability). Understanding this mechanism is pivotal for unraveling the intricate relationships governing soil microorganism life cycles.

The experiment conducted at Caltrano revealed significant differences between productive plants (engaged in active mycorrhizal symbiosis) and non-productive plants. These differences, though not structural, primarily revolve around the distinct ability to control dehydration.

The research underscores the fundamental importance of considering plant physiology to comprehend the development of truffle fruit bodies, advocating for a holistic approach beyond reliance on abiotic factors alone, which fall short of fully explaining production dynamics.

Regrettably, the data sets from field experiments are occasionally incomplete due to technical instrument damage caused by wildlife and insects. Challenges such as wild boars damaging power wires and ants oxidizing electrical contacts of dataloggers, compounded by environmental factors like wind-induced plant damage, necessitate a constant operator presence for timely repairs. Unfortunately, logistical and personal constraints hindered this constant presence, resulting in data gaps.

While replicating and measuring this mechanism in the laboratory poses challenges, preliminary results from experiments under controlled conditions align reasonably well with the initial hypothesis. Notably, findings from the *Quercus ilex* experiment suggest that the proposed interpretation of the radical exudate release mechanism is well-founded.

In conclusion, it appears plausible to assert that osmoregulation is a key mechanism underlying root exudation. Water stress prompts the plant to accumulate sugar in leaf tissues, and upon the cessation of the stress period, the plant, no longer requiring these compounds and needing to establish a new potential gradient from roots to leaves, releases them in the form of root exudates.

Future experiments aimed at replicating the exudate release mechanism could facilitate the development of protocols to control exudate release in the field (e.g., through irrigation, thinning). This could promote symbiotic soil microorganisms. Monitoring physiological parameters could serve as a foundation for truffle farmers to assess their truffle orchard and enhance productivity in the future.

6. Bibliography

Al-Karaki G, McMichael B, Zak J (2004) Field response of wheat to arbuscular mycorrhizal fungi and drought stress. Mycorrhiza 14:263–269.

Alaux P, Zhang Y, Gilbert L, Johnson D (2021) Can common mycorrhizal fungal networks be managed to enhance ecosystem functionality ? Plants People Planet 2021 :1–12.

Allison SD (2006) Brown ground: A soil carbon analogue for the green world hypothesis? Am Nat 167:619–627.

Aspelmeier S, Leuschner C (2004) Genotypic variation in drought response of silver birch (Betula pendula): Leaf water status and carbon gain. Tree Physiol 24:517–528.

Bach C, Beacco P, Cammaletti P, Babel-Chen Z, Levesque E, Todesco F, Cotton C, Robin B, Murat C (2021) First production of Italian white truffle (Tuber magnatum Pico) ascocarps in an orchard outside its natural range distribution in France. Mycorrhiza. https://doi.org/10.1007/s00572-020-01013-2

Badalotti A, Anfodillo T, Grace J (2000) Evidence of osmoregulation in Larix decidua at Alpine treeline and comparative responses to water availability of two co-occurring evergreen species. Ann For Sci 57:623–633.

Baetz U, Martinoia E (2014) Root exudates: The hidden part of plant defense. Trends Plant Sci 19:90–98. http://dx.doi.org/10.1016/j.tplants.2013.11.006

Ballhorn DJ, Schädler M, Elias JD, Millar JA, Kautz S (2016) Friend or foe - Light availability determines the relationship between mycorrhizal fungi, rhizobia and lima bean (Phaseolus lunatus L.). PLoS One 11:1–12.

Barbieri E, Ceccaroli P, Saltarelli R, Guidi C, Potenza L, Basaglia M, Fontana F, Baldan E, Casella S, Ryahi O, Zambonelli A, Stocchi V, Miller AN (2010) New evidence for nitrogen fixation within the Italian white truffle Tuber magnatum. Fungal Biol 114:936–942. http://dx.doi.org/10.1016/j.funbio.2010.09.001

Battie-Laclau P, Taschen E, Plassard C, Dezette D, Abadie J, Arnal D, Benezech P, Duthoit M, Pablo AL, Jourdan C, Laclau JP, Bertrand I, Taudière A, Hinsinger P (2020) Role of trees and herbaceous vegetation beneath trees in maintaining arbuscular mycorrhizal communities in temperate alley cropping systems. Plant Soil 453:153–171.

Bencivenga M (2005) State of the art in truffle knowledge and cultivation in Italy. Mycol Balc 2:20–5.

Bencivenga M, Di Massimo G, Donnini D, Baciarelli Falini L (2009) The Cultivation of Truffles

in Italy. Plant Divers 31:21–28.

Bertin C, Yang X, Weston LA (2003) The role of root exudates and allelochemicals in the rhizosphere. Plant Soil 256:67–83.

Bettini G, Bianchetto E, Butti F, Cantiani P, Chiellini C, De Meo I, D'Errico G, Fabiani A, Gardin L, Graziani A, Landi S, Marchi M, Mazza G, Mocali S, Montini P, Plutino M, Roversi PF, Salerni E, Samaden S, Sanz Canencia I, Torrini G (2016) SELECTIVE THINNING- Increasing mechanical stability and biodiversity in black pine plantations- SelPiBioLife technical handbook. Compagnia delle Foreste:28-29.

Birch HF (1958) The effect of soil drying on humus decomposition and nitrogen availability. Plant Soil 10:9–31.

Bonet JA, Fischer CR, Colinas C (2006) Cultivation of black truffle to promote reforestation and land-use stability. Agron Sustain Dev 26:69–76.

Bostan C, Borlea F, Mihoc C, Selesan M (2014) Ailanthus Altissima Species Invasion on Biodiversity Caused By Potential Allelopathy. Res J Agric Sci 46:95–103.

Bragato G, Fornasier F, Bagi I, Egli S, Marjanović Ž (2021) Soil parameters explain short-distance variation in production of Tuber aestivum Vittad. in an oak plantation in the central-northern part of the Great Hungarian Plain (Jászság region, Hungary). For Ecol Manage 479:118578. https://doi.org/10.1016/j.foreco.2020.118578

Bruhn J, Hall M (2011) Burgundy Black Truffle Cultivation in an Agroforestry Practice. Agrofor action:1–20.

Bruhn JN, Mihail JD, Pruett GE (2013) Truffle seedling production method has long-term consequences for tree growth and root colonization. Agroforest Syst 87:679–688. DOI 10.1007/s10457-012-9588-3

Brunner I, Herzog C, Dawes MA, Arend M, Sperisen C (2015) How tree roots respond to drought. Front Plant Sci 6:1–16. doi: 10.3389/fpls.2015.00547

Búfalo J, Rodrigues TM, de Almeida LFR, Tozin LR dos S, Marques MOM, Boaro CSF (2016) PEG-induced osmotic stress in Mentha x piperita L.: Structural features and metabolic responses. Plant Physiol Biochem 105:174–184. http://dx.doi.org/10.1016/j.plaphy.2016.04.009

Büntgen U, Bagi I, Fekete O, et al (2017) New insights into the complex relationship between weight and maturity of burgundy truffles (Tuber aestivum). PLoS One 12:1–15. https://doi.org/10.1371/journal.pone.0170375

Büntgen U, Oliach D, Martínez-Peña F, Latorre J, Egli S, Krusic PJ (2019) Black truffle winter

production depends on Mediterranean summer precipitation. Environ Res Lett 14 https://doi.org/10.1088/1748-9326/ab1880

Callister AN, Arndt SK, Adams MA (2006) Comparison of four methods for measuring osmotic potential of tree leaves. Physiol Plant 127:383–392. doi:10.1111/j.13993054.2006.00652.x

Calvo OC, Franzaring J, Schmid I, Müller M, Brohon N, Fangmeier A (2017) Atmospheric CO2 enrichment and drought stress modify root exudation of barley. Glob Chang Biol 23:1292–1304. doi: 10.1111/gcb.13503

Canarini A, Kaiser C, Merchant A, Richter A, Wanek W (2019) Root exudation of primary metabolites: Mechanisms and their roles in plant responses to environmental stimuli. Front. Plant Sci. 10:157. doi: 10.3389/fpls.2019.00157

Canarini A, Merchant A, Dijkstra FA (2016) Drought effects on Helianthus annuus and Glycine max metabolites: from phloem to root exudates. Rhizosphere 2:85–97. http://dx.doi.org/10.1016/j.rhisph.2016.06.003

Canellas LP, Olivares FL, Canellas NOA, Mazzei P, Piccolo A (2019) Humic acids increase the maize seedlings exudation yield. Chem Biol Technol Agric 6:1–14. https://doi.org/10.1186/s40538-018-0139-7

Caser M, Chitarra W, D'Angiolillo F, Perrone I, Demasi S, Lovisolo C, Pistelli L, Pistelli L, Scariot V (2019) Drought stress adaptation modulates plant secondary metabolite production in Salvia dolomitica Codd. Ind Crops Prod 129:85–96. https://doi.org/10.1016/j.indcrop.2018.11.068

Castaño C, Lindahl BD, Alday JG, Hagenbo A, Martínez de Aragón J, Parladé J, Pera J, Bonet JA (2018) Soil microclimate changes affect soil fungal communities in a Mediterranean pine forest. New Phytol 220:1211–1221. doi: 10.1111/nph.15205

Čejka T, Trnka M, Krusic PJ, Stobbe U, Oliach D, Václavík T, Tegel W, Büntgen U (2020) Predicted climate change will increase the truffle cultivation potential in central Europe. Sci Rep 10:21281 | https://doi.org/10.1038/s41598-020-76177-0

Centritto M, Magnani F, Lee HSJ, Jarvis PG (1999) Interactive effects of elevated [CO2] and drought on cherry (Prunus avium) seedlings. II. Photosynthetic capacity and water relations. New Phytol 141:141–153. doi/10.1046/j.1469-8137.1999.00327.x

Chakhchar A, Lamaoui M, Wahbi S, Ferradous A, El Mousadik A, Ibnsouda-Koraichi S, Filali-Maltouf A, El Modafar C (2015) Leaf water status, osmoregulation and secondary metabolism as a model for depicting drought tolerance in Argania spinosa. Acta Physiol Plant (2015) 37:80 DOI 10.1007/s11738-015-1833-8

Chevalier G (2012) Europe , a continent with high potential for the cultivation of the Burgundy truffle (Tuber aestivum / uncinatum). Acta Mycol. 47 (2): 127–132, 2012

Chevalier G, Pargney JC (2014) Empirical or rational truffle cultivation? It is time to choose. For Syst 23:378–384.

Clausing S, Pena R, Song B, Müller K, Mayer-Gruner P, Marhan S, Grafe M, Schulz S, Krüger J, Lang F, Schloter M, Kandeler E, Polle A (2020) Carbohydrate depletion in roots impedes phosphorus nutrition in young forest trees. New Phytol doi: 10.1111/nph.17058

Dakora FD, Phillips DA (2002) Root exudates as mediators of mineral acquisition in low-nutrient environments. Plant Soil 245:35–47.

Davies FT, Potter JR, Linderman RG (1992) Mycorrhiza and Repeated Drought Exposure Affect Drought Resistance and Extraradical Hyphae Development of Pepper Plants Independent of Plant Size and Nutrient Content. J Plant Physiol 139:289–294. http://dx.doi.org/10.1016/S0176-1617(11)80339-1

Deveau A, Clowez P, Petit F, Maurice JP, Todesco F, Murat C, Harroué M, Ruelle J, Le Tacon F (2019) New insights into black truffle biology: discovery of the potential connecting structure between a Tuber aestivum ascocarp and its host root. Mycorrhiza 29:219–226.

Daly E, Porporato A, Rodriguez-Iturbe I (2004) Coupled dynamics of photosynthesis, transpiration, and soil water balance. Part I: Upscaling from hourly to daily level. J Hydrometeorol 5:546–558.

Deng Y, Wu S, Ke J, Zhu A (2021) Effects of meteorological factors and groundwater depths on plant sap flow velocities in karst critical zone. Sci Total Environ 781:146764. https://doi.org/10.1016/j.scitotenv.2021.146764

Dichio B, Xiloyannis C, Sofo A, Montanaro G (2006) Osmotic regulation in leaves and roots of olive trees during a water deficit and rewatering. Tree Physiol 26:179–185.

Dilkes NB, Jones DL, Farrar J (2004) Temporal Dynamics of Carbon Partitioning and Rhizodeposition in Wheat. Plant Physiol 134:706–715.

Eschenbach C, Kappen L (1999) Leaf water relations of black alder [Alnus glutinosa (L.) Gaertn.] growing at neighbouring sites with different water regimes. Trees - Struct Funct 14:28–38.

Fang Y, Xiong L (2015) General mechanisms of drought response and their application in drought resistance improvement in plants. Cell Mol Life Sci 72:673–689.

Figliuolo G, Trupo G, Mang S (2013) A realized Tuber <i>magnatum</i> niche in the upper Sinni area (south Italy). Open J Genet 03:102–110.

Fischer, C. y Colinas, C. 1996. Método de control de planta de Quercus ilex inoculada con Tuber melanosporum. En "Puesta a punto de un método de control de planta de Quercus ilex inoculada con Tuber melanosporum". Informe para el Centro de Investigación Forestal de Valonsadero, Junta de Castilla y León. 66 pag.

Fischer CR, Oliach D, Bonet JA (2017) Best Practices for Cultivation of Truffles 'Best Practices for Cultivation of Truffles'. Forest Sciences Centre of Catalonia, Solsona, Spain; Yaşama Dair Vakıf, Antalaya, Turkey. 68pp. ISBN: 978-84-697-8163-0

Fracchiolla M, Montemurro P (2007) Sostanze di origine naturale ad azione erbicida. Ital. J. Agron. / Riv. Agron., 2007, 4:463-476

Frey-Klett P, Garbaye J, Tarkka M (2007) The mycorrhiza helper bacteria revisited. New Phytol 176:22–36.

Garcia-Barreda S, Camarero JJ (2020) Tree ring and water deficit indices as indicators of drought impact on black truffle production in Spain. For Ecol Manage 475:118438. https://doi.org/10.1016/j.foreco.2020.118438

Garcia-Barreda S, Marco P, Martín-Santafé M, Tejedor-Calvo E, Sánchez S (2020) Edaphic and temporal patterns of Tuber melanosporum fruitbody traits and effect of localised peat-based amendment. Sci Rep 10:1–9.

Garcia-Barreda S, Sánchez S, Marco P, Serrano-Notivoli R (2019) Agro-climatic zoning of Spanish forests naturally producing black truffle. Agric For Meteorol 269–270:231–238. https://doi.org/10.1016/j.agrformet.2019.02.020

Garcia-Forner N, Sala A, Biel C, Save R, Martínez-Vilalta J (2016) Individual traits as determinants of time to death under extreme drought in Pinus sylvestris L. Tree Physiol 36:1196–1209.

Gargallo-Garriga A, Preece C, Sardans J, Oravec M, Urban O, Peñuelas J (2018) Root exudate metabolomes change under drought and show limited capacity for recovery. Sci Rep 8:1–15.

Gioacchini AM, Menotta M, Guescini M, Saltarelli R, Ceccaroli P, Amicucci A, Barbieri E, Giomaro G, Stocchi V (2008) Geographical traceability of Italian white truffle (Tuber magnatum Pico) by the analysis of volatile organic compounds. Rapid Commun Mass Spectrom 22:3147–3153.

Glatzel G (1983) Mineral nutrition and water relations of hemiparasitic mistletoes: a question of partitioning. Experiments with *Loranthus europaeus* on *Quercus petraea* and *Quercus robur*. Oecologia 56:193–201.

Godbold DL, Hoosbeek MR, Lukac M, Cotrufo MF, Janssens IA, Ceulemans R, Polle A, Velthorst

EJ, Scarascia-Mugnozza G, De Angelis P, Miglietta F, Peressotti A (2006) Mycorrhizal hyphal turnover as a dominant process for carbon input into soil organic matter. Plant Soil 281:15–24.

Greer GK, Dietrich MA, Lincoln JM (2016) Ailanthus altissima stimulates legume nodulation in Trifolium pratense via root exudates: A novel mechanism facilitating invasion? Int J Plant Sci 177:400–408.

Grzesiak S, Iijima M, Kono Y, Yamauchi A (1997) Differences in drought tolerance between cultivars of field bean and field pea. Morphological characteristics, germination and seedling growth. Acta Physiol Plant 19:339–348. https://doi.org/10.1007/s11738-997-0011-z

Hasselquist NJ, Metcalfe DB, Inselsbacher E, Stangl Z, Oren R, Näsholm T, Högberg P (2016) Greater carbon allocation to mycorrhizal fungi reduces tree nitrogen uptake in a boreal forest. Ecology 97:1012–1022.

Heisey RM (1990) Evidence for allelopathy by tree-of-heaven (Ailanthus altissima). J Chem Ecol 16:2039–2055.

Heisey RM (1997) Allelopathy and the Secret Life of Ailanthus altissima. Arnoldia 57:28–36.

Högberg MN, Briones MJI, Keel SG, Metcalfe DB, Campbell C, Midwood AJ, Thornton B, Hurry V, Linder S, Näsholm T, Högberg P (2010) Quantification of effects of season and nitrogen supply on tree below-ground carbon transfer to ectomycorrhizal fungi and other soil organisms in a boreal pine forest. New Phytol 187:485–493.

Holz M, Zarebanadkouki M, Kaestner A, Kuzyakov Y, Carminati A (2018) Rhizodeposition under drought is controlled by root growth rate and rhizosphere water content. Plant Soil 423:429–442.

Hopkins AJM, Ruthrof KX, Fontaine JB, Matusick G, Dundas SJ, Hardy GE (2018) Forest die-off following global-change-type drought alters rhizosphere fungal communities. Environ. Res. Lett. 13 (2018) 095006 https://doi.org/10.1088/1748-9326/aadc19

Ilyas M, Nisar M, Khan N, Hazrat A, Khan AH, Hayat K, Fahad S, Khan A, Ullah A (2021) Drought Tolerance Strategies in Plants: A Mechanistic Approach. J Plant Growth Regul 40:926–944. https://doi.org/10.1007/s00344-020-10174-5

IPCC, 2014: : Climate Change 2014: Synthesis Report. Contribution of Working Groups I, II and III to the Fifth Assessment Report of the Intergovernmental Panel on Climate Change [Core Writing Team, R.K. Pachauri and L.A. Meyer (eds.)]. IPCC, Geneva, Switzerland, 151 pp.

Jiang M, Medlyn BE, Drake JE, Duursma RA, Anderson IC, Barton CVM, Boer MM, Carrillo Y, Castañeda-Gómez L, Collins L, Crous KY, De Kauwe MG, dos Santos BM, Emmerson KM, Facey SL, Gherlenda AN, Gimeno TE, Hasegawa S, Johnson SN, Kännaste A, Macdonald CA, Mahmud K, Moore BD, Nazaries L, Neilson EHJ, Nielsen UN, Niinemets Ü, Noh NJ, Ochoa-Hueso R, Pathare VS, Pendall E, Pihlblad J, Piñeiro J, Powell JR, Power SA, Reich PB, Renchon AA, Riegler M, Rinnan R, Rymer PD, Salomón RL, Singh BK, Smith B, Tjoelker MG, Walker JKM, Wujeska-Klause A, Yang J, Zaehle S, Ellsworth DS (2020) The fate of carbon in a mature forest under carbon dioxide enrichment. Nature 580:227–231. http://dx.doi.org/10.1038/s41586-020-2128-9

Johnson NC, Graham JH, Smith FA (1997) Functioning of mycorrhizal associations along the mutualism-parasitism continuum. New Phytol 135:575–585.

Jones DL, Hodge A, Kuzyakov Y (2004) Plant and mycorrhizal regulation of rhizodeposition. New Phytol 163:459–480.

Jones DL, Nguyen C, Finlay RD (2009) Carbon flow in the rhizosphere: Carbon trading at the soil-root interface. Plant Soil 321:5–33.

Karlowsky S, Augusti A, Ingrisch J, Akanda MKU, Bahn M, Gleixner G (2018) Drought-induced accumulation of root exudates supports post-drought recovery of microbes in mountain grassland. Front Plant Sci 871:1–16.

Karst J, Gaster J, Wiley E, Landhäusser SM (2017) Stress differentially causes roots of tree seedlings to exude carbon. Tree Physiol 37:154–164.

Kavi Kishor PB, Sangam S, Amrutha RN, Sri Laxmi P, Naidu KR, Rao KRSS, Rao S, Reddy KJ, Theriappan P, Sreenivasulu N (2005) Regulation of proline biosynthesis, degradation, uptake and transport in higher plants: Its implications in plant growth and abiotic stress tolerance. Curr Sci 88:424–438.

Kohli A, Narciso JO, Miro B, Raorane M (2012) Root proteases: Reinforced links between nitrogen uptake and mobilization and drought tolerance. Physiol Plant 145:165–179.

Körner C (2003) Carbon limitation in trees. J Ecol 91:4–17.

Leake J, Cameron D (2010) Physiological ecology of mycoheterotrophy. New Phytol 185:601–605.

Lehto T, Zwiazek JJ (2011) Ectomycorrhizas and water relations of trees: A review. Mycorrhiza 21:71–90.

Le Tacon, F. (2016). Influence of Climate on Natural Distribution of Tuber Species and Truffle Production. In: Zambonelli, A., Iotti, M., Murat, C. (eds) True Truffle (Tuber spp.) in the

World. Soil Biology, vol 47. 153:168 Springer, Cham. https://doi.org/10.1007/978-3-319-31436-5_10.

Le Tacon F, Zeller B, Plain C, Hossann C, Bréchet C, Robin C (2013) Carbon Transfer from the Host to Tuber melanosporum Mycorrhizas and Ascocarps Followed Using a 13C Pulse-Labeling Technique. PLoS ONE 8(5): e64626. doi:10.1371/journal.pone.0064626

Lu P, Urban L, Zhao P (2004) Granier's Thermal Dissipation Probe (TDP) Method for Measuring Sap Flow in Trees: Theory and Practice. Acta Bot Sin 46:631–646

Li S, Feifel M, Karimi Z, Schuldt B, Choat B, Jansen S (2015) Leaf gas exchange performance and the lethal water potential of five European species during drought. Tree Physiol 36:179–192.

Li M, López R, Venturas M, Pita P, Gordaliza GG, Gil L, Rodríguez-Calcerrada J (2015) Greater resistance to flooding of seedlings of Ulmus laevis than Ulmus minor is related to the maintenance of a more positive carbon balance. Trees - Struct Funct 29:835–848.

Lo Gullo M, Salleo S (1988) Different strategies of drought resistance in three Mediterranean sclerophyllous trees growing in the same environmental conditions. New Phytol 108:267–276. https://doi.org/10.1111/j.1469-8137.1988.tb04162.x

Martel MC, Margolis HA, Coursolle C, et al (2005) Decreasing photosynthesis at different spatial scales during the late growing season on a boreal cutover. Tree Physiol 25:689–699. https://doi.org/10.1093/treephys/25.6.689

Martínez-Vilalta J, Sala A, Asensio D, Galiano L, Hoch G, Palacio S, Piper FI, Lloret F (2016) Dynamics of non-structural carbohydrates in terrestrial plants: A global synthesis. Ecol Monogr 86:495–516.

Meharg AA, Killham K (1991) A novel method of quantifying root exudation in the presence of soil microflora. Plant Soil 133:111–116.

Meharg AA, Killham K (1995) Loss of exudates from the roots of perennial ryegrass inoculated with a range of micro-organisms. Plant Soil 170:345–349.

Mehmood T, Abdullah M, Ahmar S, Yasir M, Iqbal MS, Yasir M, Rehman SU, Ahmed S, Rana RM, Ghafoor A, Shah MKN, Du X, Mora-Poblete F (2020) Incredible role of osmotic adjustment in grain yield sustainability under water scarcity conditions in wheat (Triticum aestivum L.). Plants 9:1–14.

Mello A, Murat C, Bonfante P (2006) Truffles: Much more than a prized and local fungal delicacy. FEMS Microbiol Lett 260:1–8.

Millard P, Sommerkorn M, Grelet GA (2007) Environmental change and carbon limitation in trees: A biochemical, ecophysiological and ecosystem appraisal. New Phytol 175:11–28.

MiPAAF M delle politiche agricole alimentari e forestali (2018) Piano Nazionale Della Filiera del Tartufo 2017-2020. :1–153. https://www.politicheagricole.it/flex/cm/pages/ServeBLOB.php/L/IT/IDPagina/11100

Napoli C, Mello A, Borra A, Vizzini A, Bonfante P, The S, Phytologist N, Jan N (2010) Tuber melanosporum, When Dominant, Affects Fungal Dynamics in Truffle Grounds. New Phytol 185:237–247.

Nardini A, Salleo S, Tyree MT, Vertovec M (2000) Influence of the ectomycorrhizas formed by Tuber melanosporum Vitt. on hydraulic conductance and water relations of *Quercus ilex* L. seedlings. Ann For Sci 57:305–312.

Negi VS, Maikhuri RK, Rawat LS (2011) Non-timber forest products (NTFPs): A viable option for biodiversity conservation and livelihood enhancement in central Himalaya. Biodivers Conserv 20:545–559.

Nguyen C (2003) Rhizodeposition of organic C by plants: mechanisms and controls. Agronomie, EDP Sciences, 2003, 23 (5-6), pp.375-396. 10.1051/agro:2003011 . hal-00886190

Niglas A, Kupper P, Tullus A, Sellin A (2014) Responses of sap flow, leaf gas exchange and growth of hybrid aspen to elevated atmospheric humidity under field conditions. AoB Plants 6:1–14. https://doi.org/10.1093/aobpla/plu021

Oburger E, Jones DL (2018) Sampling root exudates – Mission impossible? Rhizosphere 6:116–133. https://doi.org/10.1016/j.rhisph.2018.06.004

Olivera A, Bonet JA, Oliach D, Colinas C (2014) Time and dose of irrigation impact Tuber melanosporum ectomycorrhiza proliferation and growth of *Quercus ilex* seedling hosts in young black truffle orchards. Mycorrhiza 24:73–78.

Ozturk M, Turkyilmaz Unal B, García-Caparrós P, Khursheed A, Gul A, Hasanuzzaman M (2021) Osmoregulation and its actions during the drought stress in plants. Physiol Plant 172:1321–1335.

Paganová V, Hus M, Jureková Z (2020) Physiological Performance of Pyrus pyraster L.(Burgsd.) and Sorbus torminalis (L.) Crantz Seedlings under Drought Treatment. Plants 9:1–17.

Perri S, Entekhabi D, Molini A (2018) Plant Osmoregulation as an Emergent Water-Saving Adaptation. Water Resour Res 54:2781–2798.

Preece C, Farré-Armengol G, Llusià J, Peñuelas J (2018) Thirsty tree roots exude more carbon.

Tree Physiol 38:690–695.

Preece C, Peñuelas J (2019) A Return to the Wild: Root Exudates and Food Security. Trends Plant Sci xx:1–8.

Prescott CE (2010) Litter decomposition: What controls it and how can we alter it to sequester more carbon in forest soils? Biogeochemistry 101:133–149.

Prescott CE, Grayston SJ, Helmisaari HS, Kaštovská E, Körner C, Lambers H, Meier IC, Millard P, Ostonen I (2020) Surplus Carbon Drives Allocation and Plant–Soil Interactions. Trends Ecol Evol 35:1110–1118.

R. Gobu O, Murlimanohar Baghel PB, Chourasia KN (2017) Resistance/Tolerance Mechanism under Water Deficit (Drought) Condition in Plants. Int J Curr Microbiol Appl Sci 6:66–78.

Raglione M (Consiglio NR e S in A (2011) I suoli idonei alle varie specie di tartufi neri.

Rasmann S, Köllner TG, Degenhardt J, Hiltpold I, Toepfer S, Kuhlmann U, Gershenzon J, Turlings TCJ (2005) Recruitment of entomopathogenic nematodes by insect-damaged maize roots. Nature 434:732–737.

Requena N, Perez-Solis E, Azcon-Aguilar C, Jeffries P, Barea J-M (2001) Management of Indigenous Plant-Microbe Symbioses Aids Restoration of Desertified Ecosystems. Applied and Environmental Microbiology 67:495–498

Reyna S, Garcia-Barreda S (2014) Black truffle cultivation: A global reality. For Syst 23:317–328.

Robin C, Goutal-Pousse N, Le Tacon F (2016) Soil Characteristics for Tuber aestivum (Syn. T. uncinatum). :211–231.

Rontein D, Dieuaide-Noubhani M, Dufourc EJ, Raymond P, Rolin D (2002) The metabolic architecture of plant cells: Stability of central metabolism and flexibility of anabolic pathways during the growth cycle of tomato cells. J Biol Chem 277:43948–43960. http://dx.doi.org/10.1074/jbc.M206366200

Ruth B, Khalvati M (2011) Quantification of mycorrhizal water uptake via high-resolution on-line water content sensors. Plant Soil (2011) 342:459–468 DOI 10.1007/s11104-010-0709-3

Salerni E, Iotti M, Leonardi P, Gardin L, D'Aguanno M, Perini C, Pacioni P, Zambonelli A (2014) Effects of soil tillage on Tuber magnatum development in natural truffières. Mycorrhiza 24:79–87.

Salerni E, Perini C, Gardin L (2014) Linking Climate Variables with <i>Tuber borchii</i> Sporocarps Production. Nat Resour 05:408–418.

Samils N, Olivera A, Danell E, Alexander SJ, Fischer C, Colinas C (2008) The socioeconomic

impact of truffle cultivation in rural Spain. Econ Bot 62:331–340.

Sapes G, Demaree P, Lekberg Y, Sala A (2020) Plant carbohydrate depletion impairs water relations and spreads via ectomycorrhizal networks. New Phytologist, 229(6), 3172–3183. https://doi.org/10.1111/nph.17134

Sasse J, Martinoia E, Northen T (2018) Feed Your Friends: Do Plant Exudates Shape the Root Microbiome? Trends Plant Sci 23:25–41. http://dx.doi.org/10.1016/j.tplants.2017.09.003

Schulp CJE, Thuiller W, Verburg PH (2014) Wild food in Europe: A synthesis of knowledge and data of terrestrial wild food as an ecosystem service. Ecol Econ 105:292–305. http://dx.doi.org/10.1016/j.ecolecon.2014.06.018

Song F, Han X, Zhu X, Herbert SJ (2012) Response to water stress of soil enzymes and root exudates from drought and non-drought tolerant corn hybrids at different growth stages. Can J Soil Sci 92:501–507.

Stryamets NN, Elbakidze MM, Ceuterick MM, Angelstam PP, Axelsson RR (2015) From economic survival to recreation: Contemporary uses of wild food and medicine in rural Sweden, Ukraine and NW Russia. Journal of Ethnobiology and Ethnomedicine (2015) 11:53 DOI 10.1186/s13002-015-0036-0

Tagliaferro F, Ebone A (2007) Tecniche selvicolturali e agronomiche per il miglioramento dell'habitat di Tuber magnatum in tartufaie spontanee di boschi naturali. For Silvic For Ecol 4:88.

Tahvanainen V, Miina J, Kurttila M, Salo K (2016) Modelling the yields of marketed mushrooms in Picea abies stands in eastern Finland. For Ecol Manage 362:79–88. http://dx.doi.org/10.1016/j.foreco.2015.11.040

Taiz L, Zeiger E (2003) Plant Physiology (Third edition).

Talbott LD, Zeiger E (1998) The role of sucrose in guard cell osmoregulation. J Exp Bot 49:329–337.

Tedersoo L, Bahram M, Zobel M (2020) How mycorrhizal associations drive plant population and community biology. Science (80-) 367

Thomas PA, Leski T, La Porta N, Dering M, Iszkuło G (2021) Biological Flora of the British Isles: Crataegus laevigata. J Ecol 109:572–596.

Tognetti R, Longobucco A, Raschi A (1998) Vulnerability of xylem to embolism in relation to plant hydraulic resistance in *Quercus pubescens* and *Quercus ilex* co-occurring in a Mediterranean coppice stand in central Italy. New Phytol 139:437–447.

Treseder KK, Holden SR (2013) Fungal carbon sequestration. Science (80-) 340:1528–1529.

Vanninen P, Ylitalo H, Sievänen R, Mäkelä A (1996) Effects of age and site quality on the distribution of biomass in Scots pine (Pinus sylvestris L.). Trees 10:231–238. https://doi.org/10.1007/bf02185674

Vannini A, Lucero G, Anselmi N, Vettraino AM (2009) Response of endophytic Biscogniauxia mediterranea to variation in leaf water potential of *Quercus cerris*. For Pathol 39:8–14.

Vezzola V (2002) Coltivare il tartufo nero liscio è possibile. Inf Agrar 58:79–80.

de Vries FT, Williams A, Stringer F, Willcocks R, McEwing R, Langridge H, Straathof AL (2019) Changes in root-exudate-induced respiration reveal a novel mechanism through which drought affects ecosystem carbon cycling. New Phytol 224:132–145.

Wang B, Qiu YL (2006) Phylogenetic distribution and evolution of mycorrhizas in land plants. Mycorrhiza 16:299–363.

Waseem M, Ali A, Tahir M, Nadeem M a, Ayub M, Tanveer A, Ahmad R, Hussain M (2011) Mechanism of Drought Tolerance in Plant and Its Management Through. Cont J Agric Sci 5:10–25. http://www.wiloludjournal.com/pdf/agrsci/2011-1/10-25.pdf

Williams A, de Vries FT (2019) Plant root exudation under drought: implications for ecosystem functioning. New Phytol:0–3.

Yang SL, Chen K, Wang SS, Gong M (2015) Osmoregulation as a key factor in drought hardening-induced drought tolerance in Jatropha curcas. Biol Plant 59:529–536.

Yang X, Lu M, Wang Y, Wang Y, Liu Z, Chen S (2021) Response mechanism of plants to drought stress. Horticulturae 2021, 7, 50. https://doi.org/10.3390/ horticulturae7030050

Yuste J, Rubio JA, Pelaez HJ, et al (1999) Predawn leaf water potential and soil water content in vertical trellis under irrigated and non-irrigated conditions in tempranillo grapevines. Acta Hortic. 493:309–321

Zhao M, Running SW (2010) Drought-Induced Reduction in Global. Science (80-) 329:940–943. http://www.ncbi.nlm.nih.gov/pubmed/20724633

https://www.arpa.veneto.it/temi-ambientali/agrometeo/file-e-allegati/bollettino-mese/2023/sintesi-2023

Summary of Weather and Agrometeorological Commentary for the Summer Period, Compiled by the Regional Department for Territorial Security of the Veneto Region-summer 2023